



**University of  
Nottingham**  
UK | CHINA | MALAYSIA

---

**Functional traits and comparative  
transcriptomic insight into *Pleurotus*  
mushroom for improved cultivation in  
Malaysia**

**By**

**Leong Chia Choong**

**Thesis submitted to the University of Nottingham for the  
degree of Doctor of Philosophy**

**April 2023**

## **Abstract**

Edible mushrooms are recognised as a functional food due to their rich content of bioactive substances and low calories. *Pleurotus*, or oyster mushroom contributes to a quarter of global mushroom production while the most cultivated mushroom in Malaysia is *Pleurotus pulmonarius*. The mushroom industry is constantly facing challenges arising from mushroom spawn of low quality. To maximize production, it is therefore essential to use strains with excellent biological efficiency, measured by the fresh weight of mushroom per dry substrate used. However, the biological and biochemical process at the molecular level that underlies the biological efficiency of *P. pulmonarius* are not well-known. This research aims to identify and determine the differentially expressed genes and transcriptome profiles of selected Malaysian low- and high-yield *Pleurotus pulmonarius* strains. The association between antioxidant activities, nutritional profile, and biological efficiencies of *Pleurotus* strains were established. Mechanism underlying the biological efficiency and complete growth of selected *P. pulmonarius* samples was further investigated through transcriptomic profiling. By using three newly developed DNA barcodes, sixteen strains were identified as *Pleurotus pulmonarius* and eight as *Pleurotus eryngii*. Generally, *P. pulmonarius* showed antioxidant activities and phytochemical contents that were superior to *P. eryngii*. Biological efficiencies of ten identified *P. pulmonarius* strains were further established. Subsequently, comparative transcriptomic profiling was performed, with MP35 and MP42 classified as the high-yield type, whereas MP12 and MP28 designated as the low-yield type based on findings from the biological efficiency assessments. Differential expression analysis revealed 27449 unigenes exhibiting significant ( $P < 0.05$ ) dysregulation, where 13707 genes were upregulated and 13742 were downregulated in the high-yield group as compared to the low-yield group. Through KEGG enrichment analysis, four potential differential expressed gene were discovered. Aspartyl protease, *CATALASE1*, GTPase activating protein SEC23, palmitoyltransferase and copper amine oxidase from various significantly enriched pathways were verified

using real time polymerase chain reaction (qPCR). Palmitoyltransferase, copper amine oxidase and *CATALASE1* were downregulated while GTPase-activating protein and aspartyl protease were upregulated according to NGS results. The relative gene expression from qPCR results follows the same trend for each gene. The application of the identified five genes can be used as molecular biomarkers to differentiate high and low yield *P. pulmonarius* strain before large-scale commercial cultivation. These results provide valuable information on species identification, strain selection and cultivation strategies of *P. pulmonarius* for improving mushroom agriculture industry.

## **Acknowledgement**

First and foremost, I would like to thank my supervisor Dr Ho Wan Yong for her unwavering support and invaluable feedback throughout the writing process. Her guidance and expertise were instrumental in shaping this work. Without her help and patience, this thesis would not have been possible.

I would also like to express my deepest gratitude to my co-supervisor Dr Yeap Swee Keong for his invaluable support and guidance throughout my research journey.

I would also like to extend my heartfelt thanks to my laboratory members, Dr Koh May Zie, Ms Ho Jinn Shyuan and Dr Rachel Diem, who provided invaluable insights and suggestions that helped improve the quality of my work.

I am also grateful to Mr Wong Siak Chung, Ms Siti, Ms Asma, Ms Syikin and Mr Wan for their aid and guidance throughout my PhD career in the lab. Their passion for teaching and commitment to excellence inspired me to pursue this research.

Additionally, I would like to thank my partner Ms Jessica Ooi for her support and love throughout my PhD career.

Finally, I would like to express my gratitude to my family, especially my father for his unwavering support for my PhD. This would not be possible without him.

## **Declaration**

I hereby confirm that:-

- This thesis is my original work.
- Quotations, citations and illustration have been referenced.
- This thesis has not been submitted previously or concurrently for any other degree at any other institutions.
- Intellectual property from the thesis and copyright of thesis are fully owned by the University of Nottingham, Malaysia Campus.

A handwritten signature in black ink, appearing to read 'Reynard', is written over a horizontal line.

Signature: \_\_\_\_\_

Date: 30/4/2023

## **Abbreviation**

18S	18S ribosomal RNA
ANOVA	Analysis of variance
BLAST	Basic local alignment search tool
BP	Biological Process
bp(s)	Base pair(s)
CC	Cellular Components
Cq	Cycle of quantification
DEG	Differential expressed gene
dNTP(s)	deoxynucleoside triphosphate (s)
EDTA	Ethylenediaminetetraacetic acid
et al.	et alia
FDR	False discovery rate
GO	Gene ontology
kb	Kilo base pair
MF	Molecular Function
	National Center for Biotechnology
NCBI	Information
NGS	Next generation sequencing
PCR	Polymerase chain reaction
qPCR	Quantitative polymerase chain reaction
RE	Restriction endonuclease
RIM	Root induction media
RIN	RNA integrity number
rpm	Revolutions per minute
rRNA	Ribosomal RNA
RT	Reverse transcription
	Reverse transcription quantitative real time
	Quantitative reverse transcription
RT-qPCR	polymerase chain reaction

## **Lists of Figures and Tables**

### **Figures**

Figure 2.1 <i>Pleurotus pulmonarius</i> cultivated in a mushroom house (own photo)	17
Figure 2.2 <i>Pleurotus ostreatus</i> , accessed 12 January 2023	17
Figure 2.3 <i>Pleurotus eryngii</i> , accessed 12 January 2023	18
Figure 2.4 <i>Pleurotus populinus</i> accessed 12 January 2023	18
Figure 2.5 <i>Pleurotus citrinopileatus</i> , accessed 12 January 2023	19
Figure 2.6 <i>Pleurotus djamor</i> , accessed 12 January 2023	19
Figure 2.7 Life cycle of a <i>Pleurotus</i> mushroom (Adebayo & Martínez, 2015).	21
Figure 2.8 Image of a basidiocarp (Debivort, 2006)	22
Figure 2.9 Basidiospore on the gills of a <i>Pleurotus pulmonarius</i> (own photo)	22
Figure 2.10 Schematic of the Inferred Barcoding Gap.	31
Figure 2.11 Overview of RNA-Seq (Kukurba & Montgomery, 2015)	41
Figure 3.1 Gel electrophoresis image of random samples a) ITS and rpb2 marker gene for strain MP12, MP25 and MP51 with negative control, b) IGS1 marker gene for strain MP20, MP31, MP50 with negative control	47
Figure 3.2 Frequency distributions of intra- and inter-specific Kimura-2-Parameter pairwise distances for ITS region	51
Figure 3.3 Frequency distributions of intra- and inter-specific Kimura-2-Parameter pairwise distances for IGS1 region	51
Figure 3.4 Frequency distributions of intra- and inter-specific Kimura-2-Parameter pairwise distances for rpb2 region	52
Figure 3.5 Phylogenetic tree of 24 <i>Pleurotus</i> sample constructed based on ITS gene sequence and constructed with the Maximum Likelihood algorithm (MEGA 7). Sequence of AB234030.1 ( <i>Pleurotus ostreatus</i> isolate 6689) were downloaded from NCBI GenBank as outgroup. Numbers of the branches indicate bootstrap value with 1000 replications.	55
Figure 3.6 Phylogenetic tree of 24 <i>Pleurotus</i> sample constructed based on IGS1 gene sequence and constructed with the Maximum Likelihood algorithm (MEGA 7). Sequence of AB234030.1 ( <i>Pleurotus ostreatus</i> KBPO2) were	

downloaded from NCBI GenBank as outgroup. Numbers of the branches indicate bootstrap value with 1000 replications. 57

Figure 3.7 Phylogenetic tree of 24 *Pleurotus* sample constructed based on RPB2 gene sequence and constructed with the Maximum Likelihood algorithm (MEGA 7). Sequence of JN126371.1 (*Pleurotus ostreatus* JZB2101007) were downloaded from NCBI GenBank as outgroup. Numbers of the branches indicate bootstrap value with 1000 replications 59

Figure 4.1 Antioxidant and phenolics values of mycelia aqueous extract (a) Total phenolic content, (b) DPPH radical scavenging activity, (c) FRAP value. Blue indicates *P. pulmonarius*, red indicates *P. eryngii* and black indicates unidentified sample. 76

Figure 4.2 Antioxidant activity and phenolics of *P. pulmonarius* fruiting bodies aqueous extract (a) Total phenolic content ; (b) DPPH Radical scavenging activity and (c) FRAP value 78

Figure 4.3 Morphological features of all 10 *P. pulmonarius* samples 84

Figure 4.4 Two weeks old mycelia of *Pleurotus eryngii* (MP5; Top left), *Pleurotus ostreatus* (MP6 ; Top right) and *Pleurotus pulmonarius* (MP42; Bottom) 85

Figure 4.5 Five days old MP35 mycelia showing a visible clamp connection. 100x magnification under light microscope, methylene blue stain 1% 86

Figure 4.6 Morphology of 10 *P. pulmonarius* strain, (a) Fruiting body number; (b) Cap diameter; and (c) Stipe length 87

Figure 5.1 Gel electrophoresis image of high and low yield *P. pulmonarius* RNA extracts 101

Figure 5.2 GO functional annotation of all unigenes (Red bar is biological process, green bar is cellular component while blue bar is molecular function 103

Figure 5.3 KEGG classification of all unigenes. Alphabet A to E represents different KO pathway (A: Cellular Process, B: Environmental Information Processing, C: Genetic Information Processing, D: Metabolism, E: Organismal Systems) 104

Figure 5.4 Volcano plot of each differentially expressed unigenes 106



Figure 5.5 Heatmap of all the DEG among high and low yield *P. pulmonarius*. Yellow to green represent upregulation while red to black represent downregulation. High yield types were arranged to the right side while low yield types were on the left side. 107

Figure 5.6 GO Enrichment Analysis of significant differentially expressed genes. 108

Figure 5.7 Top significant enriched KEGG pathways of differentially expressed gene between high yield and low yield *P. pulmonarius* 109

Figure 5.8 Heat map of the RNA-Seq based on FPKM and on selected unigenes tested using qRT-PCR validation. Yellow to green represent upregulation while red to black represent downregulation. High yield types were arranged to the right side while low yield types were on the left side. 111

Figure 5.9 Tryptophan metabolism pathways from KEGG database. The red box indicates known DEG that can be found in *P. pulmonarius* transcriptome in this study while green box indicates known gene based on the basidiomycete *Agaricus bisporus* genome. 115

Figure 5.10 Protein processing in endoplasmic reticulum pathways from KEGG database. The red box indicates known DEG that can be found in *P. pulmonarius* transcriptome in this study while green box indicates known gene based on the basidiomycete *Agaricus bisporus* genome. 117

Figure 5.11 Autophagy - yeast pathways from KEGG database. The red box indicates known DEG that can be found in *P. pulmonarius* transcriptome in this study while green box indicates known gene based on the basidiomycete *Agaricus bisporus* genome. 119

Figure 5.12 Phenylalanine metabolism pathways from KEGG database which is under the biosynthesis of secondary metabolite pathway. The red box indicates known DEG that can be found in *P. pulmonarius* transcriptome in this study while green box indicates known gene based on the basidiomycete *Agaricus bisporus* genome. 121

## Tables

Table 3.1 List of primers and their respective sequence	45
Table 3.2 Identification of <i>Pleurotus</i> species based on BLAST results from the aligned sequence of each marker gene.	48
Table 3.3 Genetic distance percentage generated using Kimura 2-parameter model analysis for the candidate DNA barcode.	53
Table 3.4 List of samples identified as <i>Pleurotus pulmonarius</i> compared with the database provided from MARDI.	60
Table 3.5 List of samples identified as <i>Pleurotus eryngii</i> compared with the database provided from MARDI.	61
Table 3.6 List of samples with ambiguous identity as compared with the database provided from MARDI.	62
Table 4.1 Biological efficiency, yield, and complete growth of the ten <i>P. pulmonarius</i> sample	75
Table 4.2 Pearson correlation between yield and DPPH value; FRAP value; TPC value.	79
Table 4.3 Pearson correlation between antioxidant values of fruiting bodies and mycelia in each of the antioxidant tested.	80
Table 4.4 Moisture, ash, crude protein, and lipid presented from analysis of ten <i>P. pulmonarius</i> , in triplicate. Different lowercase superscript letters in the same column indicate a statistical difference at $p < 0.05$ using one-way ANOVA.	81
Table 4.5 Ranking of main attributes evaluated for fruiting bodies in this study.	91
Table 5.1 List of primers used for qRT-PCR validation.	98
Table 5.2 Reading from Nanodrop in terms of concentration and absorbance value.	100
Table 5.3 De novo assembly statistics	102
Table 5.4 Differential expression of selected unigenes for qRT-PCR validation. One-way anova test was performed to obtain the P-value.	109

## **Table of Contents**

Abstract.....	2
Acknowledgement .....	4
Declaration.....	5
Abbreviation .....	6
Lists of Figures and Tables .....	7
Table of Contents.....	11
Chapter 1: Introduction .....	14
1.1 Background .....	14
1.2 Outline of key issues .....	14
1.3 Core objectives .....	15
Chapter 2: Literature review.....	16
2.1 <i>Pleurotus</i> genus.....	16
2.2 <i>Pleurotus</i> life cycle .....	20
2.2.1 <i>Pleurotus pulmonarius</i> .....	23
2.2.2 <i>Pleurotus ostreatus</i> .....	23
2.2.3 <i>Pleurotus eryngii</i> .....	24
2.3 Cultivation of <i>Pleurotus</i> species.....	24
2.4 Spawn time and preparation of substrate.....	25
2.5 Biological efficiency and initiation of primordial .....	27
2.6 Postharvest and processing of <i>Pleurotus</i> .....	28
2.7 Taxonomy and diversity of <i>Pleurotus</i> spp.....	29
2.8 Species identification of <i>Pleurotus</i> mushrooms .....	30
2.8.1 Internal transcribed spacer.....	31
2.8.2 Intergenic spacer.....	31
2.8.3 Largest subunit RNA polymerase II.....	32
2.8.4 Combination of multiple gene marker.....	32
2.8.5 Phylogenetic analysis .....	33
2.8.6 Antioxidant, reactive oxygen species and antioxidant capacity of <i>Pleurotus</i> mushroom.....	34
2.8.7 Nutritional value of <i>Pleurotus</i> .....	37
2.8.8 Proximate analysis .....	37
2.8.9 High throughput transcriptomics sequencing .....	39
2.8.10 Reverse transcription quantitative real time polymerase chain reactions (RT-qPCR) .....	40

Chapter 3: Molecular identification and phylogenetic studies of Malaysian <i>Pleurotus</i> species.....	42
3.1 Introduction .....	42
3.2 Materials and Methods.....	43
3.2.1 <i>Pleurotus</i> mycelia culture .....	43
3.2.2 DNA extraction of <i>Pleurotus</i> mycelia .....	43
3.2.3 PCR amplification ITS, IGS1 and rpb2 genes .....	44
3.2.4 Sequence data analysis, BLAST search and phylogenetic analysis .....	45
3.3 Results.....	46
3.3.1 PCR Amplification and Sanger sequencing .....	46
3.3.2 Assessment of barcoding gaps and Inter- and intra-specific variations of <i>Pleurotus</i> .....	50
3.3.3 Phylogenetic analysis of <i>Pleurotus</i> spp.....	54
3.3.4 Comparison of identified isolates with external database from MARDI. ..	60
3.4 Discussion .....	63
Chapter 4: Antioxidant activities, proximate analysis, and biological efficiency of <i>Pleurotus</i> species in Malaysia .....	68
4.1 Introduction .....	68
4.2 Materials and Methods.....	69
4.2.1 Sample selection .....	69
4.2.2 Spawn and substrate preparation .....	69
4.2.3 Cultivation .....	69
4.2.4 Harvesting and measurement .....	70
4.2.5 Preparation of <i>Pleurotus</i> mycelia and fruiting bodies aqueous extract ....	70
4.2.6 Bioactivities screening .....	71
4.2.7 Proximate analysis .....	72
4.3 Results.....	74
4.3.1 Growth parameters and yield of fruiting bodies .....	74
4.3.2 Antioxidant activity of aqueous extract.....	76
4.3.3 Proximate analysis .....	81
4.3.4 Morphological characteristic of 10 selected <i>P. pulmonarius</i> fruiting bodies .....	83
4.4 Discussion .....	88
Chapter 5: Comparative transcriptomics analysis of high and low yield edible mushroom <i>Pleurotus pulmonarius</i> in Malaysia .....	93
5.1 Introduction .....	93
5.2 Materials and Methods.....	94

5.2.1 Mycelia culture and fruiting bodies growth .....	94
5.2.2 RNA extraction .....	94
5.2.3 Library preparation and RNA-Seq .....	95
5.2.4 De novo transcriptome assembly and homology search.....	95
5.2.5 Identification of differentially expressed genes. ....	96
5.2.6 Validation of differentially expressed gene through Quantitative real time PCR (qPCR) Analysis. ....	97
5.3 Results.....	98
5.3.1 Total RNA quality and quantity.....	98
5.3.2 Illumina sequencing and reads assembly. ....	102
5.3.3 Functional annotation of the transcriptome .....	102
5.3.4 Identification and Functional Enrichment Analysis of Differentially expressed unigenes.....	105
5.3.5 Validation of DEGs by qPCR .....	109
5.4 Discussion .....	112
5.4.1 Specific unigenes chosen from KEGG Enrichment Analysis.....	113
5.4.2 Aspartyl protease.....	121
Chapter 6: Summary, conclusion, and future prospects. ....	123
References .....	126
Appendix .....	152

## Chapter 1: Introduction

### 1.1 Background

The oyster mushroom, which is also known as *Pleurotus*, belongs to the family Pleurotaceae in the Basidiomycota division. *Pleurotus* mushrooms are the second most produced mushroom globally, trailing only *Lentinula* (Royse). In comparison to other basidiomycetes, *Pleurotus* has a larger number of cultivated species (Singh & Kamal, 2017). The most cultivated type of oyster mushroom in Malaysia is the grey oyster mushroom (*Pleurotus pulmonarius*), which accounts for 90.89% of production, followed by Lingzhi (*Ganoderma lingzhi*) (1.64%) and King oyster (*Pleurotus eryngii*) (1.17%) (Rosmiza et al., 2016).

With its high protein, vitamins and amino acids content, oyster mushrooms are generally considered as a functional food with high nutrition (Musieba et al., 2013). Not only that, but oyster mushrooms are also known for their antioxidant, anti-inflammatory, antihypertensive, antimicrobial and cytotoxicity properties (Corrêa et al., 2016).

### 1.2 Outline of key issues

The oyster mushrooms samples in the MARDI's library lacks proper identification as its identification is based on the traditional methods by using morphological traits such as colour and cap shape. This issue is can be more complicated for two different factors. One, with species such as *P. eryngii* where species complex exists (Shnyreva & Shnyreva, 2015). Two, the morphological appearance of oyster mushroom can change depending on the cultivation conditions (temperature, humidity, absence of light) and substrate type (Avin et al., 2012). The more appropriate method of identifying edible mushroom is to use DNA barcoding such as the internal transcribed spacer (ITS).

In Malaysia, the most popular cultivated edible mushroom is *P. pulmonarius*, yet problems like the poor quality of initial mushroom spawn persist. This can

negatively impact the farmers livelihood as poor-quality spawn produce fewer fruiting bodies in a longer period. Edible mushroom pricing is based on the weight; hence it is vital to use good quality mushroom spawn that produces more fruiting bodies in a shorter period (Jeznabadi et al., 2016). Edible mushrooms should also be subjected to nutritional analysis as this is an important step to commercialise a food product. This nutritional analysis includes antioxidants content, total phenolic content, and proximate analysis (Nielsen, 2017).

Lastly, once we have established high and low yield oyster mushroom through cultivation, we can perform next generation sequencing (NGS) to compare the gene expression of high and low yield oyster mushrooms. This can provide information on the genes that might play a role in determining the yield and complete growth of oyster mushrooms. We hypothesize that the genes detected in NGS between high and low yield oyster mushroom are the important genes that plays a role in specific pathways to determine the yield, complete growth, and antioxidant properties.

### **1.3 Core objectives**

The core objective of this research is to identify differentially expressed genes via transcriptomic profiling of selected high and low yield *P. pulmonarius* in Malaysia. The specific objectives of this research is as follow:: -

1. To design three novel DNA barcode for the identification of Malaysia oyster mushroom
2. To compare antioxidant, phenolic and nutritional content of identified *P. pulmonarius* in both mycelia and fruiting bodies.
3. To perform whole transcriptomic analysis followed by differential expressed gene analysis between high and low yield *P. pulmonarius* fruiting bodies.

## Chapter 2: Literature review

### 2.1 *Pleurotus* genus

Commonly known as the oyster mushroom, the genus *Pleurotus* originated from the Basidiomycota class (Barh et al., 2019). About 40 varieties of species belong to the genus *Pleurotus* with few of high economic importance and distributed in a large range of temperate and tropical climates, such as *Pleurotus ostreatus*, *Pleurotus eryngii* and *Pleurotus pulmonarius* (Golak-Siwulska et al., 2018).

Paul Kummer defined the genus *Pleurotus* (Fr) Kummer (Basidiomycota, Agaricales) back in 1871. *Pleurotus* mushrooms are high in nutritional values while possessing a wide variety of environmental and biological applications (Knop et al., 2015). The abundance of vitamins, fibers minerals and proteins in *Pleurotus* mushrooms has led the genus to be considered a functional and healthy food. Due to the beneficial compositions of *Pleurotus* mushrooms, it is considered as an alternative to vegetables, meats, and fishes (Mostak Ahmed et al., 2016).

The *Pleurotus* species are cultivated globally as commercially important edible mushrooms. Mushrooms from the genus *Lentinula* ranked first in terms of cultivation number while *Pleurotus* ranked second worldwide. This is due to *Pleurotus* mushroom shorter shelf life as compared to the *Lentinula* (Singh & Kamal, 2017). China alone has accounted for 87% of *Pleurotus* production worldwide while the rest of the world only produce 13% (Royse et al., 2017).

The most prominent species in the *Pleurotus* genus are *P. pulmonarius* (Figure 2.1), *P. ostreatus* (Figure 2.2), *P. eryngii* (Figure 2.3), *P. populinus* (Figure 2.4), *P. citrinopileatus* (Figure 2.5), and *P. djamor* (Figure 2.6). In Malaysia, the most demanded and cultivated mushrooms are from the *Pleurotus* genus. Contrary to the global rankings, the production of oyster mushroom in Malaysia, specifically *Pleurotus pulmonarius* contributes to about 91% of total mushroom production (Rosmiza et al., 2016).





Figure 2.1 *Pleurotus pulmonarius* cultivated in a mushroom house (own photo)



Figure 2.2 *Pleurotus ostreatus*, accessed 12 January 2023

<https://www.cabidigitallibrary.org/cms/10.1079/cabicompendium.42037/asset/a4140790-eabe-454d-ab04-347b611f9fe9/assets/graphic/pleuos01.jpeg>



Figure 2.3 *Pleurotus eryngii*, accessed 12 January 2023

<<https://hifasdaterra.com/en/medicinal-mushrooms/king-oyster-pleurotus-eryngii>>



Figure 2.4 *Pleurotus populinus* accessed 12 January 2023

<[https://www.mushroomexpert.com/images/kuo6/pleurotus\\_populinus\\_02.jpg](https://www.mushroomexpert.com/images/kuo6/pleurotus_populinus_02.jpg)>





Figure 2.5 *Pleurotus citrinopileatus*, accessed 12 January 2023 <  
[https://live.staticflickr.com/962/27422363907\\_8fcdf67e07\\_b.jpg](https://live.staticflickr.com/962/27422363907_8fcdf67e07_b.jpg)>



Figure 2.6 *Pleurotus djamor*, accessed 12 January 2023 <  
<https://mushroommountain.com/wp-content/uploads/2019/03/pinkoyster2.jpg>>

The worldwide mushroom market expanded from \$57.18 billion in 2022 to \$62.44 billion in 2023. Forecasts indicate that the mushroom market is projected to reach \$90.88 billion in 2027 (The Business Research Company, 2023). This forecasted increase in demand provides a great opportunity for the Malaysia mushroom industry to develop and increase its mushroom exports to be able to compete with top mushrooms suppliers such as China. Cultivation of *Pleurotus* species is usually on a large scale, utilizing agricultural waste with easy and low-cost production techniques (Raman et al., 2018).

*Pleurotus* species secretes extracellular enzyme to aid in breaking down organic materials to obtain nutrient for growth. A wide variety of lignocellulosic waste such as paddy straw, rubber saw dust, and wheat straw has been shown to be viable cultivation substrates for *Pleurotus* species (Raman et al., 2021). By using these agriculture waste as substrates, cultivation of *Pleurotus* helps in waste recycling while providing necessary functional food. After cultivation, the spent substrates were also shown to be beneficial by functioning as animal feeds, fertilizers, and production of biogas. (Kakon et al., 2012).

## **2.2 *Pleurotus* life cycle**

The oyster mushroom life cycle initiates with the germination of a basidiospore in an optimal substrate (Figure 2.7). The spore subsequently forms a monokaryon mycelium which contains genetically identical nuclei ( $n$ ) and is capable of independent growth. The formation of fertile dikaryon ( $n+n$ ) occurs when two monokaryon mycelia come into close contact by plasmogamy (Adebayo & Martínez, 2015). A dikaryon possesses two genetically different nuclei in each hyphae (one from each monokaryon) and a clamp connection between each hyphae throughout the whole mycelia. Once appropriate temperature, lighting conditions and humidity are present, the dikaryotic mycelia will differentiate into primordia (tiny pinheads) and eventually a fruiting body with specialized structure known as basidia on the gills of the mushroom (Adebayo & Martínez, 2015). The process of karyogamy (fusion of

two haploid nuclei) and meiosis (recombination and segregation) will take place on the basidium (Figure 2.8) which results in four haploid nuclei moving to the edge of basidium to form four new basidiospores. As the fruiting bodies mature, the basidiospores (Figure 2.9) are released, initiating the life cycle again (Adebayo & Martínez, 2015).

In the event of artificial culturing such as for research or commercial purposes, the basidiospore or/and sporophore (fruiting bodies) tissue can be placed on a nutritional agar medium under aseptic conditions. This will eventually give rise to mycelia growth and the mycelium is inoculated on a suitable substrate such as grains, wheat and straws which are called spawn (Adebayo & Martínez, 2015).

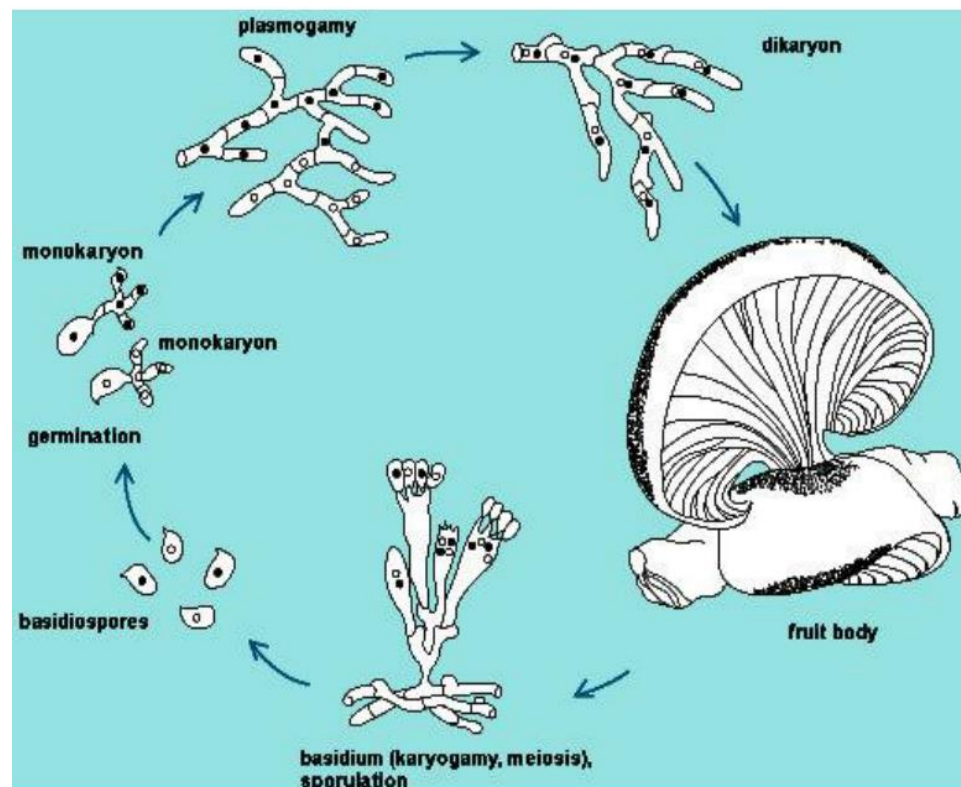


Figure 2.7 Life cycle of a *Pleurotus* mushroom (Adebayo & Martínez, 2015).

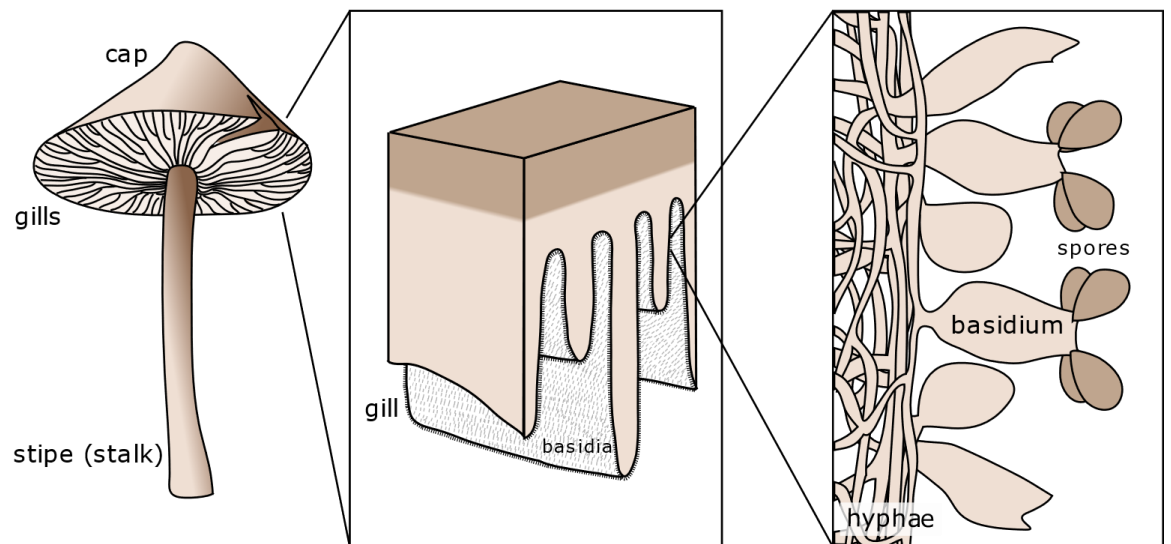


Figure 2.8 Image of a basidiocarp (Debivort, 2006)



Figure 2.9 Basidiospore on the gills of a *Pleurotus pulmonarius* (own photo)



### 2.2.1 *Pleurotus pulmonarius*

*Pleurotus pulmonarius* (Fr.) Quel, commonly also known as grey oyster mushroom (Jonathan et al., 2012). *P. pulmonarius* (Figure 2.1) often have a small cap about 10-13 cm in size, while having light brown or cream for colour. The cap can be shaped as shell, or paddle. During early stages of growth fruiting body it is shaped like an oyster with a bent and ruffled edge at times. The gills converged deeply towards the stem and are very dense and narrow. This species has a distinct stem which can reach up to 1.5 cm in thickness and 6cm in height. The stem is lateral and grows thinner towards the base. *P. pulmonarius* has an indistinct odor and tastes slightly mild and sweet (Dawidowicz, 2021). *P. pulmonarius* can be found worldwide except for Antarctica. It grows in condensed clumps or single specimen on deciduous and conifers trees. Not only that, *P. pulmonarius* can be found grown on logs, carps of trees and dead trunks of other trees such as oaks, beeches, poplars and willows. *P. pulmonarius* can produce fruiting bodies in warm seasons during summertime to early autumn (June to October). *P. pulmonarius* is often time confused with its closely related species, the *Pleurotus ostreatus* and *Pleurotus dryinus* due to its similar morphology.

### 2.2.2 *Pleurotus ostreatus*

*Pleurotus ostreatus* (Jacq.) P.Kumm is also known as oyster mushroom due to its fruiting bodies resembling a colony of oysters. *P. ostreatus* (Figure 2.2) has a cap diameter of 12-18 cm in size, often larger than *P. pulmonarius*. The fruiting bodies of *P. ostreatus* are generally dark brown to gray in colour. *P. ostreatus* found in the wild appears around autumn seasons (October – November) with some occurrence during warm winters or early spring. While tolerant to lower temperatures, *P. ostreatus* has stringent light requirements as under low light, it does not produce any fruiting bodies or very smalls ones (Wojewoda, 2003). The odor of *P. ostreatus* is of bittersweet smell of benzaldehyde and a hint of anise and almond (Beltran-Garcia et al., 1997). Just like *P. pulmonarius*, it can be also found on dead wood and living trees

specifically beech, willow, poplar, hornbeam, and common walnut (Piska et al., 2017).

### 2.2.3 *Pleurotus eryngii*

*Pleurotus eryngii* (DC: Fr.) Quel., which are known as king oyster mushroom it's a valuable edible mushroom species due to its highly nutritional and medical values. *P. eryngii* (Figure 2.3) are considered the best *Pleurotus* species for its culinary qualities such as excellent texture and flavour, longest shelf life among *Pleurotus* and its consistency in the stem and cap (Moonmoon et al., 2010) In the wild, *P. eryngii* is a weak parasite as it can grow on a root of a living plant from the genus *Eryngium* family Apiaceac (Zervakis et al., 2014). Fruiting bodies of *P. eryngii* are pale cream to gray for the cap while the stipe is white and thick. *P. eryngii* is the most diverse species in the *Pleurotus* genus with at least six different varieties in its species complex (Estrada et al., 2010).

## 2.3 Cultivation of *Pleurotus* species

*Pleurotus* mushrooms do not need specific and sophisticated controlled environment conditions as they are able to grow in high humidity, extensive range of temperatures and tolerant to high concentration of carbon dioxide. As such, cultivation of *Pleurotus* is increasingly gaining popularity globally spawn (Adebayo & Martínez, 2015). *Pleurotus* mushrooms are also ubiquitous and found all over the world whether it is tropical or temperate zone. In Southeast Asia, cultivation of *Pleurotus* mushrooms has been a large source of income for the farmers.

By using solid state fermentation, cultivation of *Pleurotus* mushroom aids in the reusing of waste byproduct from agriculture industry. Numerous agricultural wastes and by-products such as wheat and rice straw, sugar cane leaves, mango seeds, banana leaves and peanuts hull are used as a substrate to grow oyster mushroom. The commonly utilized substrates for cultivation in Asia are cotton wastes and rice straw (Sardar et al., 2017). Generated from the cotton spinning industry, cotton wastes substrates are the most suitable and cheapest which has attracted and encouraged many Korean farmers into



*Pleurotus* cultivation (Jang et al., 2016). The biological efficiency of multiple *Pleurotus* species on compost and non-compost substrate ranged from 45% to 120% (Jatwa et al., 2016).

Historically, China was the first to be introduced to *Pleurotus* cultivation by the West during World War 1 and has since attained about one quarter of the world's mushrooms production by the year 2010. In Japan, *Pleurotus ostreatus* was cultivated starting early 1950s, and in 1993, the bottled techniques for *Pleurotus eryngii* cultivation was introduced. The Japanese has adapted the bottle technique with either corncob or sawdust as a substrate in large scale production (Yamanaka, 2011). Multiple species of *Pleurotus*, namely *P. ostreatus*, *P. eryngii*, *Pleurotus djamor*, *Pleurotus citrinopileatus*, and *Pleurotus sajor-caju* are mainly cultivated in South Korea with *P. eryngii* being the most popular (Berch et al., 2007). Production of *Pleurotus* in South Korea amounted to about half of total edible mushroom production (Soylu & Kang, 2016). On the other hand, *P. pulmonarius* were cultivated on a large scale in Southeast Asia (Bao et al., 2004).

## **2.4 Spawn time and preparation of substrate**

Spawn is defined as mushroom seed, and it is used to grow the mushroom mycelia in a solid substrate during cultivation. The proper duration of spawn run, and suitable substrate usage can be challenging, despite the simplicity in large-scale *Pleurotus* cultivation. Sawdust, hardwood, straw-based substrate, and broadleaf with added supplements are usually used in commercial cultivation. These substrates are pre-treated in a sterile environment to eradicate any contaminants (Bernardi et al., 2013). Using pretreated conifer wood chips as substrate, *Pleurotus* species will colonize and produce fruiting bodies but if non-pretreated wood chips were used, inhibition of mycelia colonization will occur due to inhibitory components (Croan, 2004).

Generally, for cultivation of *Pleurotus* species in a farm or mushroom house, the temperature will be used are between 25°C to 30°C. The duration of spawn run to primordial initiation was usually between 24-30 days. The duration of

spawn run and temperature requirement for fruiting also varies based on the species that is cultivated. The presence of light is not a requirement during the spawn running and spawning is performed in a cleaned area of a large chamber.

There are different standards of spawn preparation based on the different species. For example, one kg of grains was washed thoroughly using tap water and subsequently boiled in 1.5 liters of water for 30 mins until the grain became soft and were soaked for 12 hours or overnight. These grains were then spread out on a sterile surface to drain the excess water. After the excess water was drained, 15g of calcium carbonate was added to the grains to prevent it from clumping. Two hundred grams of grains were weighed and put into polypropylene bags with cottons plugs and were sterilized at 121 °C for 20 mins. After cooling the bags at room temperature, mycelium from a *Pleurotus* agar culture was placed onto the sterile grain through the opening of the cotton plugs and incubated for mycelium propagation (Hsu et al., 2018).

Alternatively, sawdust can be a suitable replacement for grains with both the substrates using rice and wheat bran as supplements. More recently, liquid spawn, stick and stalk spawn are being utilized for cultivation (Zhang et al., 2019). Liquid spawn is usually 2% (2g of mycelial in 100g of web substrate). Various types of production methods were used for *Pleurotus* cultivation such as jars, bags, trays, shelf, grid-frame, and wall-frame. Shelf cultivation, bags and bottles are the most practiced methods of cultivation. The shelf cultivation method is high production and low cost. As for the bag cultivation method, spawns are placed in rows horizontally and at the top of the chamber. Plastic bottle cultivation is more efficient within a small space while providing high yield (Zmitrovich & Wasser, 2016).

Spawn bottles and bags were arranged vertically during spawn running and the incubation temperature was set to 25°C and 90% relative humidity. The optimum temperature for growth for *Pleurotus tuber-regium* was 30-35°C (Manandhar, 2004), although the optimum temperature for *Pleurotus* spp were generally between 21-25°C.

*Pleurotus* spawn run usually lasts for 12- 26 days at 23-25 °C. The longest maximum spawn run duration of *P. pulmonarius* was 25 days (Akinmusire et al., 2011). The spawns were allowed to colonize the whole bottles or bags until they became fully white and then transferred to the cultivation room. The room was maintained at 15-23 °C with relative humidity of 85-95% with the photoperiod of 12 hours per day of light intensity at 150-350 lux for commercial cultivation (Kibar & Peksen, 2008). To improve the production of oyster mushroom, supplementation of substrate with extra sources of nitrogen is recommended. For its initial substrate colonization, *Pleurotus* mushroom has a low nitrogen requirement (Naraian et al., 2009). *P. tuber-regium* produces sclerotium beneath the soil and it's considered a tuberous mushroom (Bamigboye et al., 2019). The cultivation requirements for *P. tuber-regium* are different from the others *Pleurotus* species, for example it requires casing to produce high yield fruiting bodies. The sclerotium and fruiting bodies of *P. tuber-regium* are a cheap protein source and highly nutritional (Ijeh et al., 2009). Various bagging cultivation systems have been tested (Mandeel et al., 2005). For instance, by utilizing plastic bags it resulted in higher yield as compared to methods such as racks, cylindrical bags, and trays (Jegadeesh et al., 2018). By hanging these plastics bags in rows, the contamination level was reduced while allowing for good air flow around the bags.

## **2.5 Biological efficiency and initiation of primordial**

Generally, the primordial initiation occurs around 16 to 27 days after spawn running (Owaid et al., 2015). Mature fruiting bodies can be observed within 3-4 days after formation of the pinhead. The mature fruiting body will be harvested, and the bed surfaces will be scraped to 1-2cm deep in preparation for the second harvest. A similar procedure will also be performed for the third harvest. The entire cropping cycle are usually completed within 50-55 days (Jegadeesh et al., 2018).

The biological efficiency of a specific species varies in relation to the substrate used. For example, the biological efficiency of was significantly higher when it

is grown in composted sawdust with bran mixture as opposed to fresh sawdust substrate for *Pleurotus* species (Ho et al., 2020) . As for the king oyster, *P. eryngii*, the soybean substrate supplemented with sawdust or cottonseed hull produced significantly higher fruiting bodies yield (Estrada & Royse, 2007). A study on *P. ostreatus* using eight different alternate substrates has shown that rice straw performed the best, producing about 50% of the biological efficiency (Obodai et al., 2003).

## **2.6 Postharvest and processing of *Pleurotus***

The browning of *Pleurotus* species during postharvest is contributed by the phenolic compound oxidation (Xiao et al., 2011). The naturally high moisture content of fresh mushroom increases its risk of microbial contamination. As such, they are easily perishable and unsuitable for long distance transportation or prolonged storage. Only proper processing method can preserve and increase the fresh mushroom shelf life.

The tried-and-true method of drying in preservation of food has been utilized for years to improve shelf life (Özünlü & Ergezer, 2021). The process of drying ensures that the water activity of a specific food is minimized to ensure physiochemical stabilization and reduction of microbial activities. The microwave hot-air flow rolling dry-blanching (MARDB) pretreatment method has been tested in *P. eryngii*. By using the optimal pretreatment parameters, the MARDB method has significantly enhanced the quality of *P. eryngii* in aspect of water, polysaccharide content, colour, while reduced the drying time and completely deactivated the enzyme that contributed to browning such as polyphenol oxidase and peroxidase (Su et al., 2020).

Another common method for postharvest processing of edible mushrooms is the low-temperature storage. The reported shelf life of freshly harvested *P. ostreatus* which were treated with low-temperature ranges from 8 to 11 days at 0°C (Choi & Kim, 2002). Li et al., (2021) performed low-temperature storage on *Pleurotus tuoliensis* at 4°C for 12 days and discovered that this temperature

helped to maintain high phenolic content, nutritional quality, enzymatic activity, and low membrane lipid peroxidation as compared to 25°C for 6 days.

Modified atmosphere packaging (MAP) is an effective and economical postharvest processing method that is usually complemented with low-storage temperature control method (Oliveira-Bouzas et al., 2021). MAP uses a mixture of gas in varying proportions such as carbon dioxide, nitrogen, ethylene, and oxygen while controlling air pressure, humidity, and temperature in the gas conditioning warehouse. This serves the purpose of reducing the metabolic rate and inhibiting the cellular respiration for the mushroom to maintain dormancy which helps in achieving long term preservation (Loredana et al., 2023). A study on *P. sapidus* treated with varying mixtures of gas demonstrated that a increased carbon dioxide packaging (HCP) (20% CO<sub>2</sub>/ 15% O<sub>2</sub>) maintained its total phenolic content while retaining its colour and odor as compared to low carbon dioxide packaging (2% CO<sub>2</sub> / 30% O<sub>2</sub>) (Wan-Mohtar et al., 2019).

## **2.7 Taxonomy and diversity of *Pleurotus* spp**

The morphology of *Pleurotus* species is inconsistent, depending on the climate condition and types of substrates used during cultivation (Won-sik, 2004). As such the phylogenetic and taxonomical identification can be difficult which leads to misidentification. Not only that, geographic separation of the same species also has differences in the isolates genetically (Stajic et al., 2005). Various molecular techniques have been performed to elucidate the taxonomical hierarchy and phylogenetic relationship of *Pleurotus* species (Barh et al., 2019). Molecular approach like random amplified polymorphic DNA (RAPD), internal transcribe spacer region (ITS), and restriction fragment length polymorphism (RFLP) has been commonly used to identify *Pleurotus* species (Adeniyi et al., 2018; Gupta et al., 2011; J. Li et al., 2017; Urbanelli et al., 2007). The molecular identification of *Pleurotus* species is relevant as it serves as a

requirement for commercial mushroom production and breeding programs (Raman et al., 2021).

## **2.8 Species identification of *Pleurotus* mushrooms**

Species identities are very important as this could help farmers in selecting the species of interest for cultivation and selective breeding. Furthermore, most regulators worldwide consider species identity as a crucial requirement for goods manufacturing practice, to avoid mislabeling of commodities (Raja et al., 2017). However, identification of *Pleurotus* mushrooms has been severely restricted due to multiple reasons. Cultivated *Pleurotus* mushrooms have principally been identified through their morphological traits such as colour, length, thickness, shape, maturation duration and yield (Zervakis et al., 1994). However, this method of species identification can often be unreliable due to environmental conditions affecting most morphological traits, leading to misidentification, and resulting in wrong taxonomic conclusion (Ravash et al., 2010). Other than the fruiting bodies of *Pleurotus*, identification is also challenging during the mycelia growth stage as the mycelia characteristic between species are similar. It is also vital to identify the species at the mycelia stage, as the mushroom growers can get an informed knowledge to decide on which species to cultivate instead. Different species of *Pleurotus* will have varying growth conditions, hence the mushroom growers can accommodate the specific conditions for optimal growth of the specific species.

Consequently, DNA based identification has been established to differentiate species of fungi. Fungal species classifications using DNA barcode is a successful, effective, and reliable tool and can be utilized at any stage of mushroom life cycle. Molecular techniques such as Amplified Fragment Length Polymorphism (Urbanelli et al., 2007) and the small subunit rRNA have been used to identify the mushroom species (Gonzalez & Labarère, 2000).

The requirement for an ideal DNA barcode is having a short sequence of the candidate marker and high success rate of both amplification & sequencing (Wang et al., 2019). Not only that, a high inter-specific variation and low intra-

specific variation is also required in which this will create a “barcoding gap” (Figure 2.10) with a discrete distribution and no overlaps (Hebert et al., 2003; Lahaye et al., 2008).

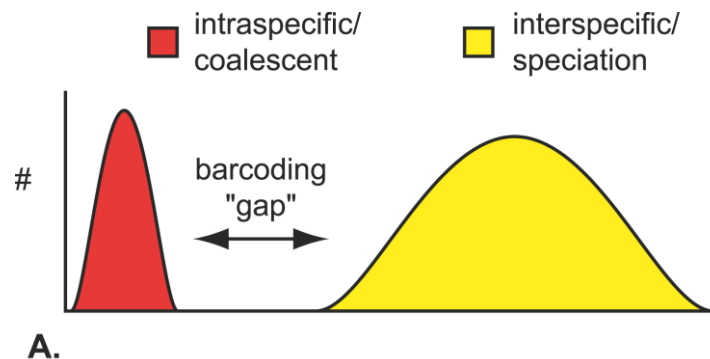


Figure 2.10 Schematic of the Inferred Barcoding Gap. Retrieved from <https://doi.org/10.1371/journal.pbio.0030422.g002>

### 2.8.1 Internal transcribed spacer

The internal transcribed spacer region (ITS) is an area of spacer DNA placed in between a small subunit of ribosomal RNA and the large subunit of rRNA. ITS region has the highest probability of successful identification for a wider span of fungi species (Schoch et al., 2012). Even though a certain report claims that ITS is not as powerful a tool to differentiate many fungal species that are closely related (Kiss, 2012), it is still one of the most widely used DNA marker due to its higher PCR amplification success rate. The main DNA barcode for fungi is the ribosomal internal transcribed spacer (ITS), a highly variable region between the conserved sequence of the small subunit, 5.8S, and large subunit of ribosomal RNA which was developed by (Schoch et al., 2012). However, the ITS region is still imperfect as this DNA barcode frequently failed to differentiate closely related fungal species (Schoch & Seifert, 2012).

### 2.8.2 Intergenic spacer

Other than ITS, another noncoding region namely intergenic spacer (IGS) is also found in a few studies for species identification in fungi. IGS are highly variable

DNA units which are found in between conserved sequences of 25S, 5S and 18S in the rRNA gene (Babasaki et al., 2007). IGS1 region is normally shorter than IGS2 and can be used easily for distinguishing species identity (Saito et al., 2002). Both ITS and IGS are vital molecular markers for intraspecies comparison within the same fungal genus and genetic polymorphism and analysis of interspecies mutation (Bunyard et al., 1996).

### 2.8.3 Largest subunit RNA polymerase II

The second largest subunit of RNA polymerase II (*rpb2*) is a single copy gene and an enzyme that transcribes the pre-messenger RNA (Matheny et al., 2006). The *rpb2* gene contains 12 conserved domains across kingdoms that are used to design primers for PCR (Liu et al., 1999). Protein-coding gene regions such as *rpb2* often have an increased chance of accurate identification as compared with ribosomal marker. The downside of protein-coding region is their low PCR amplification rate and low sequencing success (Schoch et al., 2012). Studies on fungi belonging to *Cortinarius* and *Inocybe* using *rpb2* gene in combination with other gene markers for phylogenetic analysis have been done (Frøslev et al., 2005). *Rpb2* has also been used in phylogenetic studies in *Pleurotus eryngii* species complex, such as in combination with the translation elongation factor (EFA1) and ITS (Zhao et al., 2016)

### 2.8.4 Combination of multiple gene marker

It's doubtful that a single gene marker would be capable of identifying every sample to the species level, given how the fungal kingdom's age and genetic diversity. Not to mention that all primers set have a range of biases, which leads to the uses of more than one primer combination as an appropriate solution (Bellemain et al., 2010). All marker groups success chance in differentiation closely related species are relatively equal at approximately 70% and by utilizing more marker for each study, it would increase the average delimitation success (Dupuis et al., 2012). Combination of ITS and IGS sequence are recommended for phylogenetic analysis of *Pleurotus* as both



these DNA presented enough variation between species, have distinct sequence, provided simple amplification, and are located between ideal conserved ribosomal gene (Avin et al., 2014). To overcome the issues of certain markers as mentioned on the ITS and rpb2 section, combination of ITS, IGS1 and rpb2 for the phylogenetic analysis of *Pleurotus* genus will be evaluated.

#### 2.8.5 Phylogenetic analysis

Phylogenetics is the study of evolutionary history and relationships of organisms (Kakon et al., 2012). In molecular phylogenetic analysis, the sequence of a common gene or protein can be used to determine the evolutionary relationship among organisms.

Phylogenetic analysis aids in clarifying the taxonomical status of many *Pleurotus* species and determine the names of the mushrooms accurately in scientific literature (Bao et al., 2004). Baillingu, an oyster mushroom widely cultivated in China, has its status elevated to an independent species from the use of phylogenetic analysis (Zhao et al., 2016).

### 2.8.6 Antioxidant, reactive oxygen species and antioxidant capacity of *Pleurotus* mushroom

A biological antioxidant prevents the oxidation of significant biomolecules such as DNA, protein, and fatty acids. Oxidation processes are caused by a reactive oxygen species (ROS) (Halliwell & Gutteridge, 2007). ROS is a type of reduced form of oxygen. As such, excessive amount of ROS or deficiency of antioxidant can be damaging to biological functions and structures which is known as oxidative stress (Beckman & Ames, 1998).

Certain ROS species have an unpaired electron particle in orbital which are known as free radical. Some ROS that are considered non-radical such as singlet oxygen and hydrogen peroxide, however their reactivity is still greater than normal ground-state oxygen molecules, making them able to oxidize important biomolecules on interaction. Various ROS possess important physiological functions such as hydrochlorous acid in immune defense, nitric oxide, which is a vasodilator and hydrogen peroxide plays important role in intracellular signaling molecule (Wink et al., 2011).

The most popular antioxidant is ascorbic acid (commonly known as Vitamin C). In fact, there are thousands of distinct antioxidants in plants and fungi such as Vitamin E, a group of tocotrienols and tocopherols and large families of carotenoids and flavonoids (Tam et al., 2005). These antioxidants work in various mechanisms such as prevention of ROS generation, enzymes that destroy ROS, reducing agents that “negate” free radical by electron or hydrogen donation, while some absorb excess energy from ROS (Halliwell & Gutteridge, 2007).

The exposure of continuous ROS on the human body has let us evolve an effective antioxidant defense system to manage the threat of oxidation (Benzie, 2003). However, even with our innate antioxidant defense, it is not fully adequate and requires dietary input of antioxidants (Norat et al., 2014). The main source of antioxidants in human diet are plant-based foods and beverages such as vegetables, fruits, coffee, and tea (Benzie & Wachtel-Galor,

2012). Mushrooms have become more attractive as functional food due to their antioxidant properties and nutritional value which contain high proteins and low-fat content (Reis et al., 2012). Bioactive compounds such as phenolics, polysaccharides, ascorbic acid and tocopherols which contribute to antioxidant activities are found in various parts such as fruiting bodies, mycelium and culture in different mushrooms species. Proteoglycan extracted from *P. ostreatus* have been found to exhibit antioxidant activities (Xia et al., 2011) while ergothionine, an excellent antioxidant has been found in both fruiting bodies and mycelia of multiple *Pleurotus* species (Chen et al., 2012). Notably, edible mushrooms do not contain flavonoids, one of the secondary metabolites related to plants that possess antioxidant capabilities. This is because mushroom does not have the main enzyme in its metabolic pathway to synthesize flavonoids (Gil-Ramírez et al., 2016).

The significance of antioxidant in food cannot be understated, hence multiple techniques have been developed to determine the total antioxidant content in food using the basic principles of measuring the reductive action of redox-active antioxidants as they reduce a specific component. The antioxidant activity can be determined using various spectrophotometric techniques such as Folin-Ciocalteu method (Ainsworth & Gillespie, 2007), ferric reducing antioxidant power (FRAP) (Benzie & Strain, 1996) and 2,2-diphenyl-1-picrylhydrazyl (DPPH) assay (Blois, 1958). Depending on assay methods, the activity of antioxidant varies, thus it is recommended to employ multiple different methods for the determination of antioxidant activity (Schlesier et al., 2002).

#### 2.8.6.1 2,2- Diphenyl-1-picrylhydrazyl (DPPH) radical scavenging capacity assay

Goldschmidt & Renn, (1922) discovered the DPPH radical. Blois, (1958) would eventually develop it as an antioxidant determinant in 1958. The DPPH radical has a deep purple colour due to the unpaired electron absorbing at 517nm (Gupta, 2015). During assay, another electron or hydrogen atom donated by an antioxidant to the radical will transform DPPH into its reduced form. This reaction would result in decolourization of deep purple into pale The

decolourization over multiple different concentrations of the same sample helps as an indicator of the sample antioxidant efficiency and can be reported as EC50 value. The EC50 value is defined as the concentration of antioxidants needed to decrease the starting DPPH concentration by 50% (Zhong & Shahidi, 2015).

#### 2.8.6.2 Ferric Ion Reducing Antioxidant Power (FRAP)

Developed by Benzie & Strain (1996), the Ferric Ion Reducing Antioxidant Power (FRAP) or originally known as ferric reducing ability of plasma, relies on the reduction of complex ferric–tripyridyltriazine ( $\text{Fe}^{3+}\text{TPTZ}$ ) under acidic conditions (pH 3.6) The final product is the ferrous complex [ $\text{Fe}^{2+}\text{TPTZ}$ ] which has an intense blue colour which reads at absorbance of 593nm. FRAP assay results are usually expressed as equivalent of Trolox, gallic acid, ascorbic acid, or quercetin (Zengin et al., 2015).

#### 2.8.6.3 Folin-Ciocalteu Assay for Total Phenolic Content

The most-established way to quantify phenolic content of a food or plant samples is the Folin-Ciocalteu assay. This assay is a colourimetry method based on single electron transfer reactions of the Folin-Ciocalteu reagent and the innate phenolic compounds in the samples (Sánchez-Rangel et al., 2013). The electron reduction capacity of a phenolic radical is less than an oxygen radical, making phenolic compound a good oxygen radical scavenger. The Folin-Ciocalteu assay is rapid, reproducible, easy to perform and can test multiple samples at a time. Not only that, but there is also a direct correlation between antioxidant activity and phenolic content (Bastola et al., 2017). Folin-Ciocalteu (FC) reagent is widely commercially available and comes in a strong yellow colour. The reaction of phenolic compound and FC reagent occurs under alkaline condition which is aided by the addition of sodium carbonate. The phenolic proton dissociates under alkaline (pH 10) to form phenolate ion that will reduce the FC reagent from strong yellow into blue colour The final

absorbance reading will be taken at 765nm using a spectrophotometer and gallic acid is the most used standard for this assay (Aktumsek et al., 2011).

### 2.8.7 Nutritional value of *Pleurotus*

*Pleurotus* flavour and aromas characteristics depend on the composition of amino acids, lactones, terpenes, and carbohydrates (Smiderle et al., 2012). The highly popular *P. ostreatus* is normally used stirred fried recipe and in preparation of soups. *P. eryngii* is ideal for vegetarian dishes and being prepared and served in multiple ways such as boiled, stewed, braised, or grilled (Reis et al., 2012). Proteins found in mushrooms contain all the essential amino acids which are necessary for human diet, which are suitable as meat substitute as well (Kakon et al., 2012). Not only that, due to *Pleurotus* cell wall constitute mainly of chitin, it's a great source of dietary fiber with considerable number of vitamins including ascorbic acid, thiamine, riboflavin and ergosterine (Maftoun et al., 2015).

*Pleurotus* spp fresh fruiting bodies usually have 85-90% of moisture content (Khan & Tania ,2012). The moisture content of a mushroom also varies depending on the species, growth, harvest, and storage conditions (Reis et al., 2012). The nutritional composition of major species of *Pleurotus* for carbohydrates ranges from 85 – 88%, protein contents ranges from 0.9 – 2%, lipid contents ranges from 0.8-9.6 %, fibers content ranges from 2-3 % and ash content ranges from 1 -2 % (Atri et al., 2013). However, a review of *Pleurotus* from Khan & Tania (2012) has found a more varied results of the nutritional value in which the carbohydrates values from 36 – 60%, lipids content from 0.2% to 8 % and proteins from 11 to 42%.

### 2.8.8 Proximate analysis

*Pleurotus* mushroom as food product requires nutritional analysis as part of the nutritional labelling, development of food product, quality management, and/or research program to measure its composition and to ensure the safety

and quality (Nielsen, 2017). The proximate composition is moisture, lipid, ash, and protein which are the contents of food macro components.

The moisture in food is vital as it can influence food quality, cost of shipping and consistency in expressing other analytical results on dry weight basis (Pomeranz et al., 1994). The most common method for moisture analysis is forced draft oven drying. The water evaporates from the sample by heating the sample in an oven usually at 100°C, with the calculated weight loss equal to the moisture content. While forced draft oven is simple for large samples number and official method for moisture analysis of food, it is often time consuming which can take up to 24 hours. A swifter method, namely the rapid moisture analyzer technology (Figure 2.15), is currently being used by the food industry. This technology utilizes two different heating elements which are ceramic and halogen heaters. While being rapid, it is also sensitive which can detect moisture levels of 50 ppm up to 100% of the sample weights of 150mg to 55g. Placing the food sample on a filter paper or aluminum pan with the heating controls increase up to 200°C, helps to raise the food sample to a constant temperature. With the moisture evaporation, the analyzer automatically weighs and calculates the percentage of solid.

Ash, the second macro component of proximate analysis is the total mineral content in a food product. Ash content is the inorganic residue formed from the process of either ignition or full oxidation by an organic matter of a food. The few common methods of ash content determination are by dry or wet techniques (Nielsen, 1998). Firstly, the dry ashing method requires the food sample to be placed in a crucible and heated in a muffle furnace at 500 -600°C. The high temperature burns all the organic materials, only the inorganic materials remain to be quantified. This procedure is easy and has high throughput, however it is time-consuming, taking up to 18 hours for full incineration. Secondly, the wet ashing method uses acids and/or oxidizing agent to oxidize the organic matter of a food sample. By using the wet liquid process, high temperature is not necessary. This method is suitable for analysis

of specific minerals, as there is minimum or no loss from volatilization. The disadvantages of wet ashing are it requires constant attention from the operator, a small number of samples can be processed at a time and a fume hood is required as the reagents are usually corrosive.

Lipids in food are a variety of soluble compounds in organic solvents while only rarely soluble in water. Lipid analysis commonly uses solvent extraction methods. The Soxhlet method developed by Franz Ritter von Soxhlet in 1879 (Zygler et al., 2012), a semicontinuous technique utilizes a solvent such as petroleum ether which are boiled in a round bottom flask.

The other food macro component in proximate analysis is protein content. Protein content analysis is vital for assessment of nutritional value, nutritional labelling and for isolation and purification purposes. The most popular method of protein analysis based on nitrogen content is the Kjeldahl method. This method utilizes sulfuric acid supplement with catalyst to extract nitrogen contents from the food samples. The nitrogen is converted to ammonium sulfate and neutralized with alkali and finally distilled with boric acid solution. The boric anions formed from the distillation are then titrated with a standardized acid until a specific pH or a colour is obtained. The nitrogen content of the sample is based on the volume of standardized acid used in titration. Kjeldahl method has been as official methods for crude protein content determination for years (Abrams et al., 2014).

#### 2.8.9 High throughput transcriptomics sequencing

The total RNA in a living organism is defined as whole transcriptome (Pereira et al., 2017). To aid in the study of massive gene expression profiling, high throughput sequencing technology such as RNA-sequencing analysis is available in the modern day. Due to its high accuracy, sensitivity, and reproducibility, RNA-seq is very popular as a tool for whole transcriptome studies as compared to microarray. RNA-seq works by the sequencing of complementary DNA which were reverse transcribed originally from RNA of the organisms of interest. Once the sequencing is complete, it can be used to

quantify the level of gene expression (Wang et al., 2009). The RNA-Seq technology is flexible as it can be used with or without a reference genome in which the case of without a reference genome, a de novo assembly must be conducted prior. Not only that, RNA-seq sensitivity is an advantage in terms of detection of novel genes and splice variants (Conesa et al., 2016). RNA-Seq workflow includes cost estimating, samples preparation, cDNA library construction, the whole sequencing and lastly data analysis (Kukurba & Montgomery, 2015). There are multiple options to be considered before initiating an RNA-seq workflow including the selection of sequencing platform such as Illumina or Ion Torrent, the number of replicates involves, the sequencing depth and coverage, the read length and the library preparation methods (Conesa et al., 2016)

#### 2.8.10 Reverse transcription quantitative real time polymerase chain reactions (RT-qPCR)

Reverse transcription real time quantitative polymerase chain reaction (RT-qPCR) is commonly used as a validation tool for the results generated by RNA-Seq. By using RT-qPCR, the relative gene expression of a gene of interest can be quantified and compared against the log<sub>2</sub>fold change of the RNA-seq results. To perform RT-qPCR, total RNA from the organisms of interest is extracted and used as the template to convert into cDNA using an enzyme called reverse transcriptase. Once the cDNA is ready, it is used as a template for qPCR in which amplification of the cDNA is measured in real time and the endpoint of the amplification is identified (Bustin, 2000). The endpoint is identified by the threshold cycle value which the fluorescent signal crosses a set threshold.

The RT-qPCR studies performed in this research project will follow the Minimum Information for Publication of Quantitative Real Time PCR Experiment (MIQE) guidelines (Bustin et al., 2009).



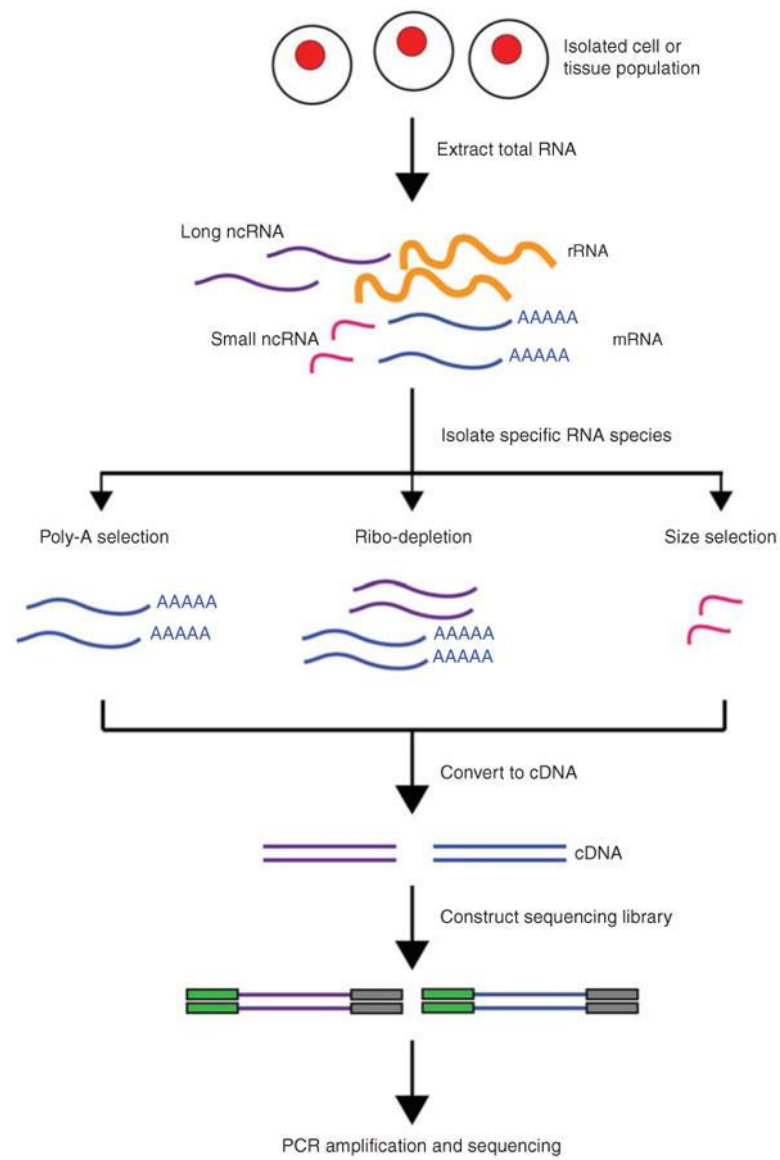


Figure 2.11 Overview of RNA-Seq (Kukurba & Montgomery, 2015)

## **Chapter 3: Molecular identification and phylogenetic studies of Malaysian *Pleurotus* species.**

### **3.1 Introduction**

Defining the species belonging to the *Pleurotus* genus can be challenging because of their similarity in their morphological traits such as colour and the shape of cap, particularly in cases involving species complexes such that exist in *P. eryngii* (Shnyreva & Shnyreva, 2015). The appearance of the fruiting body of oyster fungi can vary greatly when grown under different cultivation conditions (Avin et al., 2014). As a result, the traditional approach of defining edible mushrooms based on their physical characteristics is losing relevance to some degree, while molecular analysis techniques are gaining more popularity.

The internal Transcribed Spacer (ITS) region is the most used genetic marker for identifying mushrooms species and utilized in phylogenetic analysis of fungi (Schoch et al., 2012). It is located between the small and large subunits of the ribosomal RNA gene in the fungal genome. Additionally, the intergenic spacer (IGS1) region from the ribosomal RNA was also utilized in pair with ITS region to elucidate *P. eryngii* species complex across geographic distribution in a phylogenetic analysis (Zervakis et al., 2014). Not only that, the gene encoding second largest subunit of RNA polymerase II (*rpb2*) have been found useful in differentiation among closely related species in the order Agaricales (Frøslev et al., 2005). The *rpb2* gene has also been used in the elucidation of phylogenetic relationship of *P. eryngii* (Estrada et al., 2010). The necessity of using multiple gene markers for the studies of phylogenetics is due to the lack of genetic makeup variation in the ITS region, hence it is not suitable for complete phylogenetic studies within species (Ro et al., 2007).

The main objective of this chapter is to identify the species of 30 unidentified *Pleurotus* samples from MARDI's mushroom bank and determine their phylogenetic relationship. The specific objectives include: -

1. To develop new DNA barcode genetic markers for identification of *Pleurotus* species.
2. To identify the species of cultured *Pleurotus* using a combination of three newly developed genetic markers.
3. To determine the phylogenetic relationship between the identified *Pleurotus* species.

## **3.2 Materials and Methods**

### **3.2.1 *Pleurotus* mycelia culture**

Thirty mycelia culture were provided by MARDI (Sepang, Malaysia) and used in this study. Initial *Pleurotus* inoculum was obtained from an original petri dish stock with a cutout of the inoculum of 8mm x 8mm dimension. The cutout of the inoculum was placed on a fresh potato dextrose agar (PDA) for two weeks at 25°C in the dark. Mycelia were scrapped out gently using sterile spatula and stored in a glass bottle at -20°C freezer until further processing.

### **3.2.2 DNA extraction of *Pleurotus* mycelia**

DNA extractions were performed using Promega Wizard Genomic DNA Extraction kit (Promega, United States) according to the manufacturer's protocol. A total of 40 mg of cryogenically grounded fine powdered *Pleurotus* mycelia was used. The next step involves addition of 600 µl of Nuclei Lysis Solution, vortexing for 3 seconds and incubation at 65 °C for 15 minutes. After incubation, 3 µl of RNase solution was added to the lysate and mixed by inversion 5 times. The mixture was incubated at 37°C for 15 minutes to allow for RNase activity. Before moving forward to the next step, the samples were allowed to cool for 5 minutes at room temperature. Next, a total of 200 µl of Protein Precipitation Solution was added and vortex vigorously at high speed for 20 seconds. After protein precipitation step, the lysate was centrifuged at 16,000 RCF for 3 minutes to pellet the unwanted products through removing the supernatant carefully. Addition of 600 µl of room temperature isopropanol into the supernatant and gently mixing by inversion helps in the formation of thread-like DNA strand. The DNA strands are pelleted by another

centrifugation step at 16,000 RCF for 1 minute. The supernatant was carefully removed and 600 µl 70% ethanol was added to the DNA pellet to wash it by gently inverting the tube multiple times. Centrifugation steps at 16,000 RCF for 1 minute were repeated. The supernatant is once again carefully removed by using pipette while avoiding aspirating the loose DNA pellet. The tube containing the DNA pellet was inverted onto a clean absorbent paper to air-dry for 15 minutes. After air-drying, 100 µl of DNA rehydration solution were added and incubated at 65 °C for 1 hour. During the incubation, the solutions were mixed periodically by gently tapping. DNA concentrations were determined using Epoch Microplate Spectrophotometer (Agilent, United States). DNA solutions were then diluted to 50 ng/µl with sterile water for standardization of protocol and stored at -20°C until further used.

### 3.2.3 PCR amplification ITS, IGS1 and rpb2 genes

BIOTAQ PCR kit (Meridian Bioscience, US) was used to carry out PCR reaction. Reaction mixture (50 µl) contained 5 µl of 10X NH<sub>4</sub> Reaction buffer, 2.0 µl of 50mM MgCl<sub>2</sub> solution, 5.0 µl of 100mM dNTP mix, 1.0 µl of BIOTAQ DNA polymerase (2U), 1.0 µl of 10uM each primer, 3 µl of DNA template (150g) and 33 µl of sterile water. PCR cycling was done in a Biorad T100 Thermal Cycler (Biorad Laboratories, USA). Three primers sets were used to amplify the gene of interest as listed in Table 3.1. These primers were designed using Primer Premier software (Premier Biosoft, US). ITS sequence was designed based on NCBI accession AY450345.1, IGS1 based on AB234031.1 and rpb2 based on JQ513872. PCR cycle conditions for ITS amplifications were 94°C/3min; 30 cycles of 94°C/45sec, 56°C/30sec, 72°C/1min; and final extension step of 72°C/10min. PCR cycle conditions for IGS1 amplifications 94°C/3min; 30 cycles of 94°C/45sec, 64°C/30sec, 72°C/1min; and final extension step of 72°C/10min. PCR cycle conditions for rpb2 amplifications were 94°C/3min; 30 cycles of 94°C/45sec, 54°C/30sec, 72°C/1min; and final extension step of 72°C/10min. PCR products were then visualized and verified using gel electrophoresis in 1% agarose gel stained with 3 µl RedSafe (Intron Biotechnology, US). DNA loading buffer (6X) of 1 µl plus 5 µl PCR product were loaded on the gel and

electrophoresed for 60 min at 80 V. The successful PCR products were then sent to 1<sup>st</sup> BASE (Apical Scientific, Malaysia) for Sanger sequencing.

Table 3.1 List of primers and their respective sequence

Marker	Forward primer (5' to 3')	Reverse primer (5' to 3')	Amplicon size (bp)
ITS	TATGGAGTTGTTGCTGGC	CTTGTTTCGCTATCGGTCT	935
IGS1	CGGTAGAGTAGCCTTGTT G	GTGCTTTCAGAGTCCTATG G	719
rpb2	CAGGTGCTTAATCGCTAC A	AGGAAGTTGGTCAGGAAG A	946

### 3.2.4 Sequence data analysis, BLAST search and phylogenetic analysis

Sequences chromatograms obtained from Sanger sequencing were visualized and edited using Mega version 7.0 software. Sequences alignments were done using MUSCLE algorithm (Edgar, 2004) in MEGA (7.0) and manually trimmed. Aligned and trimmed sequence for a specific sample were then subjected to BLAST enquiry to determine the species. Alignment was performed separately for ITS, IGS1 and rpb2. Data retrieved from GenBank (accession number AY450345.1 (ITS), AB234030.1 (IGS1) and JN126371.1(rpb2)) were included in the alignment as an outgroup. Phylogenetic reconstruction of ITS, IGS1 and rpb2 were performed based on the Maximum Likelihood method (Kumar et al., 2016) in MEGA (7.0). The analysis confidence was assessed by bootstrap test with 1000 replications.

### 3.3 Results

#### 3.3.1 PCR Amplification and Sanger sequencing

In this study, ITS, IGS1 and rpb2 were used as the biomarker for species identification. The species of the samples were confirmed only when all 3 markers portrayed consistent identification. Among the 30 *Pleurotus* mycelia isolates, 16 isolates were identified as *Pleurotus pulmonarius*, 8 isolates were identified as *Pleurotus eryngii* while the identity of 6 samples could not be confirmed due to a few unresolved issues including the presence of mixed trace in the sequencing data and contradicting findings among the 3 markers. Mixed trace refers to the sequencing trace with more than two peaks at the same location which causes ambiguous base calling. The presence of mixed trace impeded the alignment of align forward and reverse sequences, thereby disabling the alignment to the marker sequences. In samples such as MP25, mixed trace was detected only for IGS1 while for other samples such as MP37 and MP29, the issue persisted in all 3 marker sequences. In another scenario, the sequencing data of MP6 was successfully aligned in BLAST but to different species. The contradicting results between ITS/rpb2 and IGS1 rendered the available data unreliable to conclude the species type. Table 3.2 shows the overall data for all the isolates and BLAST results from each marker gene. Appendix 1 – Table 1, Table 2, and Table 3 shows the detailed results for each marker genes for % identity, size of sequence compared and accession number. Figure 3.1 shows the PCR amplicon size of ITS, IGS1 and rpb2 marker gene.

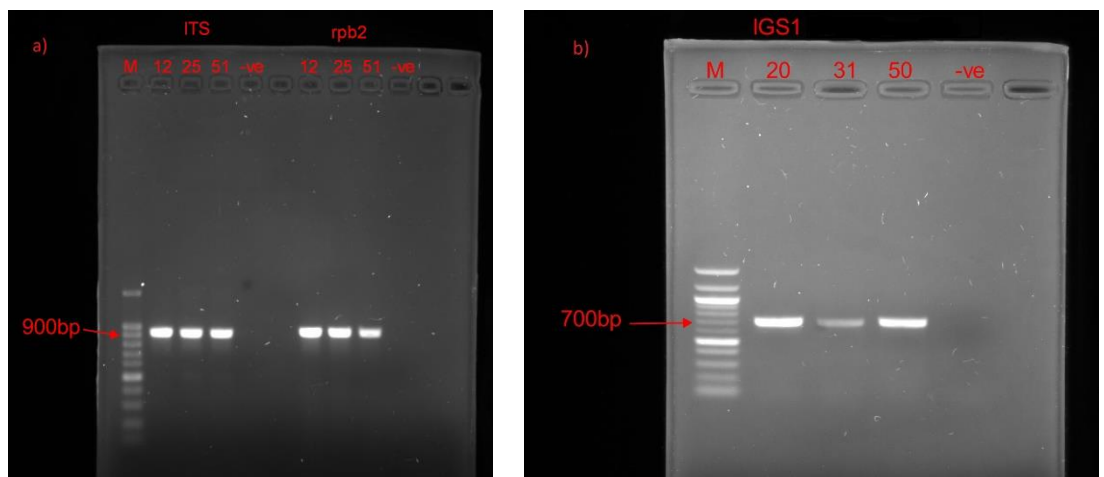


Figure 3.1 Gel electrophoresis image of random samples a) ITS and rpb2 marker gene for MP12, MP25 and MP51 with negative control, b) IGS1 marker gene for MP20, MP31, MP50 with negative control.

Table 3.2 Identification of *Pleurotus* species based on BLAST results from the aligned sequence of each marker gene.

BLAST results				
Number	Sample ID	ITS	IGS1	rpb2
1	MP5	<i>P. eryngii</i>	<i>P. eryngii</i>	<i>P. eryngii</i>
2	MP11	<i>P. eryngii</i>	<i>P. eryngii</i>	<i>P. eryngii</i>
3	MP14	<i>P. eryngii</i>	<i>P. eryngii</i>	<i>P. eryngii</i>
4	MP16	<i>P. eryngii</i>	<i>P. eryngii</i>	<i>P. eryngii</i>
5	MP22	<i>P. eryngii</i>	<i>P. eryngii</i>	<i>P. eryngii</i>
6	MP27	<i>P. eryngii</i>	<i>P. eryngii</i>	<i>P. eryngii</i>
7	MP30	<i>P. eryngii</i>	<i>P. eryngii</i>	<i>P. eryngii</i>
8	MP50	<i>P. eryngii</i>	<i>P. eryngii</i>	<i>P. eryngii</i>
9	MP2	<i>P. pulmonarius</i>	<i>P. pulmonarius</i>	<i>P. pulmonarius</i>
10	MP9	<i>P. pulmonarius</i>	<i>P. pulmonarius</i>	<i>P. pulmonarius</i>
11	MP12	<i>P. pulmonarius</i>	<i>P. pulmonarius</i>	<i>P. pulmonarius</i>
12	MP24	<i>P. pulmonarius</i>	<i>P. pulmonarius</i>	<i>P. pulmonarius</i>
13	MP25	<i>P. pulmonarius</i>	<i>P. pulmonarius</i>	<i>P. pulmonarius</i>
14	MP28	<i>P. pulmonarius</i>	<i>P. pulmonarius</i>	<i>P. pulmonarius</i>



15	MP31	<i>P. pulmonarius</i>	<i>P. pulmonarius</i>	<i>P. pulmonarius</i>
16	MP34	<i>P. pulmonarius</i>	<i>P. pulmonarius</i>	<i>P. pulmonarius</i>
17	MP35	<i>P. pulmonarius</i>	<i>P. pulmonarius</i>	<i>P. pulmonarius</i>
18	MP36	<i>P. pulmonarius</i>	<i>P. pulmonarius</i>	<i>P. pulmonarius</i>
19	MP41	<i>P. pulmonarius</i>	<i>P. pulmonarius</i>	<i>P. pulmonarius</i>
20	MP42	<i>P. pulmonarius</i>	<i>P. pulmonarius</i>	<i>P. pulmonarius</i>
21	MP43	<i>P. pulmonarius</i>	<i>P. pulmonarius</i>	<i>P. pulmonarius</i>
22	MP51	<i>P. pulmonarius</i>	<i>P. pulmonarius</i>	<i>P. pulmonarius</i>
23	MP52	<i>P. pulmonarius</i>	<i>P. pulmonarius</i>	<i>P. pulmonarius</i>
24	MP53	<i>P. pulmonarius</i>	<i>P. pulmonarius</i>	<i>P. pulmonarius</i>
25	MP1	Mixed trace	<i>P. ostreatus</i>	<i>P. ostreatus</i>
26	MP3	<i>P. ostreatus</i>	<i>P. ostreatus</i>	Mixed trace
27	MP6	<i>P. ostreatus</i>	<i>P. pulmonarius</i>	<i>P. ostreatus</i>
28	MP20	<i>P. ostreatus</i>	<i>P. eryngii</i>	Mixed trace
29	MP29	Mixed trace	Mixed trace	Mixed trace
30	MP37	Mixed trace	Mixed trace	Mixed trace

### 3.3.2 Assessment of barcoding gaps and Inter- and intra-specific variations of *Pleurotus*

The three main criteria for a perfect DNA barcode are short sequence, high success rate for amplification and sequencing, and lastly it has high interspecific variation and low intraspecific variation. With these criteria, there will be a discrete distribution with no overlap in the DNA barcode that is known as a barcoding gap (Figure 2.10) (Hebert et al., 2003; Lahaye et al., 2008).

A frequency distribution graph was generated from the pairwise genetic distance in MEGA7 to determine the inter- and intra-specific distance. In all three DNA barcode tested, there is no visible overlap in the frequency distribution (presence of barcoding gap) (Figure 3.2,3.3,3.4). This result shows that three of the DNA barcodes have a distinct gap between the inter- and intra-specific variation, which satisfied the criteria for being ideal. The differences in genetic distance between inter- and intra-specific is the largest in rpb2 region followed by IGS1 and lastly ITS.

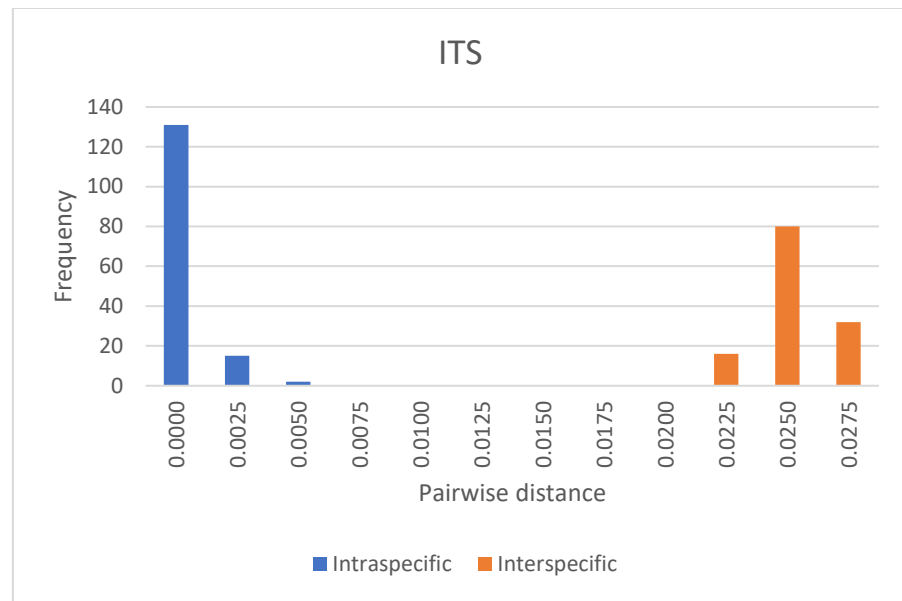


Figure 3.2 Frequency distributions of intra- and inter-specific Kimura-2-Parameter pairwise distances for ITS region

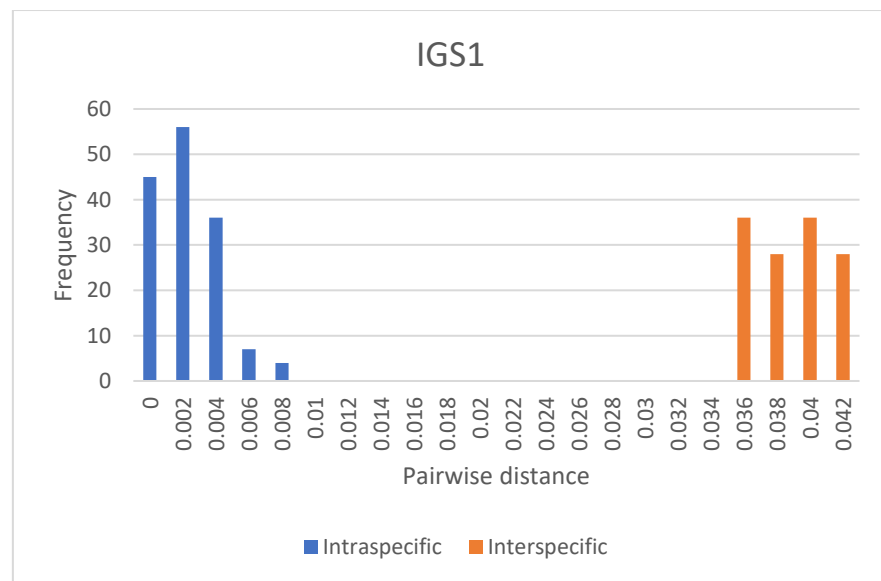


Figure 3.3 Frequency distributions of intra- and inter-specific Kimura-2-Parameter pairwise distances for IGS1 region

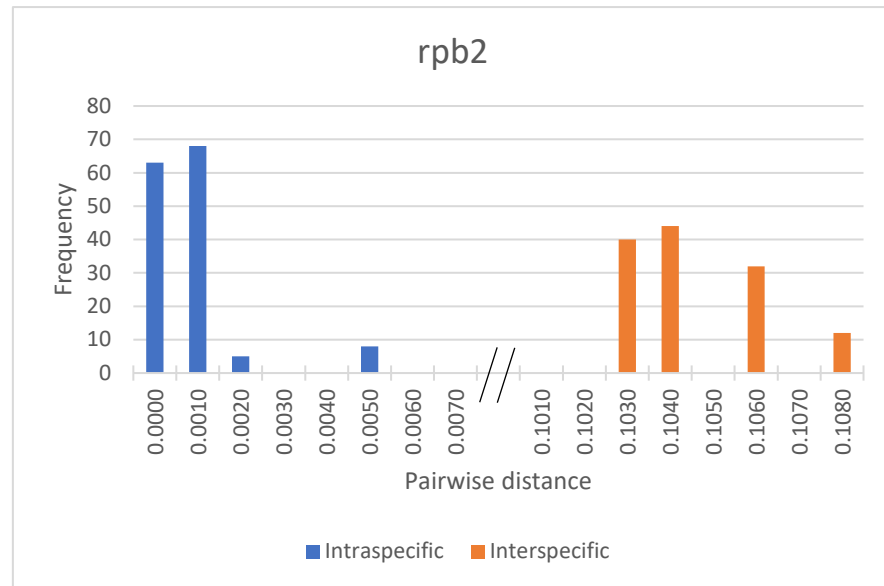


Figure 3.4 Frequency distributions of intra- and inter-specific Kimura-2-Parameter pairwise distances for rpb2 region

The pairwise intra- and interspecific distance in the three DNA barcodes were shown in Table 3.3. The mean interspecific distance of ITS is 6x greater than its mean intraspecific distance. As for IGS1, its mean interspecific distance is 9.2x greater than its mean intraspecific distance. The rpb2 barcode mean interspecific distance is 5x greater than its mean intraspecific distance. All three DNA barcodes have higher mean interspecific distance as compared to their mean intraspecific distances. This shows that all three barcodes satisfy one of the criteria for being an ideal barcode. As rpb2 (0.0709) shows the higher value differences between mean intra- and interspecific variation, it has an excellent potential for species-level identification as compared to ITS (0.0142) and IGS1 (0.0326).

Table 3.3 Genetic distance percentage generated using Kimura 2-parameter model analysis for the candidate DNA barcode.

<b>Barcode</b>	<b>Intraspecific distance (%)</b>			<b>Interspecific distances (%)</b>		
	<b>Min</b>	<b>Max</b>	<b>Mean</b>	<b>Min</b>	<b>Max</b>	<b>Mean</b>
ITS	0.0000	0.0068	0.0028	0.0110	0.0240	0.0170
IGS1	0.0019	0.0057	0.0040	0.0197	0.0468	0.0366
rpb2	0.0007	0.0498	0.0178	0.0514	0.1111	0.0887

### 3.3.3 Phylogenetic analysis of *Pleurotus* spp

The first phylogenetic tree that was constructed was based on the ITS sequence of the 24 samples (Figure 3.5). The resulting tree is divided into three major clades, namely *P. pulmonarius* and *P. eryngii* with *P. ostreatus* isolate 6689 sequences retrieve from NCBI GenBank as an outgroup. All 16 *P. pulmonarius* are located under one clade with no branch, suggesting that all *P. pulmonarius* are of the same variant. *P. eryngii* clade are further subdivided into three branches, suggesting that there is three variants of *P. eryngii* out of the eight isolates. All the branches shown have a bootstrap value of above 70%, meaning these clades has a 95% probability that is reliable (Hillis & Bull, 1993).

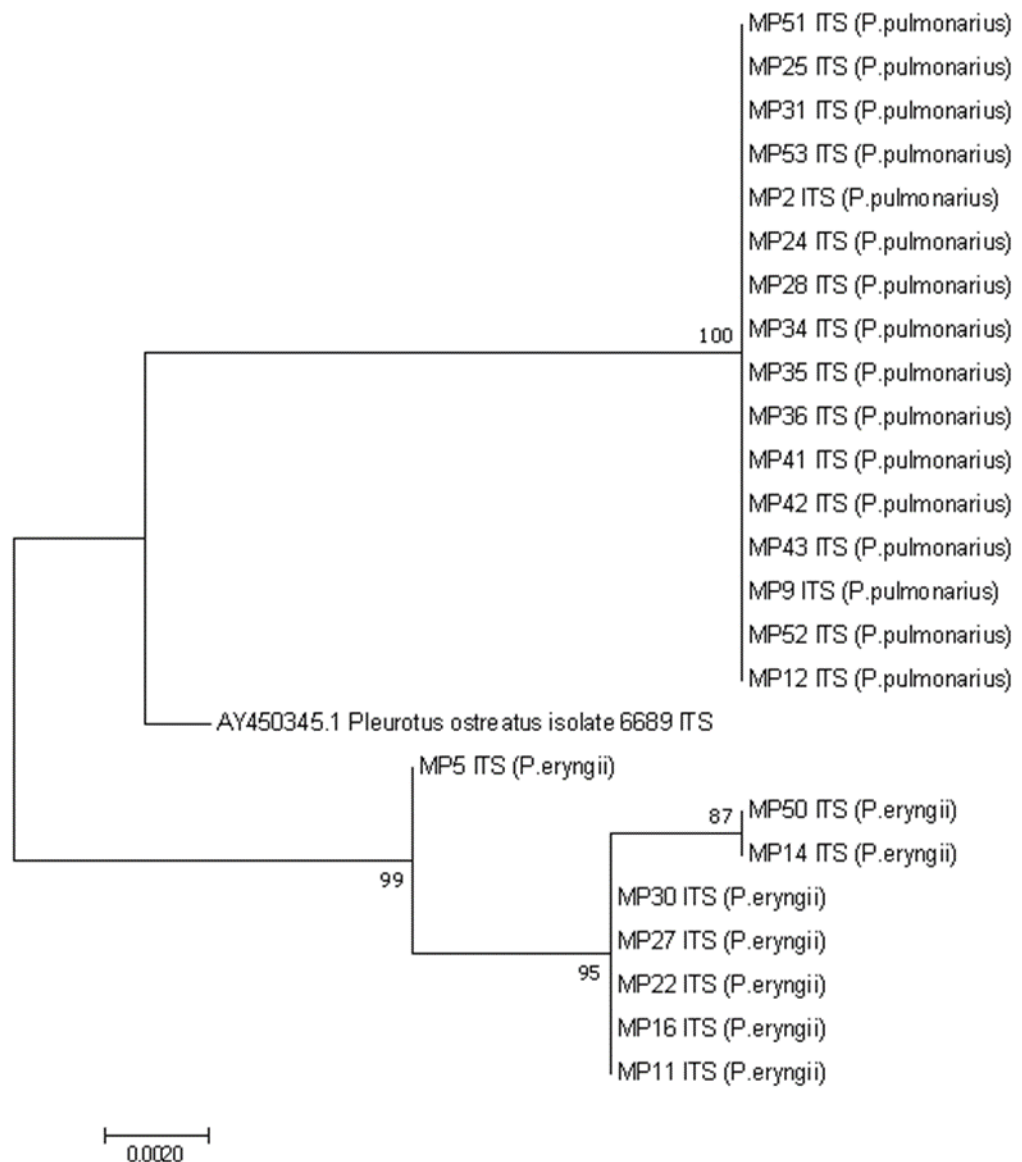


Figure 3.5 Phylogenetic tree of 24 *Pleurotus* sample constructed based on ITS gene sequence and constructed with the Maximum Likelihood algorithm (MEGA 7). Sequence of AB234030.1 (*Pleurotus ostreatus* isolate 6689) were downloaded from NCBI GenBank as outgroup. Numbers of the branches indicate bootstrap value with 1000 replications.

The second phylogenetic tree was constructed based on the IGS1 sequence of 24 samples (Figure 3.6). The *P. pulmonarius* and *P. eryngii* branches into two major groups clades, very similar to phylogenetic tree based on ITS sequence. However, the *P. pulmonarius* group further subdivided into three clades, with the bootstrap values of 21%, 21% and 44% respectively. The bootstrap values were lower than 70%, suggesting that these clades were not reliable and all the *P. pulmonarius* samples were the same variant as the ITS phylogenetic tree. As for *P. eryngii* clade, it was subdivided into three branches, with one low bootstrap value of 67% on the clade with MP16, MP27 and MP30. Like the aforementioned explanation, the clade with lower than 70% is not reliable, hence MP16, MP27 and MP30 should have been grouped with MP5. The *P. eryngii* part of the IGS phylogenetic tree differs from ITS part of phylogenetic tree in terms of number of clades and sample placement within the clades once the bootstrap value was considered. For example, ITS tree has three clades while IGS1 has two clades, and MP14 and MP50 belongs in the same clades in ITS tree while MP14, MP50, MP22 and MP11 were grouped up in the same clade in IGS1 tree.



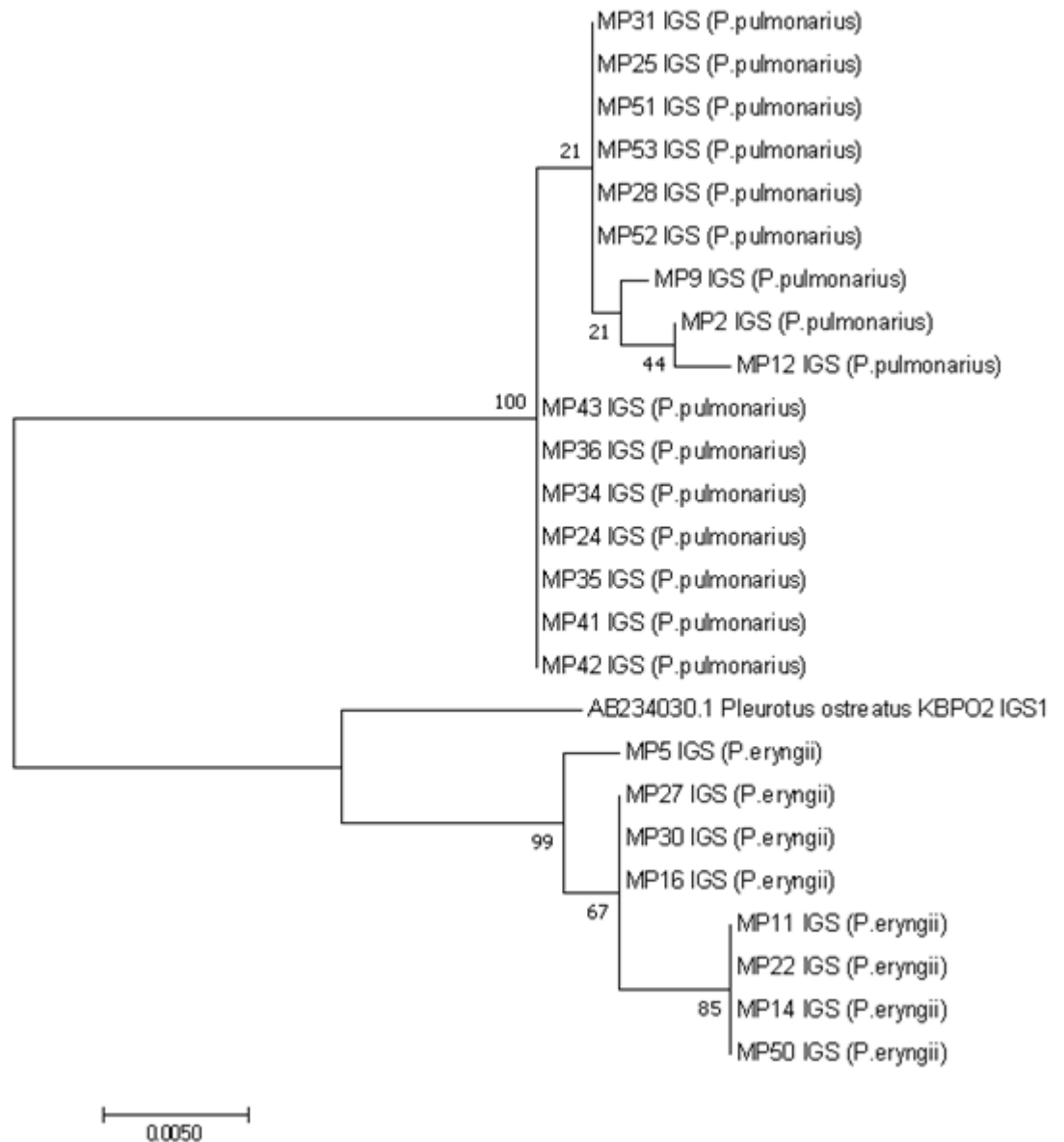


Figure 3.6 Phylogenetic tree of 24 *Pleurotus* sample constructed based on IGS1 gene sequence and constructed with the Maximum Likelihood algorithm (MEGA 7). Sequence of AB234030.1 (*Pleurotus ostreatus* KBPO2) were downloaded from NCBI GenBank as outgroup. Numbers of the branches indicate bootstrap value with 1000 replications.

The third phylogenetic tree constructed was constructed based on rpb2 sequence of 24 *Pleurotus* samples (Figure 3.7). The *P. pulmonarius* clade is subdivided into two branches, with one branch having low bootstrap value of 61%, also suggesting that it is unreliable as explained previously. The *P. eryngii* clade are subdivided into two branches with one branch having 98% bootstrap value, indicating it is reliable. The *P. eryngii* clade in rpb2 tree is similar to the IGS1 tree while different from ITS tree where the *P. eryngii* groups into 3 branches. Overall, all three phylogenetic based on ITS, IGS1 and rpb2 confirms that all 16 *P. pulmonarius* were of the same variant/strain while there is discrepancy between ITS vs IGS1/rpb2 in *P. eryngii*.

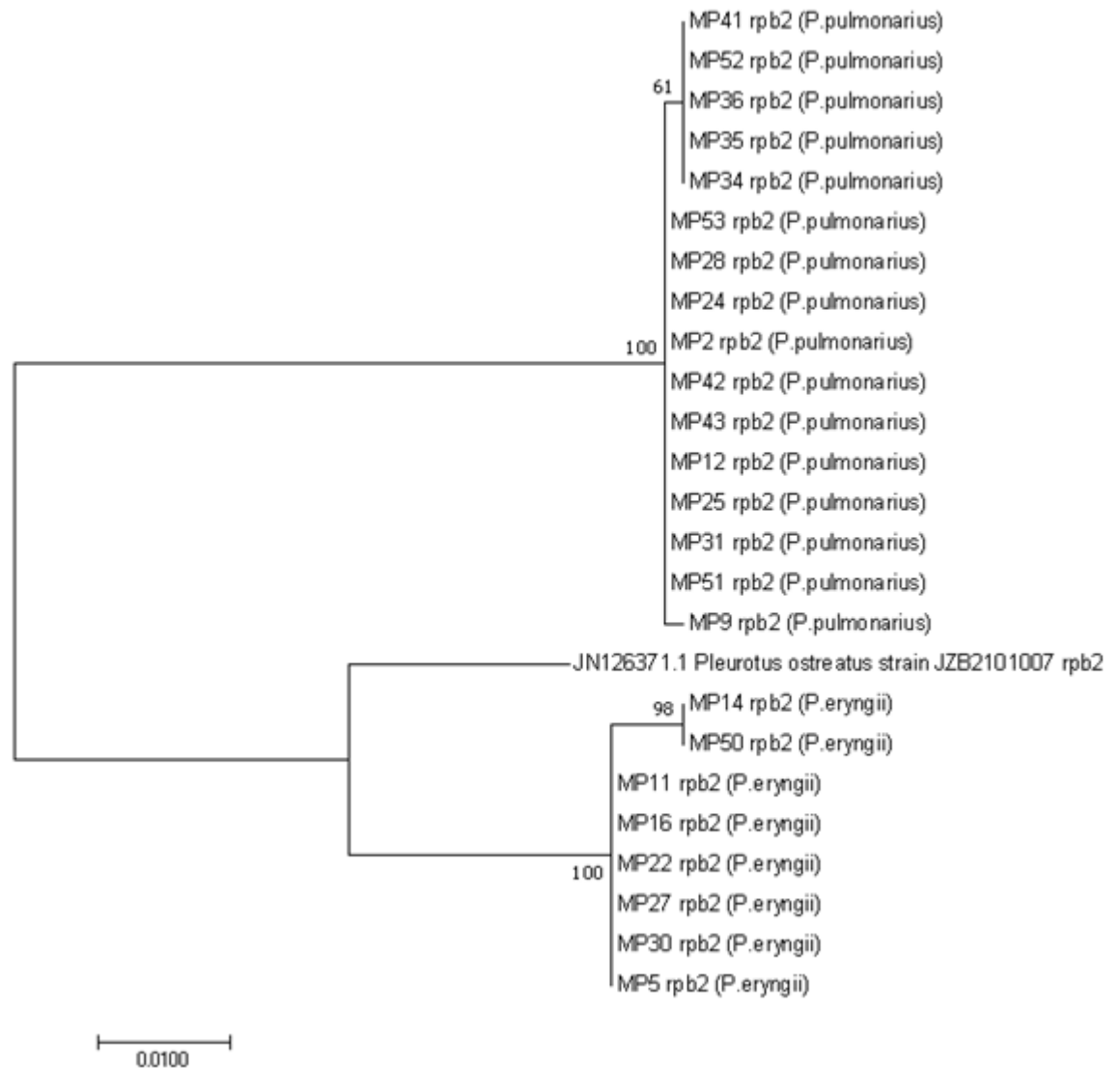


Figure 3.7 Phylogenetic tree of 24 *Pleurotus* sample constructed based on RPB2 gene sequence and constructed with the Maximum Likelihood algorithm (MEGA 7). Sequence of JN126371.1 (*Pleurotus ostreatus* JZB2101007) were downloaded from NCBI GenBank as outgroup. Numbers of the branches indicate bootstrap value with 1000 replications.

### 3.3.4 Comparison of identified isolates with external database from MARDI.

In MARDI, most of the samples were deposited into their mushroom bank collection with minimal information. Although the colour of mushroom cap for most of the samples was also recorded, this did not allow proper identification of the mushroom. Based on the findings from this study, the samples were reclassified into three groups according to the identified species, namely *P. pulmonarius* (Table 3.4), *P. eryngii* (Table 3.5) and others (Table 3.6). All five samples which had been named as *P. sajor-caju* previously were identified as *P. pulmonarius*. Likewise, all three samples which had been named as *P. florida* previously, except for MP6, were identified as *P. eryngii* whereas all five samples identified as *P. eryngii* previously were indeed true according to our findings. Among the six samples that could not be identified, one was previously recorded as *P. florida*, one as *P. nebrodensis* and no identification was available for the remaining four samples.

Table 3.4 List of samples identified as *Pleurotus pulmonarius* compared with the database provided from MARDI.

Sample	MARDI database record	Cap colour
MP2	N/A	N/A
MP9	<i>P. sajor-caju</i>	grey
MP12	N/A	N/A
MP24	N/A	grey
MP25	N/A	N/A
MP28	N/A	N/A
MP31	N/A	N/A

MP34	N/A	grey
MP35	N/A	N/A
MP36	N/A	grey
MP41	<i>P. sajor-caju</i>	grey
MP42	N/A	grey
MP43	N/A	grey
MP51	<i>P. sajor-caju</i>	grey
MP52	<i>P. sajor-caju</i>	grey
MP53	<i>P. sajor-caju</i>	grey
N/A represents missing information for the respective sample.		

Table 3.5 List of samples identified as *Pleurotus eryngii* compared with the database provided from MARDI.

Sample	MARDI database record	Cap colour
MP5	<i>P. eryngii</i>	white
MP11	<i>P. eryngii</i>	N/A
MP14	<i>P. florida</i>	white
MP16	<i>P. florida</i>	white
MP22	<i>P. eryngii</i>	N/A
MP27	<i>P. eryngii</i>	N/A
MP30	<i>P. eryngii</i>	N/A
MP50	<i>P. florida</i>	white
N/A represents missing information for the respective sample.		

Table 3.6 List of samples with ambiguous identity as compared with the database provided from MARDI.

Sample	MARDI database record	Cap colour
MP1	N/A	N/A
MP6	<i>P. florida</i>	white
MP3	N/A	N/A
MP20	<i>P. nebrodensis</i>	N/A
MP29	N/A	white
MP27	N/A	white
N/A represents missing information for the respective sample.		

### 3.4 Discussion

In this study, ITS, IGS1 and rpb2 were used as the biomarker for species identification. The species of the samples were confirmed only when all 3 markers portrayed consistent identification. Among the *Pleurotus* mycelia isolates, 16 isolates were identified as *Pleurotus pulmonarius*, 8 isolates were identified as *Pleurotus eryngii* while the identity of 6 samples could not be confirmed due to a few unresolved issues including the presence of mixed trace in the sequencing data and contradicting findings among the 3 markers. The two major species identified are *P. pulmonarius* and *P. eryngii*. *P. pulmonarius* have very similar morphology characteristic with *P. ostreatus* (Figure 2.2) and *P. populinus* (Figure 2.4), making these species difficult to distinguish. *P. pulmonarius* are usually flat in shape, short stemmed and have light beige to light brown colour depending on the incubation temperature (Figure 2.1)

Commonly known as the king oyster mushroom, *P. eryngii* originated from Europe (Vilgalys & Sun, 1994). Its natural habitat is the dead roots of the weed *Eryngium campestre*. The king oyster mushroom are the only group in the *Pleurotus* genus to be growing in association in living plants. *P. eryngii* belong in a species-complex which are poor parasites on roots and stem of umbellifers (Zervakis et al., 2001). Usually, *P. eryngii* is named together with its specific host plant, eg. *P. eryngii* var *eryngii* and *P. eryngii* var *ferulae*. While *P. eryngii* is distinct in terms of morphology as compared with other species of *Pleurotus*, the morphology of different variant of *P. eryngii* species complex is similar (Urbanelli et al., 2007). *P. eryngii* are large with thick white stem and grey-brown cap (Figure 2.3).

While most of the isolates being successfully sequenced and identified, some isolates such as MP1, MP29 and MP37 produced mixed trace during sequencing. The resulting chromatogram data has a lot of noise in it, rendering the data unreadable, hence the species of the isolate could not be identified.

This occurrence might be due to direct sequencing of diploid alleles that contains heterozygous insertion/deletion (Sousa-Santos et al., 2005). Another reason for mixed trace is existence of microsatellite repeats of A and T base pairs in the sequence. One of the methods to solve the mixed trace issue would be to perform gel purification of the PCR product and sequencing the DNA from individual gel band. However, the downside of this method is it requires more sequencing reactions and less sensitive as some PCR products might not be visible under agarose gel (Tenney et al., 2007).. According to Chapter 2.2, a monokaryon mycelium only contains a single nucleus (n) in each cell while a dikaryon possesses two genetically different nuclei (n+n) in each hyphae (one from each monokaryon). With the two different nuclei, the PCR product will be derived from two different sequences, hence resulting in mixed trace in the chromatogram.

Based on all three constructed phylogenetic trees, all sixteen *P. pulmonarius* should be the same variant. Based on the three clades of *P. eryngii* in ITS and two clades of *P. eryngii* in IGS1 and rpb2 phylogenetic tree, this suggests that the *P. eryngii* in this study have about two to three different variants. *P. eryngii* are known for having several varieties in its species complex such as *var. eryngii*, *var. ferulae* and *var. elaeoselini* (Estrada et al., 2010). The idea of a "species complex" is frequently utilized in the field of mycology to describe species that are closely related and have complete or partial intercompatibility (Bao et al., 2004). Zervakis et al. (2001) state that within the natural environment, *P. eryngii* act as facultative biotrophs, forming associations with certain genera from the Apiaceae (Umbelliferae) and Asteraceae (Compositae) families.

One of the major differences between all three of the trees constructed is that the *P. ostreatus* outgroup is different from ITS tree as compared to the IGS1/rpb2 tree. For the ITS tree, it's shown that the *P. ostreatus* share a common ancestor with *P. pulmonarius* while for IGS1/rpb2 tree, *P. ostreatus* share a common ancestor with *P. eryngii*. The three *P. ostreatus* sequence for outgroup were obtained based on the most similar sequence in BLAST with



their respective gene. Additionally, all these three *P. ostreatus* DNA sequences are from different studies with different strains and origins. Hence, this might cause the discrepancy result between the three trees. The most valuable information that can be added in is all three gene sequence from the same *P. ostreatus*. Logically, as *P. ostreatus* are very similar with *P. pulmonarius* in terms of morphology, the ITS Tree should be the most accurate. However, some studies have concluded that ITS gene marker is more suitable to be used to compare between genus, such as comparing *Lentinus* and *Shitake* with *Pleurotus*, rather than comparing between closely related species such as in this case (Avin et al., 2012). The usage of different combination of gene marker has been used in multiple studies to construct a better resolution phylogenetic tree (Avin et al., 2014; Estrada et al., 2010)

Interestingly, by comparing the data with the external database provided by MARDI, there's a trend observed. In Table 3.4, all the samples that are identified as *P. pulmonarius* are mostly considered as *P. sajor-caju* by MARDI. A study by Li & Yao, (2005), has concluded that *P. sajor-caju* should be renamed to *P. pulmonarius* instead due to morphological and microscopic traits. All the *P. pulmonarius* identified are mostly grey in colour according to the database. As for Table 3.5, 5 out of 8 samples are considered as *P. eryngii* by MARDI, which agree with our findings. However, three remaining samples, MP14, MP16 and MP50 were considered as *P. florida* by MARDI. *P. florida* have very similar sequence with *P. ostreatus* in their mitochondrial sequence (Gonzalez & Labarère, 2000). Based on the three phylogenetic trees in the results section, MP14, MP16 and MP50 are not close to *P. ostreatus* reference sequence and are grouped together in the *P. eryngii* clade. This could probably be misidentification by the MARDI side. However, without morphological data, comparing solely with phylogenetic and sequence data will not be sufficient to confidently conclude the species identity and its relative position in the phylogenetic tree.

The most vital consideration for determining optimal DNA barcodes are a high rate of amplification and sequencing while the barcode needs to have significantly greater mean inter-specific variation than mean intra-specific variation (Wang et al., 2019). This study has shown that the ITS region has achieved all three requirements for an optimal barcode, which are high success rate of amplification and sequencing, and having greater mean inter-specific variation than mean intra-specific variation among the two *Pleurotus* species. IGS1 region has the high success amplification rate and higher differences in mean intra/inter-specific variation than ITS, however all IGS1 PCR products produced multiple bands on agarose gel due to non-specific binding, making IGS1 region less optimal as a DNA barcode. The rpb2 region also has the highest differences in the mean intra/inter-specific variation as compared to ITS and IGS1. The only flaw with the rpb2 region is the presence of non-specific binding after PCR amplification in isolate MP3 which was identified as *P. ostreatus*, suggesting that the rpb2 region may not be suitable to be used for *P. ostreatus* identification.

ITS region has been suggested as the universal barcode for fungi (Schoch et al., 2012). This is because ITS region can be found in several chromosomes and exists in thousands of copies in tandem repeats, which leads to its ease of amplification (Ali et al., 2014). Not only that, several other fungi from the group Agaricales such as the genus *Cortinarius* (Liimatainen et al., 2014) and the family *Lyophyllaceae* (Bellanger et al., 2015) have shown that ITS region is the most suitable DNA barcode due to its clear barcoding gap between interspecific and intraspecific variation. Based on the phylogenetic tree analysis of ITS region in Figure 3.4, all three *Pleurotus* species have high bootstrap support (>88%). The result from this study shows that ITS is a better barcode as compared to IGS1 and rpb2. However, whether ITS is less effective in distinguishing closely related species proves that more studies are required in this subject matter. In conclusion, this study has successfully used a combination of DNA barcodes to identify 24 *Pleurotus* isolates and elucidate its relation through construction of phylogenetic tree. The identification of

*Pleurotus* is vital not only for breeding and economic purposes (He et al., 2017), but also for labelling of samples for subsequent future research.

## **Chapter 4: Antioxidant activities, proximate analysis, and biological efficiency of *Pleurotus* species in Malaysia**

### **4.1 Introduction**

Edible mushrooms are known for its health benefits due to its bioactive properties contributed by the antioxidant and phenolic contents innate to the mushroom. With this, there were numerous research conducted to investigate the antioxidant properties of edible mushrooms including Oyster mushroom. Nutritional analysis is also vital as this helps to commercialise an edible mushroom as a food product (Nielsen, 2017). Prices of edible mushrooms are usually determined by their weight (Jeznabadi et al., 2016). With this in mind, the edible mushroom strain that can produce more fruiting body in a shorter cultivation period is extremely good for the farmers in terms of business standpoint (Girmay et al., 2016)

The main objective of this study is to determine the biological efficiency of *Pleurotus* sample from Chapter 3, evaluation of its antioxidant capacity in terms of fruiting bodies and mycelia and evaluation of its nutritional profile through proximate analysis. The specific objectives were: -

1. To determine the yield and biological efficiency of mature fruiting bodies from 10 selected *Pleurotus pulmonarius* mushroom samples.
2. To assess the antioxidant activities and total phenolic content of the mycelia and mature fruiting bodies from selected *P. pulmonarius*, and *Pleurotus eryngii* samples.
3. To determine the moisture content, lipid content, ash content and protein contents of mature fruiting bodies from selected 10 *P. pulmonarius* samples.

## 4.2 Materials and Methods

### 4.2.1 Sample selection

All samples identified as *P. pulmonarius* from phylogenetic identification (Chapter 3) were cultivated to produce fruiting bodies. However, some samples failed to produce fruiting bodies while some were infected with green mould during cultivation, leaving 10 *P. pulmonarius* samples, namely MP2, MP9, MP12, MP28, MP34, MP35, MP36, MP41, MP42 and MP43 selected for further evaluation. Mycelial sample of all 16 *P. pulmonarius*, 8 *P. eryngii* and 3 unidentified sample were used for antioxidant and phenolic analysis.

### 4.2.2 Spawn and substrate preparation

5000 g of wheat grains were cleaned in tap water and left to soak for 5 hours. Excess water was removed and 100 g of powdered calcium carbonate (2%) were added to avoid the clumping of grains. 200 g of grains were packed into polypropylene bags with PVC caps and were sterilized at 121°C for 1 hour. After cooling the spawn bag, three mycelial plugs (8mm x 8mm) were removed from the stock agar and added to the sterilized wheat grain in the bag. The spawn bags were then left to grow at 25°C, 70% relative humidity in darkness for one week.

The materials used were provided by MARDI, Malaysia. Substrates were prepared using sawdust, rice bran and calcium carbonate at a ratio of 100:10:1. The dry ingredients were then mixed with tap water to obtain a moisture content of 70% (w/w). Moistened substrate (1kg) was added into polypropylene bags with PVC caps and were sterilized at 121°C for 6 hours (Chen et al., 2020). The sterilized substrate bags were cooled overnight before inoculation of spawn.

### 4.2.3 Cultivation

Twelve bags per samples was used in this study. Cultivation time span was 30 days at MARDI's Controlled Environment Mushroom House for 21-28°C in dark for colonization of mycelia (spawn run). After 30 days, the mushroom bag cap

was opened to allow for fruiting induction with the water sprinkler turned on to maintain the relative humidity at 80-90%. Triplicates were selected randomly from the twelve bags per sample for further assessment.

#### 4.2.4 Harvesting and measurement

Three flushes of mushrooms were harvested from each bag. The harvesting time for three flushes of mushroom varies with different samples. The mushrooms were harvested when the cap have fully expanded with pronounce brownish colouration and before the sporulation process. Mushroom yield per bag was determined by weight in grams. Morphological observation such as numbers of fruiting bodies per bag, cap diameter (cm) and stipe length (cm) were recorded. Biological efficiency (%) was calculated as follows:

$$\text{Biological efficiency (BE) (\%)} = \frac{\text{Fresh weight of mushroom across 3 flush}}{\text{Dry weight of substrate}} * 100\%$$

#### 4.2.5 Preparation of *Pleurotus* mycelia and fruiting bodies aqueous extract

Two weeks old mycelia samples and fruiting body sample were kept at -20°C overnight before the freeze drying process (Alpha 1-2 LDPlus, Martin Christ, Germany) for 24 hours for mycelia and 48 hours for fruiting body. The conditions of freeze drying are at -50°C and 0.12 atm pressure.

The freeze-dried samples were then grinded to fine powder using pestle and mortar. 0.5g of respective fine mushroom powder were added in 15 ml of boiling distilled water for 2 hours to generate the aqueous extracts. While the process of boiling was ongoing, addition of distilled water to the mixture to maintain the constant volume at 10 ml. The supernatant of the aqueous extract was recovered by centrifugation (Centrifuge 5810/5810R, Eppendorf, Germany) twice at 6300 RCF at room temperature. The supernatant was then

filtered with 0.45 µm syringe filter and kept at -20°C freezer until further analysis. The final extract concentration was at 50 mg/ml.

#### 4.2.6 Bioactivities screening

Only 10 samples of *P. pulmonarius* fruiting bodies were evaluated for antioxidant and phytochemical as these were the few samples that produced fruiting bodies under the experimental conditions.

##### 4.2.6.1 2,2-diphenyl-1-picrylhydrazyl (DPPH)

DPPH radical scavenging activity was determined using aqueous extract diluted with methanol with slight modification (Liew et al., 2018). For each sample, 6 different concentrations were tested (20mg/ml, 10mg/ml, 5mg/ml, 2.5mg/ml, 1.25mg/ml and 0.625mg/ml) (Appendix 2- Figure 1 and 2). The reaction mixture consisted of 50µl of extract, 50µl of methanol, 50µl of 90mM of Tris-Cl and 100 µl of 0.2mM 2,2-diphenyl-1-picrylhydrazyl radical solution in methanol. After incubation for 40 minutes under dark condition, absorbance was read using Biotek Microplate Spectrophotometer (Agilent, US) at 517nm. The antioxidant activity was calculated using the following equation.

$$\% \text{ inhibition} = \frac{A_{\text{control}} - A_{\text{sample}}}{A_{\text{control}}} * 100\%$$

Acontrol was the absorbance of the reaction mixture without sample extracts. Antioxidant activity was defined as the amount of antioxidant necessary to decrease the initial DPPH concentration by 50% (IC50). A scatter plot was generated for each sample with concentration of extract against its % inhibition to determine its IC50. (Appendix 2 – Figure 1 and 2)

##### 4.2.6.2 Ferric reducing antioxidant power (FRAP)

Ferric reducing antioxidant power assay was measured using 25mg/ml aqueous extract diluted with distilled water with slight modification (Liew et al., 2018). The FRAP cocktail ratio contained 10mM 2,4,6-Tris(2-pyridyl)-s-triazine (TPTZ), 20mM FeCl<sub>3</sub>.6H<sub>2</sub>O and 300mM sodium acetate buffer (pH 3.6). FRAP cocktail was freshly prepared on the same day of assay and warmed at 37°C for 10 minutes. The reaction mixture consisted of 25 µl of extract and

175µl of FRAP cocktail. The reaction was incubated in dark for 30 minutes and absorbance was measured at 590nm. FRAP activity was expressed as µM of  $\text{FeSO}_4$  per gram of sample. Standard calibration curve using various concentration of ferrous sulphate heptahydrate (Appendix 2 – Figure 3)

#### 4.2.6.3 Total phenolic content

Total phenolic content was measure using stock concentration (50 mg/ml) of the aqueous extract with slight modification (Liew et al., 2018). A total of 50µl of extract were added with 3ml of distilled water and 250 µl of Folin-Ciocalteu's reagent. The mixtures were vortex vigorously and let to stand at room temperature for 5 minutes. 7% sodium carbonate and distilled water was then added and let to stand for 2 hours in dark. 250 µl of the reaction mixture were removed and loaded into a 96 well plate. Absorbance was measured at 765nm, and result were expressed as mg of gallic acid/g sample. Standard calibration curve using various concentration of gallic acid (Appendix 2 – Figure 4).

#### 4.2.7 Proximate analysis

Contents of total ash, moisture, protein, and lipids were measured using the official proximate analysis techniques (Association of Official Analytical Chemists, 1997).

##### 4.2.7.1 Ash content

300mg of freeze-dried sample were weight into a crucible and used for determination of ash content. The initial crucible and samples weight were noted. The crucible with sample were placed in a muffled furnace for incineration at 550°C for 16 hours. After incineration, the crucible was left to cooldown and subsequently weigh to determine the weight loss. Total ash content was determined by this formula: -

$$\text{Ash content \%} = \frac{\text{Weight loss of sample (g)}}{\text{Initial sample weight (g)}} * 100\%$$



#### 4.2.7.2 Moisture content

500mg of fresh liquid nitrogen grinded sample were used to determine the moisture content using a rapid moisture analyzer (Sartorius, Germany) at 200°C until a constant weight are reached. Total moisture content was determined using this formula: -

$$\text{Moisture content \%} = \frac{\text{Initial sample weight (g)} - \text{Final sample weight (g)}}{\text{Initial sample weight (g)}} * 100\%$$

#### 4.2.7.3 Lipid content

The Soxhlet method using petroleum ether were used for total crude lipid content determination. 300mg of freeze-dried sample were weighted onto a thimble and place into the Soxhlet extractor. The initial weight of an empty round bottom flask was noted. 250ml of petroleum ether were added into the round bottom flask and placed onto a heating apparatus while connected to the Soxhlet apparatus. The solvent was boiled for extraction for 16 hours. After extraction, the petroleum ether was evaporated using a rotary evaporator, leaving only the lipid content in the flask which are weighed. Total lipid content was calculated using this formula: -

$$\text{Lipid content \%} = \frac{\text{Final weight of flask (g)} - \text{Initial weight of flask (g)}}{\text{Sample weight (g)}} * 100\%$$

#### 4.2.7.4 Protein content

The Kjeldahl method was used for total protein content determination. 300 mg of freeze-dried samples were weighed and set inside the digestion tube, with 2 titanium tablets as catalyst and 15 ml of sulphuric acid. Blank sample was prepared only with tablets and sulphuric acid while control samples was prepared with 100 mg of glycine, tablets, and sulphuric acid. The digestion tubes containing samples, blank and control were placed on a digestion block and the tubes were covered with an exhaust system. The heating process starts at 150°C, which after 15 minutes are increased to 250°C and after 15 minutes,

another increase to 380°C for 2 hours. Fully digested samples should be clear and neon green in colour. Digestion tubes were taken out from the digestion block and let to cool at room temperature. The digested sample then were subjected to distillation using the BÜCHI distillation unit K-350 (BÜCHI, Malaysia). The program on the distillation unit were set to utilize 90ml of water, 50ml of 4% 4.65pH boric acid solution and 50ml of 8M sodium hydroxide for each sample. When the distillation process was completed, the sample were titrated using 0.1N hydrochloric acid until it reached pH 4.65. The volume of 0.1N HCL used were recorded. Total nitrogen content was determined using this formula: -

$$\text{Nitrogen \%} = \frac{((\text{normality HCL} \times \text{corrected vol (mL)} \times 1.4007) \times 6.25)}{\text{Sample weight (g)}} * 100\%$$

#### Statistical analysis

All the analyses were performed in three technical and biological replicates which were averaged. One-way ANOVA with Tukey's posthoc test was performed using GraphPad Prism version 9.0.0 for Windows GraphPad Software, La Jolla California USA, [www.graphpad.com](http://www.graphpad.com). P-values less than 0.05 is statistically significant.

### 4.3 Results

#### 4.3.1 Growth parameters and yield of fruiting bodies

Among the 10 cultivated samples, sample MP42, MP35 and MP34 showed the highest yield and biological efficiency for first three flushes at an average of 125.3g, 123.9g and 116.8g respectively (Table 4.1). The three lowest yield Sample belongs to MP9, MP12 and MP28 at 70.2g ,62.0g and 56.8g respectively (Table 4.1).

Sample MP34 and MP9 have the least numbers of day for complete growth (days required to harvest 3 fruiting flushes.) at 59.33 days and 78.0 days respectively. Both MP34 and MP9 samples have a significantly faster growth rate as compared to the rest of the eight samples in which these eight samples have complete growth ranging from 135.33 days to 163.5 days.

While MP9 have the second fastest complete growth, it did not produce a high enough weight of fruiting body. MP42 and MP35 were the highest yield sample but both this sample also suffers from slow complete growth averaging at about 151.25 days and 135.33 days respectively.

The results show that sample MP34 possess the best traits, which has fast complete growth rate at 59.3 days and producing satisfactory biological efficiency of 43.8% within the three flushes.

Table 4.1 Biological efficiency, yield, and complete growth of the ten *P. pulmonarius* sample

Samples	Biological efficiency (%)	Yield (g)	Complete Growth (days)
MP2	36.4±0.88 <sup>abc</sup>	96.93±2.35 <sup>abc</sup>	149.56±30.8 <sup>ab</sup>
MP9	26.4±2.33 <sup>bcd</sup>	70.27±6.20 <sup>bcd</sup>	78.00±6.93 <sup>c</sup>
MP12	23.3±0.93 <sup>cd</sup>	62.00±2.48 <sup>cd</sup>	149.00±14.50 <sup>ab</sup>
MP28	21.3±1.86 <sup>d</sup>	56.83±4.95 <sup>d</sup>	158.20±26.0 <sup>ab</sup>
MP34	43.8±8.53 <sup>a</sup>	116.80±22.8 <sup>a</sup>	59.33±8.08 <sup>c</sup>
MP35	47.0±3.18 <sup>a</sup>	125.30±8.49 <sup>a</sup>	135.33±16.17 <sup>b</sup>
MP36	40.6±11.69 <sup>ab</sup>	108.30±31.2 <sup>ab</sup>	154.3±15.57 <sup>ab</sup>
MP41	38.2±1.70 <sup>ab</sup>	101.73±4.54 <sup>ab</sup>	148.73±14.01 <sup>ab</sup>
MP42	46.5±1.24 <sup>a</sup>	123.90±3.30 <sup>a</sup>	151.25±16.56 <sup>ab</sup>
MP43	39.9±3.41 <sup>ab</sup>	106.27±9.09 <sup>ab</sup>	163.50±16.52 <sup>a</sup>

Biological efficiency was determined by total weight of fruiting bodies/dry weight of substrate x 100%, yield was determined by average weight of fruiting body across 3 flush, complete growth is defined as days required to harvest 3 fruiting flushes. Different letters (a-d) denote the means were significantly different at p<0.05

### 4.3.2 Antioxidant activity of aqueous extract

The total phenolic content, DPPH radical scavenging activity and FRAP assay results for mycelia aqueous extracts are shown in Figure 4.1.

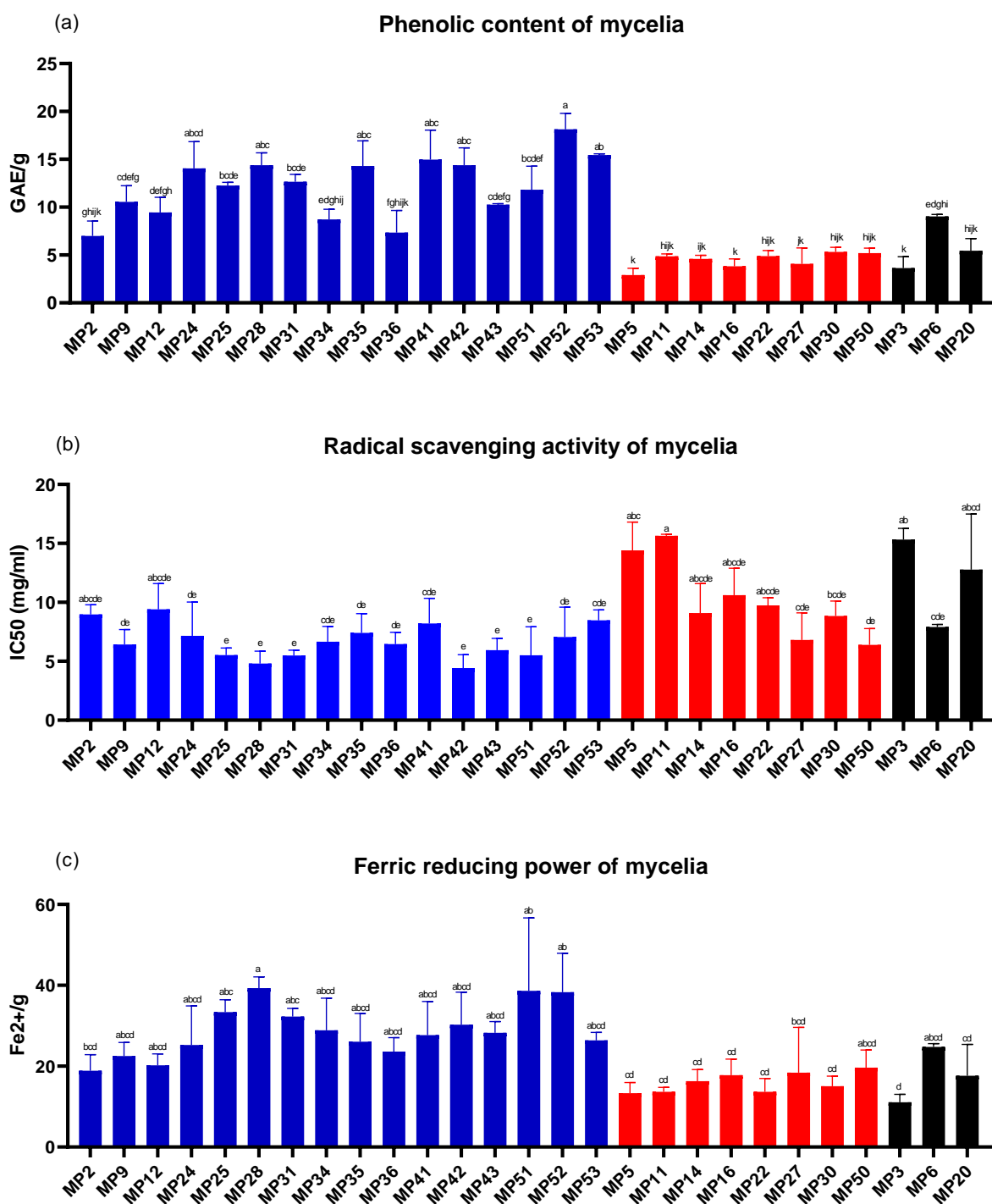


Figure 4.1 Antioxidant and phenolics values of mycelia aqueous extract (a)Total phenolic content, (b) DPPH radical scavenging activity, (c) FRAP value. Blue

indicates *P. pulmonarius*, red indicates *P. eryngii* and black indicates unidentified sample.

Total phenolic content for mycelia aqueous extract was found to be the highest in MP52 ( $18.13 \pm 1.69$  ug GAE/g), followed by MP53 ( $15.44 \pm 0.13$  ug GAE/g). *P. pulmonarius* phenolic content ranges from  $6.99 \pm 0.9$  –  $18.13 \pm 1.69$  GAE/g while *P. eryngii* phenolic content ranges from  $2.91 \pm 0.4$  –  $5.36 \pm 0.40$  GAE/g. *P. ostreatus* phenolic content ranges from  $3.62 \pm 0.7$  –  $9.03 \pm 0.12$  GAE/g.

The DPPH radical scavenging activity was found to be positively correlated with the concentration of extracts (0.625, 1.25, 2.5, 5, 10, 20 mg/ml). IC<sub>50</sub> value was defined as the amount required to inhibit 50% of the DPPH radical, meaning the lower IC<sub>50</sub> the greater radical scavenging activity possess by the sample. The highest scavenging activity was found in MP42 ( $4.42 \pm 1.13$  ug/ml), followed by MP28 ( $4.82 \pm 1.05$  ug/ml). For samples that identified as *P. pulmonarius*, the IC<sub>50</sub> value ranges from  $4.42 \pm 0.65$  –  $9.40 \pm 1.26$  ug/ml, while for *P. eryngii* the value ranges from  $6.38 \pm 0.81$  –  $15.65 \pm 0.08$  ug/ml. *P. ostreatus* sample IC<sub>50</sub> values range from  $7.9 \pm 0.12$  –  $15.33 \pm 0.55$  ug/ml. The observed trend for mycelia aqueous extracts shows that *P. pulmonarius* generally has a higher DPPH radical scavenging activity as compared to the other two species.

The ferric reducing power of all extract was tested with a single concentration (25mg/ml). Optimization results showed that extracts at 25mg/ml falls within the range of the calibration curve. MP28 ( $39.32 \pm 2.75$  Fe<sup>2+</sup>/g) shows the highest ferric-reducing power, followed by MP51 ( $38.6 \pm 18.1$  Fe<sup>2+</sup>/g). *P. pulmonarius* FRAP value ranges from  $18.88 \pm 2.29$  –  $39.32 \pm 2.75$  Fe<sup>2+</sup>/g while *P. eryngii* FRAP value ranges from  $13.30 \pm 1.54$  –  $19.63 \pm 2.51$  Fe<sup>2+</sup>/g. *P. ostreatus* FRAP value ranges from  $11.08 \pm 1.14$  –  $24.78 \pm 0.45$  Fe<sup>2+</sup>/g. Similarly, the FRAP assay also shows the same trend as DPPH radical scavenging activity in which *P. pulmonarius* generally have better ferric reducing power as compared to *P. eryngii* and *P. ostreatus*.

To sum up, antioxidant properties and phytochemical of mycelial aqueous extract were generally higher in all *P. pulmonarius* samples.

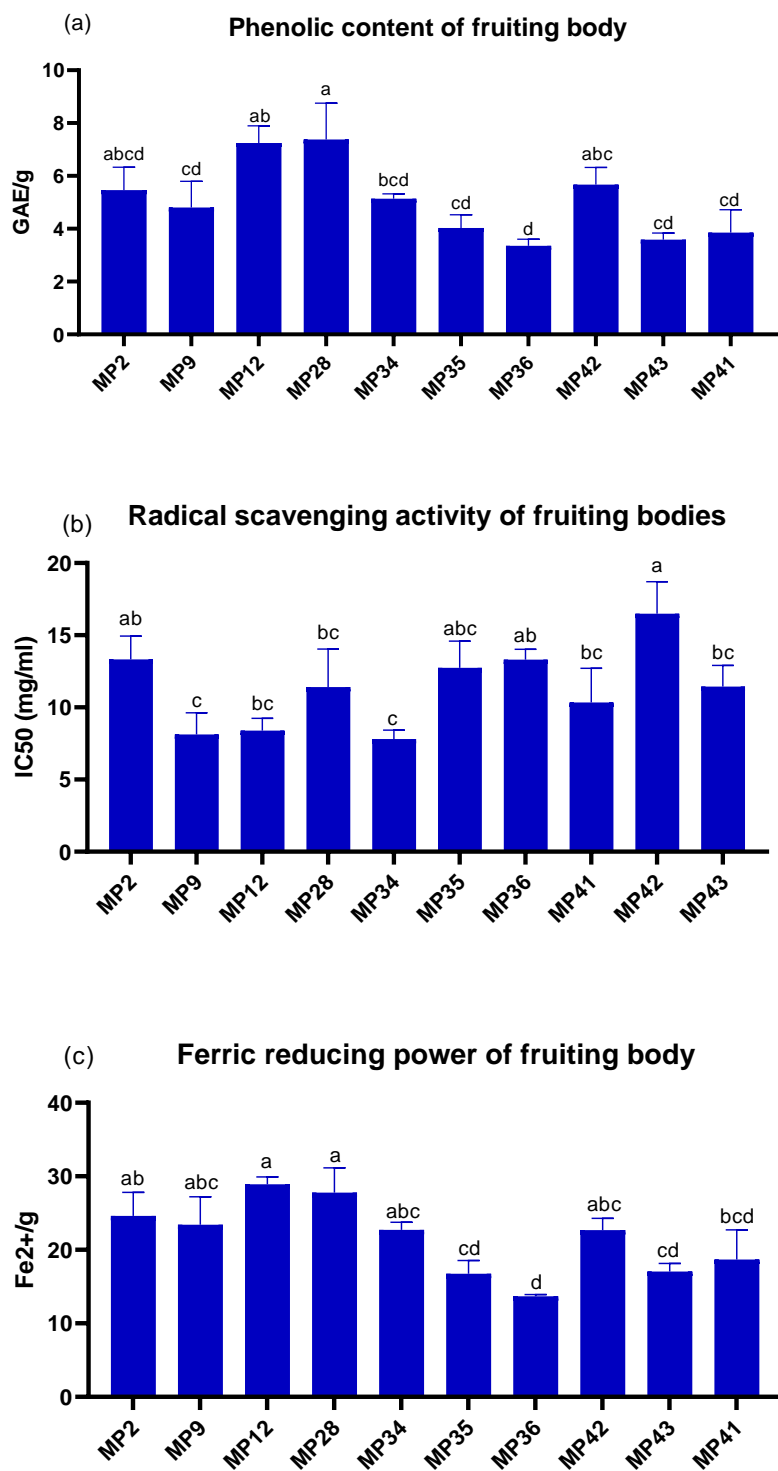


Figure 4.2 Antioxidant activity and phenolics of *P. pulmonarius* fruiting bodies aqueous extract (a) Total phenolic content ; (b) DPPH Radical scavenging activity and (c) FRAP value

The total phenolic content, DPPH radical scavenging activity and FRAP assay results for fruiting bodies aqueous extracts are shown in Figure 4.2.

Total phenolic content for fruiting body aqueous extract was found to be the highest in MP28 ( $7.38 \pm 1.38 \mu\text{g GAE/g}$ ), followed by MP12 ( $7.24 \pm 0.13 \mu\text{g GAE/g}$ ). The highest DPPH radical scavenging activity for fruiting body was MP34 ( $7.81 \pm 0.62 \mu\text{g/ml}$ ), followed by MP9 ( $8.11 \pm 1.50 \mu\text{g/ml}$ ).

Similarly, the ferric reducing antioxidant power for fruiting body aqueous was found to be highest in MP12 ( $28.93 \pm 0.99 \text{ Fe}^{2+}/\text{g}$ ) followed by MP28 ( $27.78 \pm 3.38 \text{ Fe}^{2+}/\text{g}$ ).

The phenolic content, FRAP value and DPPH scavenging activity of fruiting body were lower as compared to their mycelia counterpart.

Table 4.2 Pearson correlation between yield and DPPH value; FRAP value; TPC value.

	<u><b>Yield</b></u>		
	<b>Pearson r value</b>	<b>significance (2-tailed)</b>	<b>N</b>
DPPH IC50	0.42	0.226	10
FRAP	-0.61	0.060	10
TPC	-0.61	0.061	10

Pearson correlation coefficient ( $r$ ) between 0 to 1 is positive correlation,  $r$  value of 0 is no correlation,  $r$  value between 0 and -1 is negative correlation.

The Pearson correlation results of yield and antioxidant values were shown in Table 4.2. There was a negative medium correlation of yield with total phenolic content and yield with FRAP value and positive small correlation of yield and DPPH IC50 value (IC50 value is the lower the better antioxidant activity). This suggests that the higher the mushroom yield, the lower the FRAP antioxidant power and phytochemical content, however the results were not significant.

Table 4.3 Pearson correlation between antioxidant values of fruiting bodies and mycelia in each of the antioxidant tested.

	<b><u>Fruiting body</u></b>		
	<b>Pearson r value</b>	<b>significance (2-tailed)</b>	<b>N</b>
DPPH IC50	-0.38	0.286	10
FRAP	0.09	0.807	10
TPC	0.10	0.784	10

Pearson correlation coefficient ( $r$ ) between 0 to 1 is positive correlation,  $r$  value of 0 is no correlation,  $r$  value between 0 and -1 is negative correlation.

The Pearson correlation results of antioxidant values between fruiting bodies and mycelia were shown in Table 4.3. DPPH IC50 has moderate negative correlation in relation to fruiting bodies and mycelia while FRAP and TPC have small correlation in relation to fruiting bodies and mycelia. Like the correlation between yield and antioxidant value, the results were not significant.



### 4.3.3 Proximate analysis









Table 4.4 Moisture, ash, crude protein, and lipid presented from analysis of ten *P. pulmonarius*, in triplicate. Different lowercase superscript letters in the same column indicate a statistical difference at  $p < 0.05$  using one-way ANOVA.

	Moisture (%)	Ash (%)	Lipid (%)	Protein (%)
MP2	85.11 ± 1.29 <sup>ab</sup>	6.63 ± 0.11 <sup>abc</sup>	1.70 ± 0.51 <sup>a</sup>	18.14 ± 1.28 <sup>b</sup>
MP9	87.31 ± 0.5 <sup>a</sup>	5.86 ± 0.12 <sup>bc</sup>	2.48 ± 0.9 <sup>a</sup>	23.29 ± 0.9 <sup>a</sup>
MP12	85.76 ± 0.66 <sup>ab</sup>	7.55 ± 0.2 <sup>a</sup>	3.66 ± 0.82 <sup>a</sup>	19.45 ± 1.14 <sup>ab</sup>
MP28	88.22 ± 0.16 <sup>a</sup>	6.45 ± 0.24 <sup>abc</sup>	5.74 ± 1.31 <sup>a</sup>	17.8 ± 0.3 <sup>b</sup>
MP34	85.97 ± 0.77 <sup>ab</sup>	6.90 ± 0.49 <sup>ab</sup>	2.08 ± 0.53 <sup>a</sup>	23.88 ± 0.4 <sup>a</sup>
MP35	88.09 ± 0.37 <sup>a</sup>	7.48 ± 0.23 <sup>a</sup>	6.94 ± 0.84 <sup>a</sup>	16.97 ± 0.7 <sup>b</sup>
MP36	83.24 ± 1.12 <sup>b</sup>	7.49 ± 0.04 <sup>a</sup>	3.47 ± 0.47 <sup>a</sup>	21.05 ± 0.7 <sup>ab</sup>
MP41	86.09 ± 0.76 <sup>ab</sup>	5.54 ± 0.26 <sup>c</sup>	1.86 ± 0.14 <sup>a</sup>	20.67 ± 1.2 <sup>ab</sup>
MP42	84.50 ± 0.14 <sup>ab</sup>	6.24 ± 0.15 <sup>abc</sup>	2.14 ± 0.28 <sup>a</sup>	20.23 ± 1.3 <sup>ab</sup>
MP43	85.53 ± 0.95 <sup>ab</sup>	6.88 ± 0.43 <sup>ab</sup>	2.17 ± 0.06 <sup>a</sup>	20.32 ± 0.34 <sup>ab</sup>

The nutritional values of ten tested *P. pulmonarius* are shown in Table 4.4. All the *P. pulmonarius* have a high moisture content, ranging from 83.24% to 88.22%. The amount of lipid for all samples is very low as compared to the other components, ranging from 1.7% to 6.94%. The ash content is also low, but at a smaller range between 5.54% to 7.55%. Lastly, the protein content ranges from 16.97% to 23.88%, higher than both lipid and ash content. MP35 has the highest moisture content at 88.22%, while MP12 has the

highest ash content at 7.55%. MP2 has the lowest lipid content at 1.7% while MP34 have the highest protein content at 23.88%.

#### 4.3.4 Morphological characteristic of 10 selected *P. pulmonarius* fruiting bodies

MP2	 A single mushroom specimen with a light brown cap and a thick, pale stem. A blue ruler is visible on the left for scale.	MP35	 A cluster of mushrooms with dark brown caps and pale stems. A blue ruler is visible on the left for scale.
MP9	 A cluster of mushrooms with light brown caps. An arrow points to the cap with the label "Light Brown". A blue ruler is visible on the left for scale.	MP36	 A cluster of mushrooms with dark brown caps and pale stems. A blue ruler is visible on the left for scale.
MP12	 A cluster of mushrooms with dark brown caps. An arrow points to the cap with the label "Darker Brown". A blue ruler is visible on the left for scale.	MP41	 A cluster of mushrooms with dark brown caps and pale stems. A blue ruler is visible on the left for scale.
MP28	 A cluster of mushrooms with dark brown caps and pale stems. A blue ruler is visible on the left for scale.	MP42	 A cluster of mushrooms with dark brown caps and pale stems. A blue ruler is visible on the left for scale.

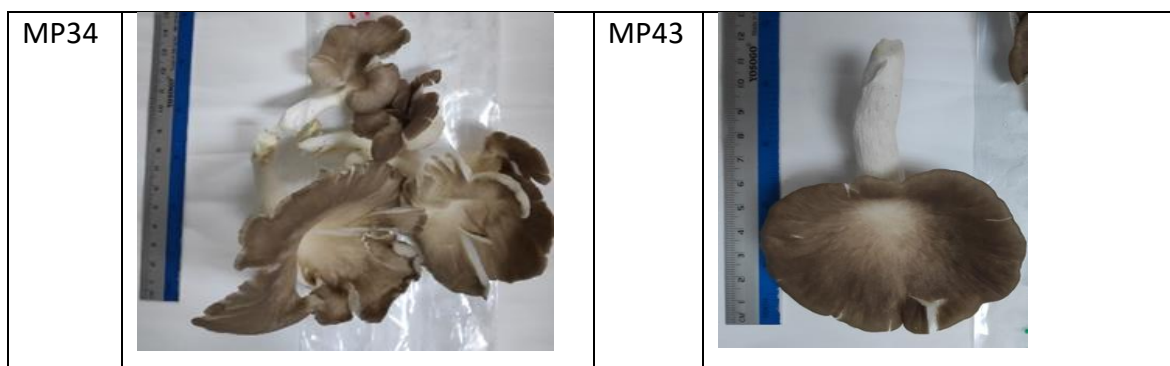


Figure 4.3 Morphological features of all 10 *P. pulmonarius* samples

Figure 4.3 shows the fruiting bodies of *P. pulmonarius* cultivated in this study. All 10 samples of *P. pulmonarius* have similar morphology, consist of lighter and darker brownish caps, average cap diameter of 5.5 - 7.5 cm and average stipe length of 4.0 -6.8 cm. However, the number of fruiting bodies were highly varied, ranging from 1-15 fruiting bodies per bag even for the same strain. The morphological results also complement the ITS phylogenetic tree from Chapter 3.3.3, further confirming that all the 10 *P. pulmonarius* samples in this study are the same.

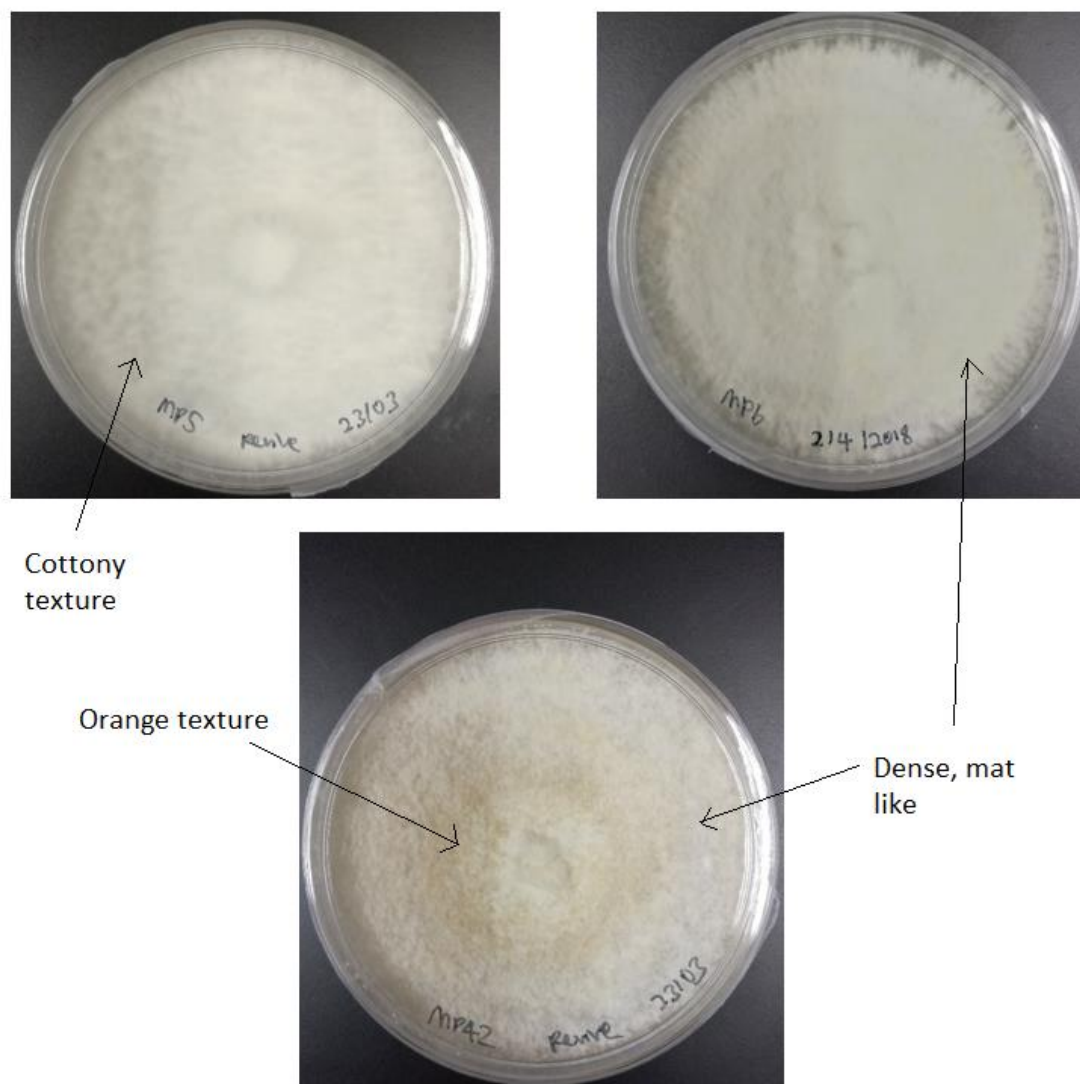


Figure 4.4 Two weeks old mycelia of *Pleurotus eryngii* (MP5; Top left), *Pleurotus ostreatus* (MP6; Top right) and *Pleurotus pulmonarius* (MP42; Bottom)

Figure 4.4 shows the mycelial morphology of 3 distinct species, from sample MP5 (*P. eryngii*), MP6 (*P. ostreatus*) and MP42 (*P. pulmonarius*). MP5 mycelia was white in colour and had cottony texture with abundant growth. MP6 mycelial was whitish with a little hint of orange, dense and compact, mat-like structure, and regular growth. MP42 mycelia was half white and half orange, dense and compact, mat-like structure, and regular growth as well.

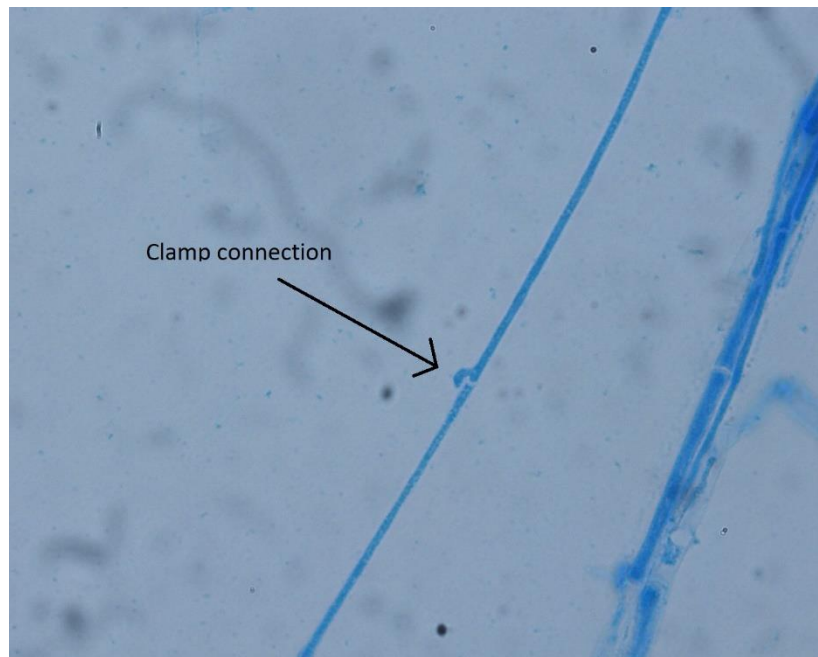


Figure 4.5 Five days old MP35 mycelia showing a visible clamp connection.  
100x magnification under light microscope, methylene blue stain 1%

Figure 4.5 shows five days old MP35 mycelia under 100X magnification of a light microscope. A visible clamp connection was formed during the elongation process. A clamp connection facilitates the mating of hyphae of different sexual types to maintain genetic variation.

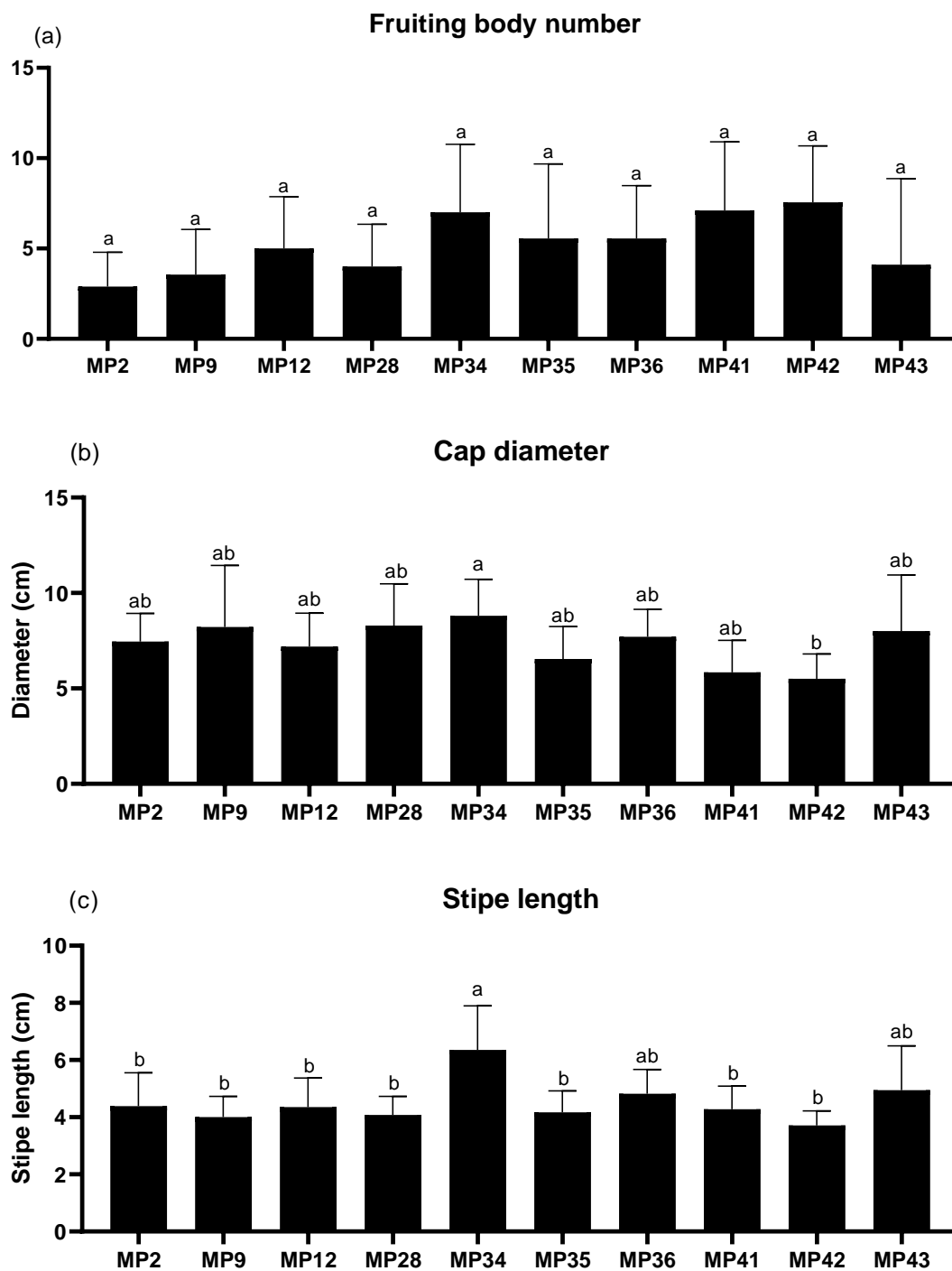


Figure 4.6 Morphology of 10 *P. pulmonarius*, (a) Fruiting body number; (b) Cap diameter; and (c) Stipe length

The morphological characteristics of the 10 *P. pulmonarius* samples are shown in Figure 4.6. Tukey method pairwise comparisons were used for statistical analysis of these 3 morphological data. MP42 ( $7.5 \pm 3.1$ ) has the highest amount of fruiting bodies number followed by MP41 ( $7.1 \pm 3.8$ ) and MP34 ( $7.0 \pm 3.8$ ). There is no significant difference found among the 10 samples. MP34 ( $8.8 \pm 1.9$  cm) has the largest cap diameter followed by MP28 ( $8.3 \pm 2.2$  cm) and MP9 ( $8.2 \pm 3.2$  cm). There is no significant difference found among the 10 samples. For the stipe length, MP34 ( $6.84 \pm 1.5$  cm) has the longest stipe followed by MP43 ( $4.9 \pm 1.5$  cm) and MP36 ( $4.8 \pm 0.8$  cm). MP34 has significantly longer stipe as compared to the rest of the sample. Generally, MP34 has better relative growth in terms of fruiting body number, cap diameter and stipe length.

#### 4.4 Discussion

The biological efficiency of 10 selected *P. pulmonarius* were shown in Table 4.1. It was observed that the biological efficiency of *P. pulmonarius* was significant when comparing the highest yield samples (MP42, MP35, MP34) and lowest yield samples (MP28, MP12, MP9). Both MP34 and MP9 have significantly shorter days for complete growth (days required to harvest 3 fruiting flushes) as compared with the rest of the samples. The shorter growing cycle aids to reduce the labor cost during harvesting and reduce the duration of the entire production (Myronycheva et al., 2017). *Pleurotus* spp secretes enzyme to degrade lignocellulosic materials for nutrients such as carbon and nitrogen as part of its metabolism (Sousa et al., 2016). The high biological efficiency of MP42, MP35, and MP34 might be attributed to its production of lignin-degrading enzyme. Some research have showed that fungus with high yield have enhanced production of lignin-degrading enzyme such as laccase and manganese peroxidase during mycelia colonization stage which decreased during fruiting stage (Elisashvili et al., 2008; Mata et al., 2007; Savoie et al., 2007). Four samples, namely MP34, MP35, MP36 and MP42 have biological efficiency of 40% and above, which are suitable for oyster mushroom cultivation (Gume et al., 2013).



Another study reported by (Myronycheva et al., 2017), has shown six *P. pulmonarius* sample with biological efficiency (%) ranging from 9.8 – 62.0%. The large range of biological efficiency results can be due to the different methods of cultivation employed by the author. This author uses larger bags with perforation along the sides which could have better air exchange as opposed to the bags without perforation used in this study.

Gallic acid, which is a phenolic compound, are known to exist in huge quantities in edible mushrooms (Puttaraju et al., 2006). Edible mushrooms are usually cooked under heat such as in soup or stirred fried and is not advisable to be consumed raw for safety reasons (Tan et al., 2015). Hence in this study, we performed hot water extraction for the antioxidant and phenolic content studies.

The 16 samples of *P. pulmonarius* based on Chapter 3.3.3 showed no variation in the phylogenetic tree suggested that all of them might belong to the same strain. However, the results for antioxidant and especially biological efficiency show significant variation among the samples of *P. pulmonarius*. Studies has shown that filamentous fungi such as *Pleurotus* spp. exhibit high levels of variation in terms of morphological, physiological and production of secondary metabolites when grown in nutrient rich laboratory environment with serial transfer of culture media (Horn & Dorner, 2002; Li et al., 1994). This phenomenon known as strain instability or degeneration (Lee et al., 2014) might be the cause of varying antioxidant level and growth in *P. pulmonarius*.

Overall, this study shows that *P. pulmonarius* have better antioxidant capacity and phytochemical compound as compared to *P. ostreatus* and *P. eryngii* during the mycelial stage as shown in Figure 4.1.

*P. pulmonarius* mycelia also have a higher antioxidant capacity as compared to their fruiting body counterpart, which contradicts the study of Sulistiany et al., (2016). The higher antioxidant capacity of the mycelia could be due to the usage of potato dextrose agar (PDA) as the growth media in which the dextrose content could promote the antioxidant activity of the mycelia (de Queiroz Cancian et al., 2018). While 10% of rice bran was also supplemented in the substrate for the fruiting body growth, the ratio was

not as high as the ratio of dextrose (20%) in PDA. Even though mycelial antioxidant shows an average increase of 1.8-fold in DPPH, 1.3-fold in FRAP and 2.3-fold in TPC value than fruiting body, lower overall yield of mycelial than fruiting body has limited its application as good source of antioxidant. Furthermore, antioxidant activity of the mushroom comparing to other functional food that are rich in antioxidant such as green tea is still low (Shannon et al., 2017). However, our data has shown the potential of using antioxidant profile to differentiate the mycelial *P. pulmonarius* than *P. ostreatus* and *P. eryngii*, which can be used as rapid screening to complement the molecular characterisation of the mycelial of *P. pulmonarius* before initiate the commercial culture.

Edible mushroom normally has high moisture contents (Adejumo & Awosanya, 2005), which conforms to our results on moisture contents. The ash contents of all samples were considerable high, suggesting that the mineral content is high too. The *Pleurotus* species contained a small amount of fat, which is also correlates with our result (Wani et al., 2010). While the moisture, ash and lipid content of our study conforms with *P. pulmonarius* studied by Nwoko et al., (2017), our results on protein content were considerably lower at around 16.97% to 23.88%, while Nwoko reported around 37%. The amount of protein found in *Pleurotus* mushrooms is influenced by both the species and the type of the substrate utilized (Erjavec et al., 2012). Our study utilized rubber sawdust while Nwoko utilized various species of fruit trees logs. This occurrence is also similar in *P. florida* as cultivation with sawdust resulted in the lowest protein content as compared to other substrate such as rice straw (Mapayi et al., 2021).

Table 4.5 Ranking of main attributes evaluated for fruiting bodies in this study.

Rank	Biological efficiency	Complete growth	TPC	DPPH	FRAP
1	MP35	MP34	MP28	MP34	MP12
2	MP42	MP9	MP12	MP9	MP28
3	MP34	MP35	MP42	MP12	MP2
4	MP36	MP2	MP2	MP41	MP9
5	MP43	MP41	MP34	MP28	MP34

*Pleurotus* mycelia can be utilized as a source of high biologically active compounds since its mycelial stage antioxidant capacity are greater than fruiting bodies as shown in this study. Considering large interest for mushroom as a source for drugs and nutraceuticals development (Papaspnyridi et al., 2011), mycelial MP42, MP52 and MP28 (Figure 4.1) can potentially be utilized for extraction of biologically active compound such as phenolics. Mycelia are also advantageous as it can benefit from rapid production and reduced intensive labour as compared to fruiting body for used in extraction of biological compounds especially in submerged cultivation (Tang et al., 2007).

As the sale of mushrooms is determined by weight, this parameter stands as a primary characteristic assessed for various mushroom strains (Jeznabadi et al., 2016). Farmers benefits from rapid growing mushrooms with high yield as it is better in terms of financial returns (Girmay et al., 2016), hence the important characteristic to be evaluated is complete growth and biological efficiency.

As shown in Table 4.5, sample MP34, which ranked 3<sup>rd</sup> in biological efficiency (43.8%), shows the improved traits in terms of yield and morphological characteristic, while having an average antioxidant (ranked 1<sup>st</sup> in DPPH and 5<sup>th</sup> in FRAP) and phytochemical content (ranked 5<sup>th</sup> in TPC). More importantly, MP34 exhibits the fastest growth rate (ranked 1<sup>st</sup>), achieving 3 mature flush of fruiting bodies within 59 days. Therefore, among the tested samples, MP34 can be recommended as the preferred *P. pulmonarius* for commercial

cultivation. The high-quality sample can ensure continuous and frequent supply of local oyster mushroom without depending on import which will benefit the economic activity and boost the income of the local farmers. With a suitable sample of *P. pulmonarius* identified for optimal mushroom cultivation, further studies can be conducted on different potential agriculture waste (other than sawdust) such as cotton seed and paper waste and method of substrate/ bags preparation for oyster mushroom cultivation to further evaluate its benefit in yield, growth, and potential health benefit.

## **Chapter 5: Comparative transcriptomics analysis of high and low yield edible mushroom *Pleurotus pulmonarius* in Malaysia**

### **5.1 Introduction**

While *Pleurotus pulmonarius* takes up most Malaysia mushroom cultivation shares, the mushroom agriculture industry is still facing several problems such as poor quality of mushroom spawn the mushroom yield and cost losses to the mushroom farmers. Mushrooms are usually sold based on their weight; hence the yield of a mushroom is the most vital component during harvesting (Jeznabadi et al., 2016). To maximize production, it is essential to use the strain that produces the highest yield. However, the molecular factors which affect the yield of *P. pulmonarius* are not fully known.

RNA-sequencing is a cost-effective and a swift technology for studying differentially expressed gene in two or more sample types, especially when the reference genome of the species is not available (Wong et al., 2011). Multiple transcriptome studies have been performed on a variety of edible mushroom species such as *Cordyceps miliratis*, *Ganoderma lucidium* and *Pleurotus eryngii* which profiled and compared the gene expression these edible mushroom growth cycle. These finding have provided insightful information that can assist the strain selection and cultivation strategies of the mushroom (Xie et al., 2018; Yin et al., 2017; Yu et al., 2012). To-date, using comparative transcriptomic analysis to explore the differential gene expression between high and low yield of *P. pulmonarius* is still lacking.

In this study, we aimed to identify potential molecular markers that specifically distinguish between high and low yield *P. pulmonarius* mushroom for large-scale cultivation. *P. pulmonarius* with different biological efficiencies were selected for de-novo transcriptomic analysis using the next-generation sequencing technology. The high yield type *P. pulmonarius* is expected to have different gene expression as compared to low yield while having similar gene expression within their own groups. These differentials expressed genes (DEG) may include genes related to the pathways such as metabolic,

development, stress response, cell division and differentiation, protein transport and production of secondary metabolites.

The specific objectives of this study include: -

1. To perform de novo transcriptome sequencing analysis using total RNA from fruiting bodies of selected low- and high-yield *P. pulmonarius* strains.
2. To identify differentially expressed genes (DEGs) and the annotated pathways via gene ontology and KEGG pathway enrichment analyses.
3. To validate the selected and KEGG enriched DEGs using quantitative real time PCR (qPCR).

## **5.2 Materials and Methods**

### **5.2.1 Mycelia culture and fruiting bodies growth**

Four pure cultures of *Pleurotus pulmonarius* mushroom mycelia, namely MP42, MP35, MP12 and MP28 were prepared as per Section 4.2.1, and 4.2.2. MP42 and MP35 were considered as high yield and MP12 and MP28 were considered as low yield as per Section 4.3.

### **5.2.2 RNA extraction**

For each sample's biological replicates, multiple freshly harvested fruiting bodies that were snap froze in liquid nitrogen from three bags were pooled and homogenized during cryogenic grinding. Total RNA from fruiting bodies was extracted using RNeasy Plant Mini Kit (QIAGEN, Inc., Valencia, CA) according to the manufacturer's instructions. The amount of starting material used was 100 mg of cryogenically grounded fruiting body sample. Four hundred fifty µl of Buffer RLC with 2-Mercaptoethanol were added into the sample. This mixture with sample was transferred to the QIAshredder spin column and centrifuged at 20,000 RCF for 2 minutes. Supernatant were transferred to a new tube and 0.5 volume of

100% ethanol were added and mixed immediately. The mixed sample was transferred to a RNeasy spin column and centrifuged for 11,000 RCF for 15 seconds. DNase digestion was performed in the column using 5U of Ambion DNase I and incubated for 30 minutes at 37°C. Seven hundred microliters of Buffer RW1 were added onto the spin column and centrifuged for 11,000 RCF for 15 seconds to clean the remaining DNase I. A final column wash using 500 µl of Buffer RPE centrifuged for 11,000 RCF for 15 seconds. An additional spin at 11,000 RCF for 2 minutes was performed to ensure all residues were removed from the spin column. Twenty microliters of RNase free water were added on top of the column and incubated for 15 minutes before elution by centrifuged for 11,000 RCF for 15 seconds.

The concentration, quality and integrity of extracted RNA samples were determined using agarose gel electrophoresis and Nanodrop spectrophotometer (Thermo Scientific, USA). Further RNA integrity and quantification were performed using the Bioanalyzer 2100 system (Agilent Technologies, USA).

### 5.2.3 Library preparation and RNA-Seq

Twelve cDNA libraries were constructed using NEBNext Ultra RNA Library Prep Kit for Illumina (NEB, USA) following manufacturer's recommendations. The 12 cDNA libraries are MP42 biological replicates 1 to 3, MP35 biological replicates 1 to 3, MP12 biological replicates 1 to 3 and MP28 biological replicates 1 to 3. Paired-end sequencing on all 12 libraries were performed using Illumina HiSeq 2500 platform (Novogene, China).

### 5.2.4 De novo transcriptome assembly and homology search

Clean reads were obtained by filtering and trimming the adapters, low-quality, and duplicate sequence from the raw reads. De novo assembly was performed using CLC Genomics Workbench v10.1 software (CLC Bio, Denmark). The settings for de novo assembly were graph parameters set to automatic for word and bubble size, minimum

contig length of 200 base pairs, map reads back to contig with mismatch cost of 2, insertion cost of 3, deletion cost of 3, length fraction at 0.5 and similarity function at 0.8.

Gene functional annotation was performed using Diamond software for the NCBI non-redundant protein sequences (Nr), Swissprot and Cluster of Orthologous Groups of proteins (KOG) (Buchfink et al., 2015). NCBI Nucleotide database (nt) annotation was performed using NCBI Basic Local Alignment Search Tools (BLAST)+ executables (National Center for Biotechnology Information (US), 2008). Annotation for Kyoto Encyclopedia of Genes and Genomes (KEGG) was performed using KEGG Automatic Annotation Server (KASS) at <https://www.genome.jp/kegg/kaas/> (Moriya et al., 2007) while Protein family (Pfam) annotation was performed using hmmscan build in CLC Genomic Workbench. Gene ontology functional annotation was performed using BLAST2GO software based on the annotation results of Nr and Pfam (Conesa et al., 2005).

GO enrichment pathway analysis was performed using ShinyGO with setting set to “*Agaricus bisporus* StringDB” at <http://bioinformatics.sdstate.edu/go/> (Ge et al., 2020). KEGG pathway enrichment analysis was performed using KOBAS with the species chosen for basidiomycetes *Agaricus bisporus* var. *bisporus* H97, statistical methods set to Fisher’s exact test and FDR correction method to Benjamini and Hochberg (1995) at <http://kobas.cbi.pku.edu.cn/> (Bu et al., 2021).

### 5.2.5 Identification of differentially expressed genes.

Differential expression analysis was calculated using CLC Genomic Workbench v10.1 software (CLC Bio, Aarhus, Denmark). RNA-Seq analysis tool were chosen in the software with the following settings: - the de novo assembled sequences selected as reference, mismatch cost set to 2, insertion cost to 3, deletion cost to 3, length fraction to 0.8, and similarity fraction to 0.8.



### 5.2.6 Validation of differentially expressed gene through Quantitative real time PCR (qPCR) Analysis.

Five DEGs were identified by RNA-Seq and KEGG Enrichment method for validation by RT-qPCR. Total RNA from high- and low-yield fruiting bodies were extracted using the same procedure as in section 5.2. RNA from each sample was reverse transcribed using NEXscript cDNA synthesis kit (Geneslabs, Korea).

cDNA conversions were performed using NEXscript cDNA synthesis kit (NEXDiagnostic, Korea) as per manufacturer's protocol. A mixture of 1 µl of Oligo DT, template RNA of total 2 µg and additional RNase-free water up to 10 µl total were incubated at 65°C for 5 minutes. After incubation, the initial mix of template RNA with oligo DT were added with 4 µl of 5x reaction buffer (50mM Tris-HCl, 150mM NaCl, 0.1 mM EDTA, 1 mM dithiothreitol, 0.1% NP-40 alternative, 50% glycerol), 1 µl of RTase (200U/ µl), 1 µl of DTT (8mM), 1 µl of dNTP mix (2.5mM) and RNase free water up to 20 µl. The reaction mixture was incubated at 50°C for 60 minutes and reactions were terminated by incubating at 95°C for 5 minutes.

Primers for the 5 DEGs and 2 housekeeping genes were designed using Primer Premier 6.24 software (Premier Biosoft, US) and are shown in Table 5.1. Reaction mixture (10 µl) contained 5 µl of 2X NEXpro qPCR Master Mix (SYBR), 1.0 µl of 10uM each primer, 2 µl of cDNA template and 1 µl of RNase free water. The qPCR reactions were cycled on an Eco Real-Time PCR system (Illumina, USA). Amplification conditions were 95°C for 10 mins for polymerase activation followed by 40 cycles of 95°C for 10 seconds, 65°C for 30 seconds, and 72°C for 15 seconds. The melt curve conditions are as follows: 95°C for 15 seconds, 55°C for 15 seconds and 95°C for 15 seconds. Each reaction was performed in duplicates and used the electron transfer gene and GTP-binding as housekeeping gene. Relative gene expression levels were calculated using the  $2^{-\Delta\Delta C_t}$  method (Livak & Schmittgen, 2001)

Table 5.1 List of primers used for qPCR validation.

Gene ID	Annotation	Primer (5' -3')
885	Aspartyl protease	FWD - GTATATCCACGGTCGCCACCAC RV- CGGACGCATTGACGCCATTG
11935	Electron transfer (reference gene 1)	FWD - CTGTTGCCTCCCGTGCCTTT RV - GCGACAACCTTCACTTCATCCG
10629	GTPase-activating protein S23	FWD - CGTCACGCATTACCAACATTG RV - ATCCAGCCACCTCAAGACATCC
3921	<i>CATALASE1</i> mRNA	FWD - GCACCGAAGGAACCGACCATCA RV - ACGCATTGCGCCGACGCAGAT
10258	Palmitoyltransferase (YKT6)	FWD - CCAGAGCGTCCAGGAGAACAAAT RV - TGGCAGTGAAGTCGTCCAGAAT
640	Copper amine oxidase	FWD - GCTCGTCGTCAGCATGGTCT RV - CGATGGTGCCGTCCTGATAGAA
8888	GTP-binding protein (reference gene 2)	FWD - AACCTTCCTCCTCAGCGTACT RV - AGAACTCCAGCGTCAGGCAGAT

## 5.3 Results

### 5.3.1 Total RNA quality and quantity

The whole RNA quantity and quality quantified using Nanodrop is shown in Table 5.2. Sample absorbance values for A260/280 and A260/230 represent the purity of the nuclei acid samples. A260/280 ratio of about 2.0 is generally considered pure for RNA and A260/230 ratio of about 2.0-2.2 for both DNA and RNA. Figure 5.1 shows the gel electrophoresis image of all the RNA. All samples showed RNA integrity number (RIN) of 7.5 and above except for MP42 R1 and MP42 R2 (Appendix 3 – Figure 1). This was an error caused by the calibration software as shown in Appendix 3 – Figure 2 and Figure 3 The pink and green line should be positioned at the base of 18S and 26S peaks respectively.

All RNA samples electropherogram have similar patterns which confidently shows that all samples should have similar RIN value. Figure 5.1 shows the gel electrophoresis image of both the high and low yield type *P. pulmonarius* RNA samples and shows clearly two visible intact bands (28S and 18S) with no signs of degradation.

Table 5.2 Reading from Nanodrop in terms of concentration and absorbance value.

<b>Sample Name</b>	<b>Nucleic Acid(ng/μl)</b>	<b>A260/A280</b>	<b>A260/A230</b>
MP35 R1	300.8	2.17	2.38
MP35 R2	732.4	2.16	1.96
MP35 R3	352.4	2.16	1.95
MP42 R1	400.2	2.18	2.56
MP42 R2	419.9	2.19	2.34
MP42 R3	406.20	2.19	1.76
MP12 R1	1001.8	2.17	2.09
MP12 R2	545.8	2.16	2.68
MP12 R3	805.0	2.17	2.44
MP28 R1	1386.3	2.17	2.62
MP28 R2	465.6	2.19	2.58
MP28 R3	1437.8	2.18	2.41

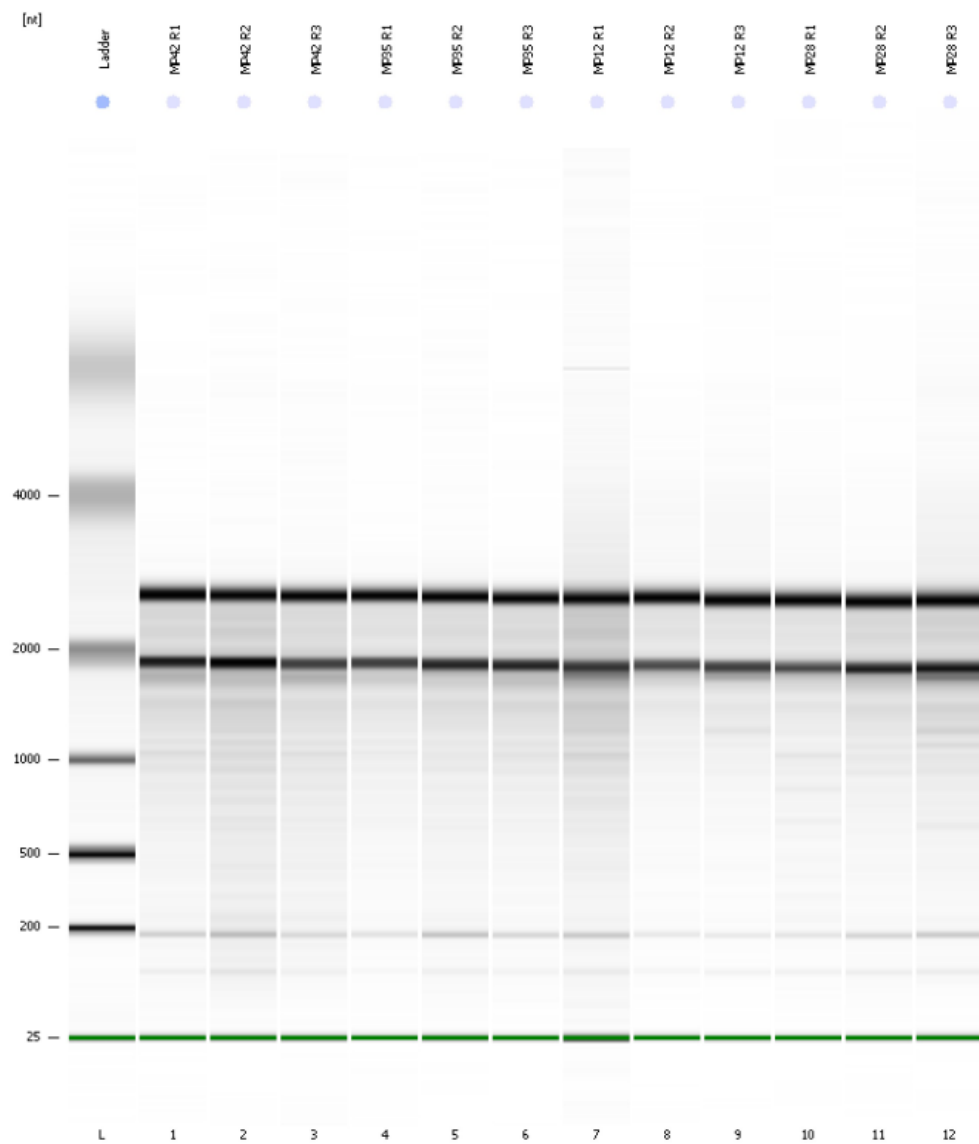


Figure 5.1 Gel electrophoresis image of high and low yield *P. pulmonarius* RNA extracts

### 5.3.2 Illumina sequencing and reads assembly.

Altogether, 1,036,603,062 raw reads were generated from 12 cDNA libraries of *P. pulmonarius* samples representing two groups, namely high yield (MP42, MP35) and low yield (MP12 and MP28). A total of 984,518,500 high quality cleans read were obtained after data filtering and trimming (Table 5.3). De novo assembly was performed and 85,072 unigenes were produced with an average length of 656bp and an N50 of 991bp. Table 5.3 shows the summary for the de novo assembly statistics.

Table 5.3 De novo assembly statistics

Item	Numbers
Total number of raw reads	1,036,603,062
Total numbers of clean reads	984,518,500
Total number of unigenes	85,072
Average unigene length	656
N75	442
N50	991
N25	2032

### 5.3.3 Functional annotation of the transcriptome

A total of 50,471 (59%) unigenes were associated with known protein in NCBI Nucleotide (NT) database, followed by NCBI protein (Nr) database (30,097; 35%), Gene Ontology (GO) database (28750: 33.8%), Pfam database (7255: 8%), and Clusters of Orthologous Groups (KOG) database (4148: 4.9%).

The breakdown of GO functional annotation is shown in Figure 5.2. The main biological process (BP) GO term identified in all the unigenes were “metabolic process” (16557 unigenes) and “cellular process” (11760 unigenes), while the “binding” (15852 unigenes) and “catalytic activity” (17893 unigenes) GO term were the most common in molecular function (MF). These results on MF and BP agree with the findings on transcriptomic of *P.*

*tuolensis* (Wang et al., 2022). The top GO terms for cellular components (CC) were “cell” (7705 unigenes) and “cell parts” (7680 unigenes).

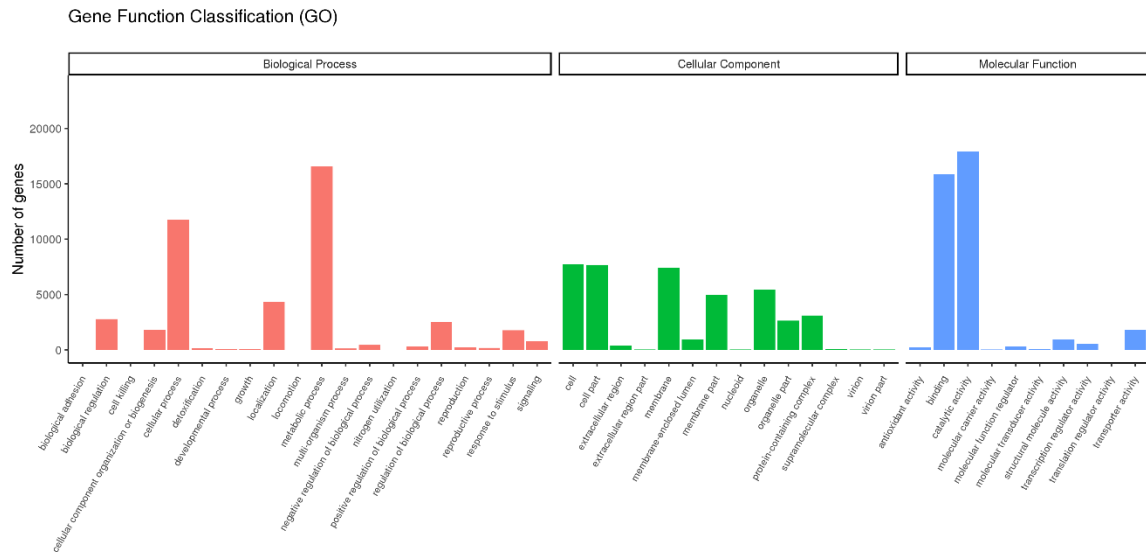


Figure 5.2 GO functional annotation of all unigenes (Red bar is biological process, green bar is cellular component while blue bar is molecular function)

The KEGG classification for all unigene is shown in Figure 5.3. The top 5 KEGG pathways were “Carbon metabolism” (2843 unigenes) and “Amino acid metabolism” (1612 unigenes) under Metabolism, “Translation” (1855 unigenes) and “Folding, sorting and degradation” (1855 unigenes) under Genetic Information Processing and “Signal transduction” (1393 unigenes) under Environmental Information Processing. These results also agree with (Wang et al., 2022) on *P. tuolensis*, in which its top KEGG pathways were “carbon metabolism”, “amino acids metabolism”, “translation” and “signal transduction”.

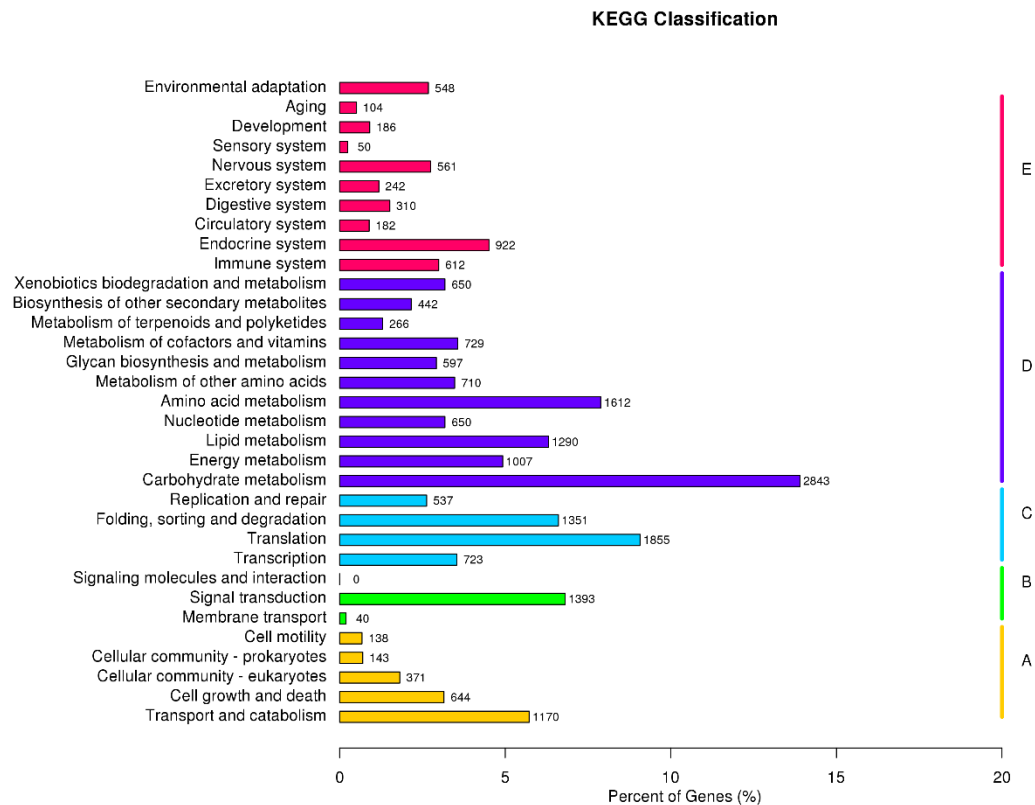


Figure 5.3 KEGG classification of all unigenes. Alphabet A to E represents different KO pathway (A: Cellular Process, B: Environmental Information Processing, C: Genetic Information Processing, D: Metabolism, E: Organismal Systems)



#### 5.3.4 Identification and Functional Enrichment Analysis of Differentially expressed unigenes.

To identify and evaluate differentially expressed unigenes, we compared the normalized read counts in FPKM of the high yield and low yield samples according to  $\log_2(\text{Fold Change}) > 1$  and  $p\text{-value} < 0.05$ . The comparative analysis revealed 27449 significantly DEGs ( $p_{\text{adj}} < 0.05$ ) which includes 13707 upregulated and 13742 downregulated genes. A volcano plot showing the  $-\log_{10}(P\text{-value})$  versus  $\log_2\text{fold change}$  of all the upregulated and downregulated genes are shown in Figure 5.4. Split down in the middle, the dots on the left hand side represents downregulated genes while on the right hand side represent upregulated genes and the most statistically significant genes were located towards the top. Additionally, a heatmap of all the DEG is shown in Figure 5.5. Generally, high yield and low yield sample shown to have very different gene expression pattern across groups but similar expression patterns within groups which supports the hypothesis.

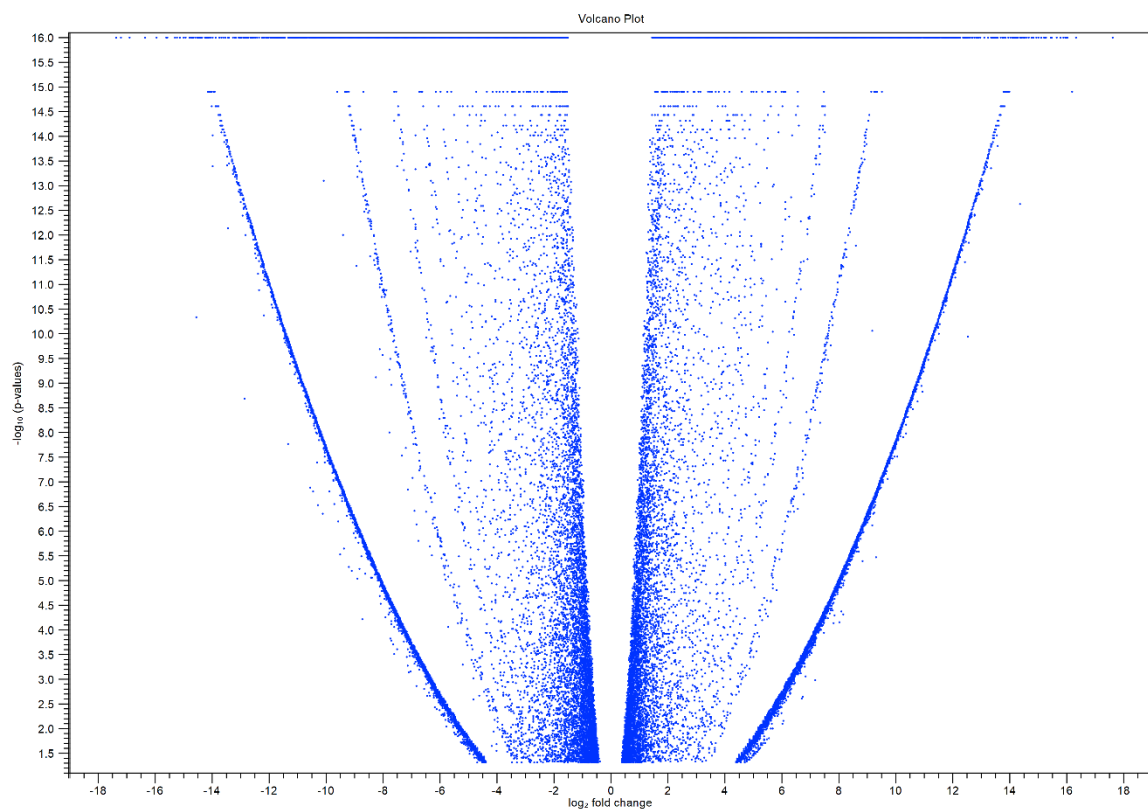


Figure 5.4 Volcano plot of each differentially expressed unigenes

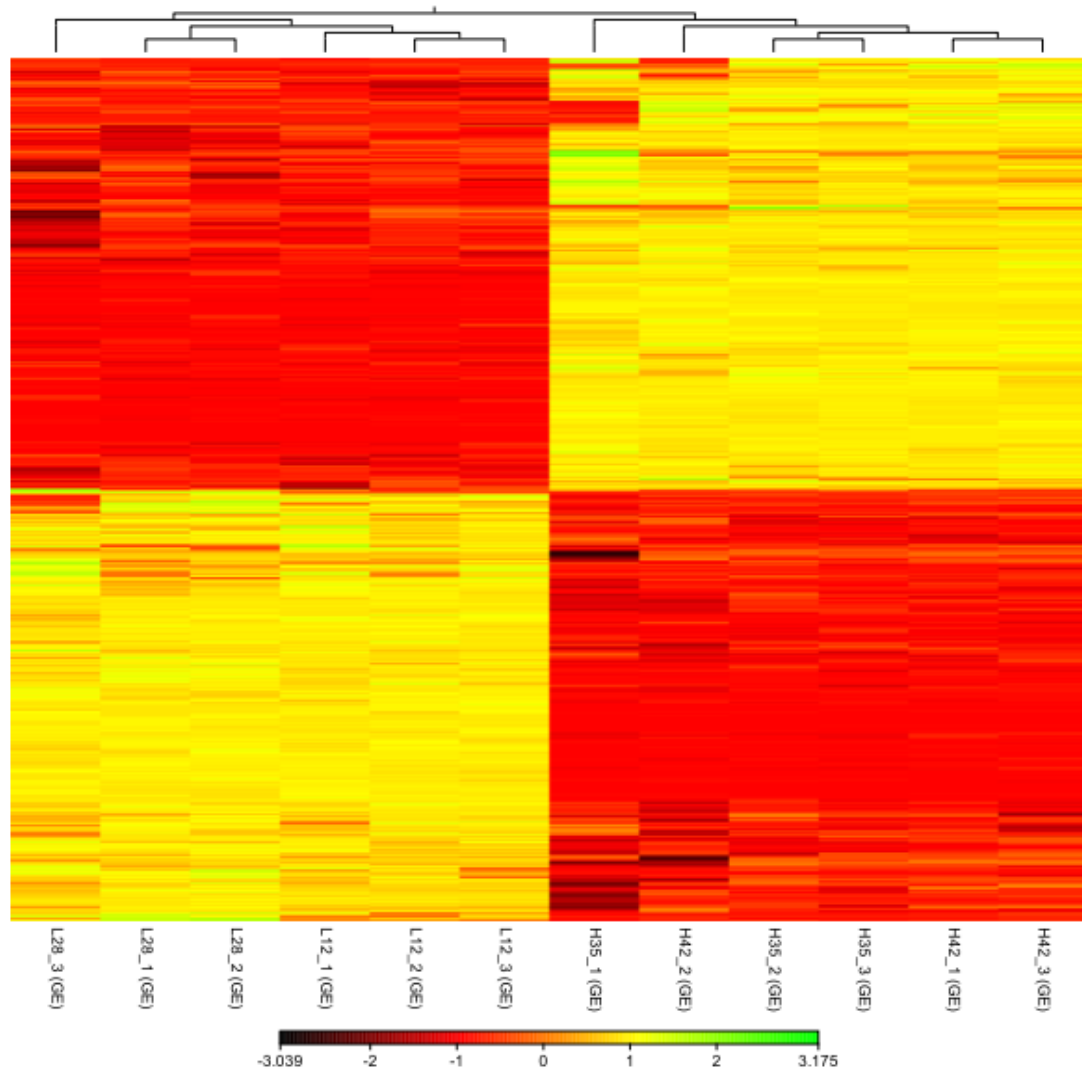


Figure 5.5 Heatmap of all the DEG among high and low yield *P. pulmonarius*. Yellow to green represent upregulation while red to black represent downregulation. High yield types were arranged to the right side while low yield types were on the left side.

While standard GO classification matches the gene to its GO functions to obtain annotation information, GO enrichment analysis involves the assessment of the level of enrichment of a cluster of genes that share common GO functions, with the aim of analyzing genes that have similar functions.

GO enrichment analysis of the DEG was conducted to identify the functions of the DEG by providing it GO terms that were significantly enriched in DEG in comparison to the genomic background. Up till now, no reports of GO enrichment analysis comparing high yield and low yield type of *P. pulmonarius* have been published, hence these reports are novel and will contribute to the future studies of DEG in *P. pulmonarius*. The GO enrichment analysis results are shown in Figure 5.6. The heat shock factor (HSF) (395-fold enrichment), HS transcription factor (395-fold enrichment), HSF-type DNA binding (395-fold enrichment) and oxidoreductase activity (346-fold enrichment) were the top enriched terms.

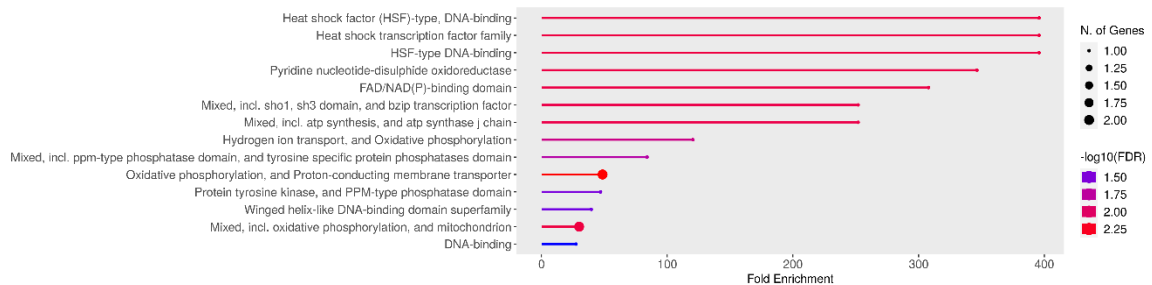


Figure 5.6 GO Enrichment Analysis of significant differentially expressed genes.

KEGG enrichment analysis was performed to better understand the functions and interactions of all the DEGs. The top pathway enrichment from the analysis were “Metabolic pathways” (556 DEG), “biosynthesis of secondary metabolite” (198 DEGs), “biosynthesis of antibiotics” (150 DEGs), “autophagy - yeast” (59 DEGs), “RNA degradation” (45 DEGs), “protein processing in endoplasmic reticulum” (61 DEGs), “glycerolipid metabolism” (35 DEGs) and “tryptophan metabolism” (35 DEGs). Figure 5.7 shows the enriched KEGG pathways. Both the GO and KEGG enrichment support our hypothesis that DEG were in fact involved in several of these processes and pathway such as heat shock in stress response, metabolic pathway, protein transport and biosynthesis of secondary metabolites.

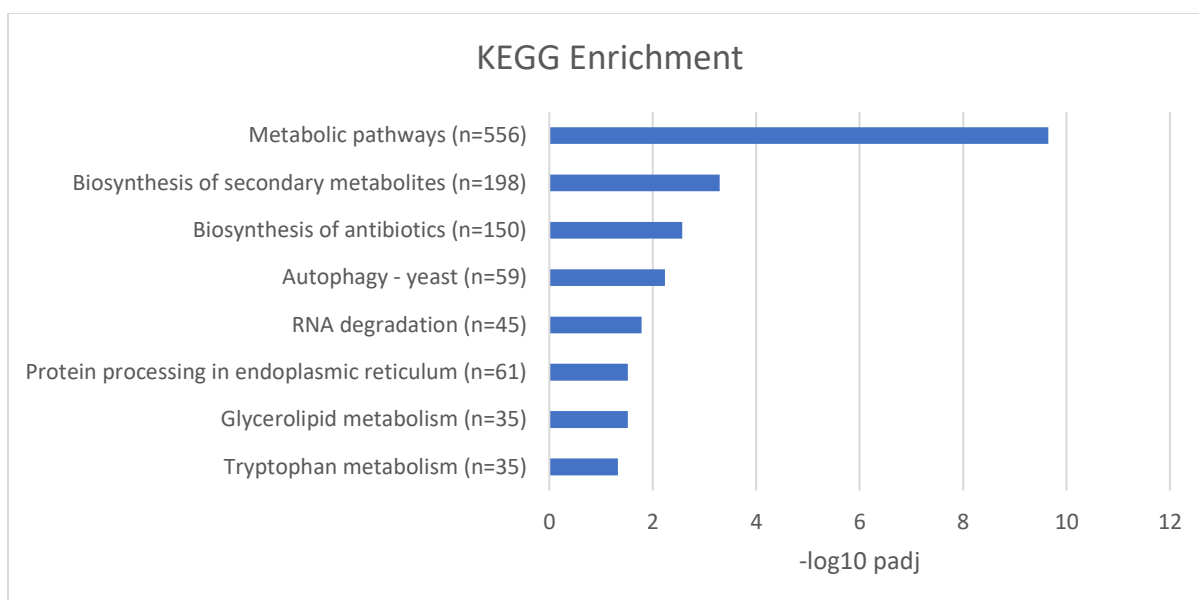


Figure 5.7 Top significant enriched KEGG pathways of differentially expressed gene between high yield and low yield *P. pulmonarius*

### 5.3.5 Validation of DEGs by qPCR

To validate the results of the RNA-seq analysis, five genes were chosen to confirm the expression by quantitative real time polymerase chain reaction (qPCR). The selected genes were aspartyl protease, GTPase-activating protein S23, *CATALASE1*, palmitoyltransferase and copper amine oxidase 1. Figure 1, 2, 3 and 4 in Appendix 4 shows the melt curve analysis of the 5 selected genes plus 2 housekeeping genes. These genes were chosen due to their high log2 fold change value in both extremes (positive and negatives with relation to KEGG pathways. For instance, GTPase activating protein gene is highly upregulated in relation to KEGG term of tryptophan metabolism and copper amine oxidase is highly downregulated in biosynthesis of secondary metabolite, while also gene known for their important role in mushroom growth. These genes relative expression show similar trends according to its log2 fold change results from the RNA-seq analysis output (Table 5.4). The  $2^{-(\Delta\Delta Ct)}$  method calculate the relative gene expression between samples. If low yield type has a higher gene expression value than high yield type, this means the gene is downregulated and vice versa. Two upregulated genes, namely aspartyl protease and GTPase-activating protein S23 show log2 fold change value

of 14.15 and 11.94. While three downregulated genes, namely *CATALASE1*, copper amine oxidase 1, palmitoyltransferase show log2fold change value of -10.92, -15.92, and -13.79 respectively. Figure 5.8 shows the heat map for the selected unigenes used in qPCR. Electron transfer genes and GTP-binding protein were selected as reference genes according to Castanera et al., (2015) . Additional information regarding the selected DEG can be found in Appendix 5 – Table 1 , Table 2 and Table 3.

Table 5.4 Differential expression of selected unigenes for qRT-PCR validation. One-way anova test was performed to obtain the P-value.

Gene name	Relative gene expression	P-value	RNA-Seq	P-value
			log2foldchange	
Palmitoyltransferase	-1.2	0.63	-13.79	$2.54^{-15}$
Copper amine oxidase	-2.5	0.007	-15.92	0
<i>CATALASE1</i>	-2.3	0.066	-10.92	0
GTPase-activating protein	1.03	0.83	11.94	$8.26^{-12}$
Aspartyl protease	288	0.023	14.15	0

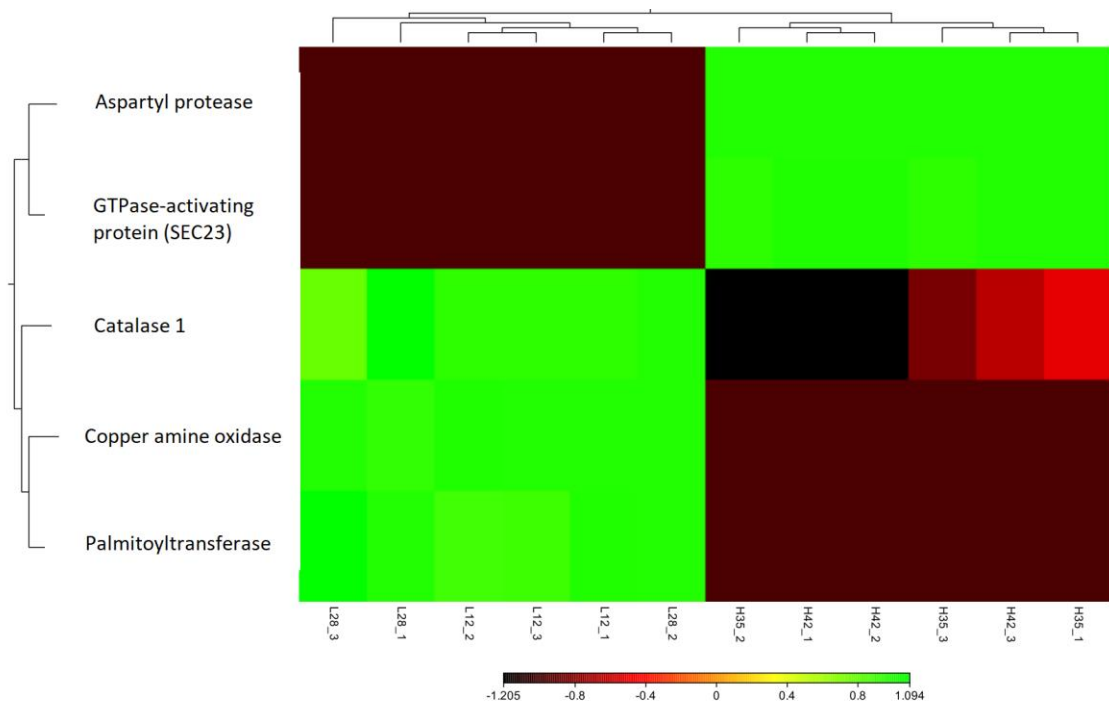


Figure 5.8 Heat map of the RNA-Seq based on FPKM and on selected unigenes tested using qRT-PCR validation. Yellow to green represent upregulation while red to black represent downregulation. High yield types were arranged to the right side while low yield types were on the left side.

## 5.4 Discussion

The final yield in weight of mushroom crop is the most important traits to improve upon, and therefore has been in the subject of multiple studies (Jeznabadi et al., 2016). Cross breeding of mushrooms with good yield (Adebayo et al., 2013), or usage of an alternative substrate such as wheat straw or cotton seed cake (Girmay et al., 2016) were commonly used to improve the yield of *Pleurotus* spp. Based on the results in Section 4.3, we observed that samples belonging to *P. pulmonarius* exhibit vast difference in growth rate and final yield with a standardized substrate and growth conditions. These results suggested that the differences in yield might be contributed by the differential expression of growth-related genes. However, no studies on transcriptomics analyses of *P. pulmonarius* of high and low yield have been performed. We performed comparative transcriptomics analysis to study the differential gene expressed and molecular process in between high yield and low yield *P. pulmonarius*. Our results will reveal genes which plays a role in growth of *P. pulmonarius* and possibly other species in the *Pleurotus* genus.

From the transcriptomic analysis results, a total of 27449 unigenes were differentially expressed in the two comparative groups, whereby 13707 unigenes were upregulated and 13742 unigenes were downregulated in the high yield group as compared to the low yield group (Figure 5.4). Further functional annotation using KEGG enrichment analysis suggested that most (556) of the differentially expressed genes were implicated in metabolic pathways, with the topmost pathway being the biosynthesis of secondary metabolite, followed by biosynthesis of antibiotics, autophagy, RNA degradation, protein processing in endoplasmic reticulum.



## 5.4.1 Specific unigenes chosen from KEGG Enrichment Analysis

### 5.4.1.1 *CATALASE1*

A total of 35 unigenes were involved in the tryptophan metabolism pathway (Figure 5.9). One of the highly downregulated unigene in this pathway is *CATALASE1* [EC: 1.11.1.6]. Catalases are tetramer metalloenzyme and have three gene families, notably manganese catalase, monofunctional catalase and bifunctional catalase (Zámocký et al., 2012). Catalase is made up of 4 subunits and generally functions as an oxidoreductase enzyme by acting on a peroxide as acceptor. The main function of catalase is catalyzing hydrogen peroxide to oxygen and water, essentially reducing oxidative damage and it's considered an antioxidant enzyme (Kwok et al., 2004). Not only that, but *CATALASE1* also converts 3-hydroxyanthranilate to cinnavalininate towards the later stage of tryptophan metabolism pathway. Other than that, catalase in lignin degradation fungi such as *Pleurotus* may protect ligninolytic peroxidases from inactivation by specifically by hydrogen peroxide (Persky et al., 2002).

Usually, a single fungus can have more than one type of catalase, with different roles in stress resistance and development (Chagas et al., 2008). For example, the ascomycota fungi, *Neurospora crassa*, has 4 catalases, namely *CATALASE1* and *CATALASE3* which are monofunctional catalase found in growing hyphae and conidia, while *CATALASE2* is a bifunctional catalase found in heat-stressed mycelia and *CATALASE4* is a monofunctional catalase with unknown role (Noguchi et al., 2007). In basidiomycetes, the button mushroom *Agaricus bisporus* whole genome sequence has revealed 3 catalases sequences (Morin et al., 2012).

The role of catalase in *P. ostreatus* was partly elucidated by Wang et al., (2017) at different stages of development and in response to heat stress in mycelia. The author found that *CATALASE2* performs a catalytic role in breaking hydrogen peroxide down during any life cycle of *P. ostreatus* while *CATALASE1* has an unknown function. The expression level of

*CATALASE1* was highly upregulated and continuous throughout the development stages especially during spore stage. However, there is no catalase activity even with high gene and protein expression. With its high level in spores, *CATALASE1* expression appears to be spore-specific only and it is an indication of its importance in sporulation.

Catalase has also been found to play a role in heavy metal mycoremediation in *Pleurotus*. Cytosolic catalase and peroxisomal catalase were overexpressed in *P. cornucopia* and *P. ostreatus* respectively under cadmium contamination (Xu et al., 2021)

In our results, the specific *CATALASE1* was downregulated in high yield *P. pulmonarius* as compared to low yield type. This may be due to presence of reactive oxygen species, as catalase usually operate in high hydrogen peroxide concentrations (Diaz & Plummer, 2018), that is affecting the low yield type, hence the increase of *CATALASE1* expression which directed the resource and energy away from further growth. The possibility of heat as a stress factor was minimized as the growth condition was constant in terms of temperature and humidity. Another possibility is that *CATALASE1* activity is negligible in *P. pulmonarius* similar to *P. ostreatus* and it does not play a role in determining the growth rate during cultivation. Notably, with its high fold change value based on RNA-Seq results, it can be a potential biomarker for low yield *P. pulmonarius*.

While unlikely, the low yield *P. pulmonarius* might contain heavy metals which can inhibit fungal growth (Li et al., 2017), hence the upregulation of catalase to combat the heavy metal stress.

Additionally, *P. ostreatus* under heat stress has been shown to have increased overall amino acid contents including L-tryptophan (Yan et al., 2020). The downregulation of catalase in tryptophan metabolism according to our results, suggest that there could be reduced metabolism of tryptophan in high yield *P. pulmonarius* which were cultivated at low temperature.

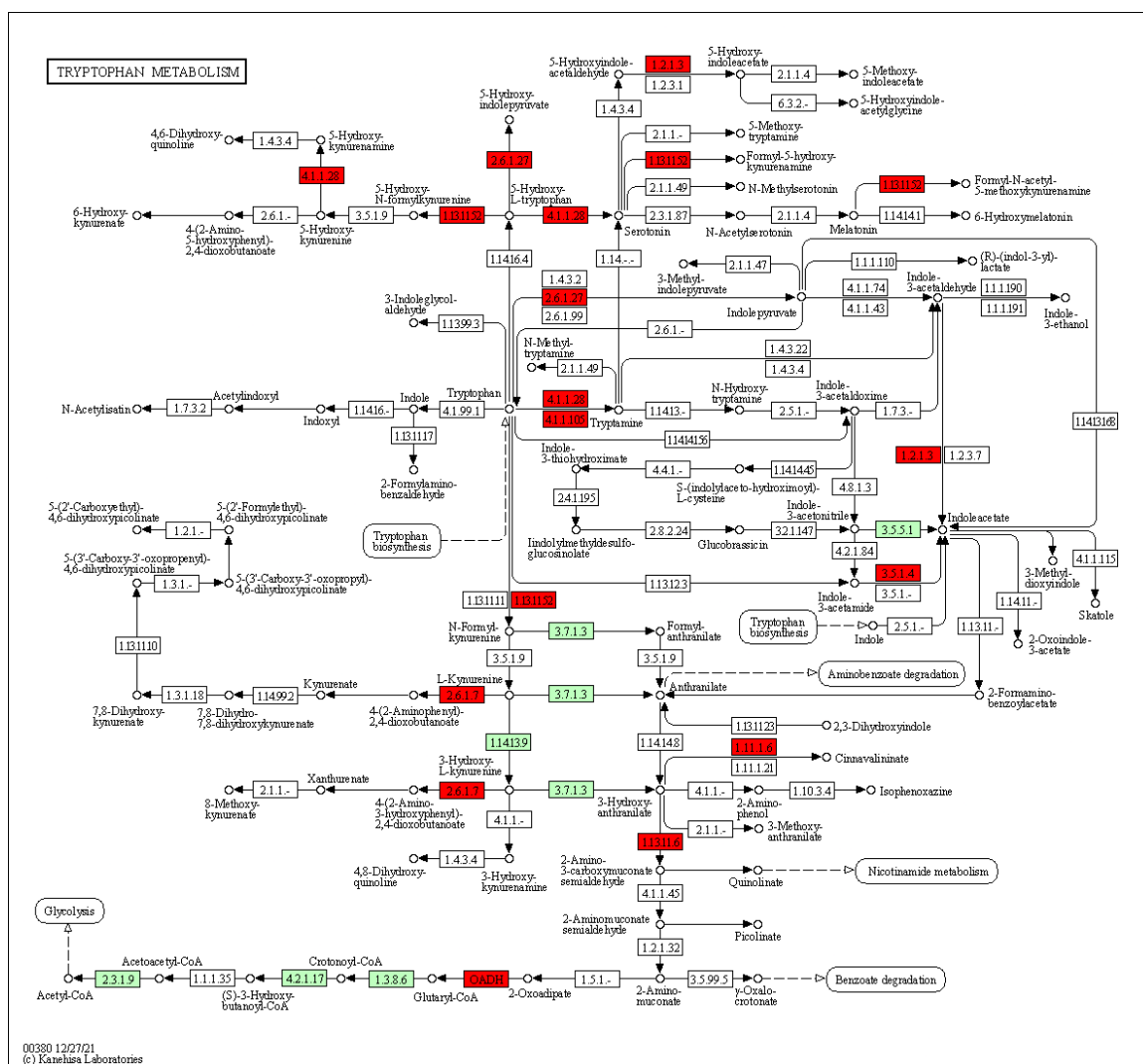


Figure 5.9 Tryptophan metabolism pathways from KEGG database. The red box indicates known DEG that can be found in *P. pulmonarius* transcriptome in this study while green box indicates known gene based on the basidiomycete *Agaricus bisporus* genome.

#### 5.4.1.2 GTPase-activating protein SEC23

Other than that, the term “protein processing in endoplasmic reticulum” is also one of the most enriched KEGG pathways with 61 unigenes (Figure 5.10). One of the upregulated unigene in this pathway is GTPase-activating protein S23 (SEC23). The SEC23/24 helical domain is one of the three components responsible for the formation of coat protein

complex II (COPII)- coated vesicle which carries protein from the endoplasmic reticulum into the Golgi apparatus (Lederkremer et al., 2001). SEC23 functions as a GTPase-activating protein (GAP) mediated by an arginine residue that is inserted into the active site of Sar1.

While there are limited studies on GAP SEC23 specifically on the fungi kingdom, most studies in relation to GAP on fungi were on small G protein (Ras). GAPs control small GTP-binding proteins like Ras by boosting the G-protein's inherent GTPase activity, leading to the molecule becoming inactive and bound to GDP (Boguski & McCormick, 1993). GAP Ras in dikaryon *S. commune* has been found to influence both colony growth and fruiting body development (Yamagishi et al., 2004). Furthermore, GAP controlling FgFab1 gene in the fungus *Fusarium graminearum* were found to be vital in vegetative growth and conidiation (Zheng et al., 2021). These GAP studies on these fungi may suggest that the GAP SEC23 in *P. pulmonarius* functions in protein transport that regulates fruiting body development and growth as supported by upregulation of GAP SEC23 in high yield type (Zheng et al., 2021).



with exposed carbohydrate head group towards the extracellular space. The role of GSL have been associated with cell division, adhesion, and motility, signal transduction pathways such as carbohydrate-carbohydrate interactions and finally control of cell phenotypes (Hakomori, 2008).

Heat stress in the fungi *S. cerevisiae* activates serine palmitoyltransferase, which leads to increase in sphingoid bases (Dickson et al., 1997). Furthermore, serine palmitoyltransferase was also upregulated in reaction to stress such as damage to the DNA and nutrient starvation, which in turns contributes to degradation of nutrient permeases which is vital for growth (Chung et al., 2000). The role of serine palmitoyltransferase is not well studied in basidiomycetes and specifically *Pleurotus* while role of GSL is mostly studied in pathogenic fungi such as *Cryptococcus neoformans* (Guimarães et al., 2014). Additionally, many studies on antifungal have targeted inhibition of serine palmitoyltransferase due to its important role in GSL synthesis (Vicente et al., 2003). This suggests that serine palmitoyltransferase plays a vital role in fungal development and may perform similar roles in the growth of *Pleurotus*.



#### 5.4.1.4 Copper amine oxidases

The KEGG term “Biosynthesis of secondary metabolite” is the second most enriched term with 198 unigene under this category. There are multiple other KEGG pathway under this term including phenylalanine metabolism (Figure 5.12). The most downregulated unigene in this term is the copper amine oxidase gene [EC: 1.4.3.21]. As the name suggests, copper amine oxidases are an enzyme which utilized copper as a cofactor, which play a vital aspect in basic cellular functions including respiration, elimination of harmful superoxide ions, transportation of iron, and metabolism of amine (Festa & Thiele, 2011). Copper amine oxidases have been identified in yeasts, fungi, bacteria plants, and humans (MacPherson & Murphy, 2007). Copper amine oxidase catalase oxygen and amine into aldehyde, ammonia, and hydrogen peroxide. Study on the fungi *S. pombe* shows that the copper transport mechanisms including the copper amine oxidase enzymes play a vital role in meiosis growth (Peter et al., 2008). While some studies have screened for copper amine oxidase in other fungi such as *Syncephalastrum racemosum* (Hirano et al., 2016) and *Aspergillus carbonarius* (Sugawara et al., 2015), these studies were lacking in the elucidation of the functional characteristics of these enzymes in terms of fungal growth. In addition, there are also no studies on copper amine oxidase in basidiomycetes as of time of writing. However, copper amine oxidases have been widely studied in plants model and shown to play a role in stress related growth response and wound healing response (Cona et al., 2014).





protease (Yin et al., 2014). Aspartyl protease is special enzyme and plays a role in metabolism, cellular signaling and have special application in pharmaceutical and chemical industry (Kudryavtseva et al., 2008). In fungi, aspartyl protease is involved in germination and sporulation and appears to be involved heavily during the whole life cycle of *Pleurotus citrinopileatus* (Cui et al., 2007). Production of aspartyl protease are stimulated by the reduction of nitrogen content in the substrate (Watkinson et al., 2001). This observation is further reinforced by Johnston et al., (2000) in which protease production are detected in low nitrogen substrate. Multiple *Pleurotus* species also produce aspartyl protease to aid in the ligninolysis process and at specific life cycle, protease also degrades laccase enzymes (Cha et al., 2010; Cui et al., 2007; Palmieri et al., 2000).

## **Chapter 6: Summary, conclusion, and future prospects.**

The three DNA barcode designed in this study has identified 16 *P. pulmonarius* and eight *P. eryngii* among the samples in MARDI library. Construction of the phylogenetic tree showed that the 16 *P. pulmonarius* were the same variant while the eight *P. eryngii* may originated from two to three different variant. Among the three designed DNA barcode, internal transcribed spacer (ITS) was the best for Malaysia *Pleurotus* identification as it has high amplification rate and greater mean on interspecific variation than mean of intraspecific variation (Chapter 3).

The antioxidant activities analysis showed that *P. pulmonarius* mycelial aqueous extract had higher antioxidant properties compared to *P. eryngii* and other *Pleurotus* samples mycelial. Interestingly, *P. pulmonarius* fruiting bodies aqueous extract had a lower antioxidant properties as compared to their mycelial counterpart. Proximate analysis of fruiting bodies of *P. pulmonarius* showed high moisture and ash content, medium protein content and low lipid content. MP35, MP42 and MP34 had the highest biological efficiency out of the ten *P. pulmonarius* samples that managed to fruit, while MP34 possesses the fastest complete growth. Henceforth, MP34 was suggested as the highest-ranked strain in this study for cultivation in the agriculture industry as it had the fastest complete growth, third highest biological efficiency with an average antioxidant properties. MP35, MP42 were considered as high yield as these samples had highest biological efficiency while MP2 and MP12 were considered as low yield as these samples had lowest biological efficiency (Chapter 4).

Comparative transcriptomics analysis of high- vs low-yield of *P. pulmonarius* samples revealed that 27449 significantly differentially expressed genes (DEG) ( $p_{adj} < 0.05$ ) which included 13707 upregulated and 13742 downregulated genes among both samples. Remarkably, heat map analysis provided a strong evidence of differential gene expression, depicting sets of expressed genes that clearly distinguished between the high-yield and low-yield groups, but were shared within their respective groups. This further supported our hypothesis that gene expression contributed significantly to the underlying biological

efficiency of *P. pulmonarius*. Kyoto Encyclopedia Genes and Genomes (KEGG) enrichment analysis of DEG revealed top five KEGG pathways which were “metabolic pathways”, “biosynthesis of secondary metabolite”, “biosynthesis of antibiotics”, “autophagy - yeast”, “RNA degradation”, “protein processing in endoplasmic reticulum”, “glycerolipid metabolism” and “tryptophan metabolism”. *Pleurotus* may produce antibiotics as part of their defense mechanisms. These antibiotics can inhibit the growth of competing microorganisms and protect the mushroom from infections during its growth. Protein processing in endoplasmic reticulum pathway plays a vital role in generating functional protein that might serves in *Pleurotus* growth and development through various cellular functions. Tryptophan is an amino acid that served as a precursor for the synthesis of various bioactive compounds. In *Pleurotus*, tryptophan metabolism contributed to the production of compounds with physiological roles in growth and development. One gene was chosen in each pathway for its high log2 fold change value in both extremes (positive and negatives with relation to KEGG pathways) and qPCR was performed to validate the transcriptomic results. The selected gene were *CATALASE1*, GTP activating protein SEC23, serine palmitoyltransferase, copper amine oxidase and aspartyl protease could be used as molecular biomarkers to differentiate high and low yield *P. pulmonarius* strain before large-scale commercial cultivation to help save cost and time (Chapter 5).

One of the recommendations for future studies is to include *P. eryngii* in all the conducted experiments. In the current study, the mushroom house used was unable to produce a low enough temperature to induce the fruiting of *P. eryngii*. By including *P. eryngii*, we could produce more data in terms of fruiting bodies biological efficiency, antioxidants and phenolic contents which could serve as an additional biomarker to identifying high and low yield *P. eryngii*. Furthermore, transcriptomics analysis of high vs low *P. eryngii* can produce differential expressed genes which in turns can identified potential genes of interest as additional biomarkers specifically for *P. eryngii*.

The second recommendation for future studies is to perform functional validation through CRISPR/Cas9 gene knockout technology for the five identified genes. Knocking out these gene and then cultivate the transgenic oyster mushroom could elucidate the

gene specific roles and functions accurately in terms of yield, complete growth, antioxidants properties and phenolic content of *P. pulmonarius*. The third recommendation for future studies is to perform genomics and proteomics studies of the current *P. pulmonarius* to further validate the current transcriptomic results. The genomic sequencing of *P. pulmonarius* is also important as there is currently no reference genome for this species. The identified five genes could also be tested on other *Pleurotus* species to determine if these genes can differentiate between high and low yield in other species other than *P. pulmonarius*.

## **References**

- Abrams, D., Metcalf, D., & Hojjatie, M. (2014). Determination of Kjeldahl Nitrogen in Fertilizers by AOAC Official Method 978.02: Effect of Copper Sulfate as a Catalyst. *Journal of AOAC INTERNATIONAL*, 97(3), 764–767. <https://doi.org/10.5740/jaoacint.13-299>
- Adebayo, E. A., Oloke, J. K., Yadav, A., Barooah, M., & Bora, T. C. (2013). Improving yield performance of *Pleurotus pulmonarius* through hyphal anastomosis fusion of dikaryons. *World Journal of Microbiology and Biotechnology* 2013 29:6, 29(6), 1029–1037. <https://doi.org/10.1007/S11274-013-1266-8>
- Adebayo, & Martínez. (2015). Oyster mushrooms (*Pleurotus*) are useful for utilizing lignocellulosic biomass. *African Journal of Biotechnology*, 14, 52–67.
- Adejumo, T. O., & Awosanya, O. B. (2005). Proximate and mineral composition of four edible mushroom species from South Western Nigeria. *African Journal of Biotechnology*, 4(10).
- Adeniyi, M., Titilawo, Y., Oluduro, A., Odeyemi, O., Nakin, M., & Okoh, A. I. (2018). Molecular identification of some wild Nigerian mushrooms using internal transcribed spacer: polymerase chain reaction. *AMB Express*, 8(1), 148. <https://doi.org/10.1186/s13568-018-0661-9>
- Ainsworth, E. A., & Gillespie, K. M. (2007). Estimation of total phenolic content and other oxidation substrates in plant tissues using Folin–Ciocalteu reagent. *Nature Protocols*, 2(4), 875–877.
- Akinmusire, O. O., Omomowo, I. O., & Oguntoye, S. I. K. (2011). Cultivation performance of *Pleurotus pulmonarius* in Maiduguri, North Eastern Nigeria, using wood chippings and rice straw waste. *Advances in Environmental Biology*, 2091–2095.

Aktumsek, A., Zengin, G., Guler, G. O., Cakmak, Y. S., & Duran, A. (2011). Screening for in vitro antioxidant properties and fatty acid profiles of five *Centaurea L.* species from Turkey flora. *Food and Chemical Toxicology*, 49(11), 2914–2920.

Ali, M. A., Gyulai, G., Hidvegi, N., Kerti, B., Al Hemaïd, F. M. A., Pandey, A. K., & Lee, J. (2014). The changing epitome of species identification–DNA barcoding. *Saudi Journal of Biological Sciences*, 21(3), 204–231.

Association of Official Analytical Chemists. (1997). Official methods of analysis of the Association of Official Analytical Chemists.

Atri, N. S., Sharma, S. K., Joshi, R., Gulati, A., & Gulati, A. (2013). Nutritional and nutraceutical composition of five wild culinary-medicinal species of genus *Pleurotus* (higher Basidiomycetes) from northwest India. *International Journal of Medicinal Mushrooms*, 15(1).

Avin, F. A., Bhassu, S., Shin, T. Y., & Sabaratnam, V. (2012). Molecular classification and phylogenetic relationships of selected edible Basidiomycetes species. *Molecular Biology Reports*, 39(7), 7355–7364. <https://doi.org/10.1007/S11033-012-1567-2>

Avin, F. A., Bhassu, S., Tan, Y. S., Shahbazi, P., & Vikineswary, S. (2014). Molecular divergence and species delimitation of the cultivated oyster mushrooms: integration of IGS1 and ITS. *The Scientific World Journal*, 2014. <https://doi.org/10.1155/2014/793414>

Babasaki, K., Neda, H., & Murata, H. (2007). megB1, a novel macroevolutionary genomic marker of the fungal phylum Basidiomycota. *Bioscience, Biotechnology, and Biochemistry*, 71(8), 1927–1939.

Bamigboye, C. O., Oloke, J. K., & Dames, J. F. (2019). Development of high yielding strain of *Pleurotus tuber-regium*: fructification, nutritional and phylogenetic studies. *Journal of Food Science and Technology*, 56(8), 3597–3608.

Bao, D., Kinugasa, S., & Kitamoto, Y. (2004). The biological species of oyster mushrooms (*Pleurotus* spp.) from Asia based on mating compatibility tests. *Journal of Wood Science*, 50(2), 162–168. <https://doi.org/10.1007/S10086-003-0540-Z/METRICS>

Barh, A., Sharma, V. P., Annepu, S. K., Kamal, S., Sharma, S., & Bhatt, P. (2019). Genetic improvement in *Pleurotus* (oyster mushroom): a review. *3 Biotech*, 9(9), 322. <https://doi.org/10.1007/s13205-019-1854-x>

Bastola, K. P., Guragain, Y. N., Bhadriraju, V., & Vadlani, P. V. (2017). Evaluation of standards and interfering compounds in the determination of phenolics by Folin-Ciocalteu assay method for effective bioprocessing of biomass. *American Journal of Analytical Chemistry*, 8(6), 416–431.

Beckman, K. B., & Ames, B. N. (1998). The free radical theory of aging matures. *Physiological Reviews*.

Bellanger, J. M., Moreau, P. A., Corriol, G., Bidaud, A., Chalange, R., Dudova, Z., & Richard, F. (2015). Plunging hands into the mushroom jar: a phylogenetic framework for *Lyophyllaceae* (Agaricales, Basidiomycota). *Genetica* 2015 143:2, 143(2), 169–194. <https://doi.org/10.1007/S10709-015-9823-8>

Benjamini, Y., & Hochberg, Y. (1995). Controlling the False Discovery Rate: A Practical and Powerful Approach to Multiple Testing. *Journal of the Royal Statistical Society: Series B (Methodological)*, 57(1), 289–300. <https://doi.org/https://doi.org/10.1111/j.2517-6161.1995.tb02031.x>

Bellemain, E., Carlsen, T., Brochmann, C., Coissac, E., Taberlet, P., & Kauserud, H. (2010). ITS as an environmental DNA barcode for fungi: an in silico approach reveals potential PCR biases. *BMC Microbiology*, 10, 1–9.

Beltran-Garcia, M. J., Estarron-Espinosa, M., & Ogura, T. (1997). Volatile Compounds Secreted by the Oyster Mushroom (*Pleurotus ostreatus*) and Their Antibacterial Activities. *Journal of Agricultural and Food Chemistry*, 45(10), 4049–4052. <https://doi.org/10.1021/jf960876i>



Benzie, I. F. F. (2003). Evolution of dietary antioxidants. *Comparative Biochemistry and Physiology Part A: Molecular & Integrative Physiology*, 136(1), 113–126.

[https://doi.org/https://doi.org/10.1016/S1095-6433\(02\)00368-9](https://doi.org/https://doi.org/10.1016/S1095-6433(02)00368-9)

Benzie, I. F. F., & Strain, J. J. (1996). The ferric reducing ability of plasma (FRAP) as a measure of “antioxidant power”: the FRAP assay. *Analytical Biochemistry*, 239(1), 70–76.

Benzie, I. F. F., & Wachtel-Galor, S. (2012). Increasing the antioxidant content of food: a personal view on whether this is possible or desirable. *International Journal of Food Sciences and Nutrition*, 63(sup1), 62–70.

Berch, S. M., Ka, K.-H., Park, H., & Winder, R. (2007). Development and potential of the cultivated and wild-harvested mushroom industries in the Republic of Korea and British Columbia. *Journal of Ecosystems and Management*.

<https://doi.org/10.22230/JEM.2007V8N3A372>

Bernardi, E., Minotto, E., & Nascimento, J. S. do. (2013). Evaluation of growth and production of *Pleurotus* spp. in sterilized substrates. *Arquivos Do Instituto Biológico*, 80, 318–324.

Blois, M. S. (1958). Antioxidant determinations by the use of a stable free radical. *Nature*, 181, 1199–1200.

Boguski, M. S., & McCormick, F. (1993). Proteins regulating Ras and its relatives. *Nature*, 366(6456), 643–654.

Bu, D., Luo, H., Huo, P., Wang, Z., Zhang, S., He, Z., Wu, Y., Zhao, L., Liu, J., Guo, J., Fang, S., Cao, W., Yi, L., Zhao, Y., & Kong, L. (2021). KOBAS-i: intelligent prioritization and exploratory visualization of biological functions for gene enrichment analysis. *Nucleic Acids Research*, 49(W1), W317–W325. <https://doi.org/10.1093/nar/gkab447>

Buchfink, B., Xie, C., & Huson, D. H. (2015). Fast and sensitive protein alignment using DIAMOND. *Nature Methods*, 12(1), 59–60. <https://doi.org/10.1038/nmeth.3176>

Bunyard, B. A., Chaichuchote, S., Nicholson, M. S., & Royse, D. J. (1996). Ribosomal DNA analysis for resolution of genotypic classes of *Pleurotus*. *Mycological Research*, 100(2), 143–150.

Bustin, S. A. (2000). Absolute quantification of mRNA using real-time reverse transcription polymerase chain reaction assays. *Journal of Molecular Endocrinology*, 25(2), 169–193.

Bustin, S. A., Benes, V., Garson, J. A., Helleman, J., Huggett, J., Kubista, M., Mueller, R., Nolan, T., Pfaffl, M. W., & Shipley, G. L. (2009). *The MIQE Guidelines: Minimum Information for Publication of Quantitative Real-Time PCR Experiments*. Oxford University Press.

Castanera, R., López-Varas, L., Pisabarro, A. G., & Ramírez, L. (2015). Validation of reference genes for transcriptional analyses in *Pleurotus ostreatus* by using reverse transcription-quantitative PCR. *Applied and Environmental Microbiology*, 81(12), 4120–4129.

Cha, W.-S., Park, S.-S., Kim, S.-J., & Choi, D. (2010). Biochemical and enzymatic properties of a fibrinolytic enzyme from *Pleurotus eryngii* cultivated under solid-state conditions using corn cob. *Bioresource Technology*, 101(16), 6475–6481.

Chagas, R. F., Bailão, A. M., Pereira, M., Winters, M. S., Smullian, A. G., Deepe Jr, G. S., & de Almeida Soares, C. M. (2008). The catalases of *Paracoccidioides brasiliensis* are differentially regulated: protein activity and transcript analysis. *Fungal Genetics and Biology*, 45(11), 1470–1478.

Chen, S.-Y., Ho, K.-J., Hsieh, Y.-J., Wang, L.-T., & Mau, J.-L. (2012). Contents of lovastatin,  $\gamma$ -aminobutyric acid and ergothioneine in mushroom fruiting bodies and mycelia. *LWT*, 47(2), 274–278. [https://doi.org/https://doi.org/10.1016/j.lwt.2012.01.019](https://doi.org/10.1016/j.lwt.2012.01.019)

Chen, F., Xiong, S., Sundelin, J., Martín, C., & Hultberg, M. (2020). Potential for combined production of food and biofuel: Cultivation of *Pleurotus pulmonarius* on soft- and

hardwood sawdusts. *Journal of Cleaner Production*, 266, 122011.

<https://doi.org/https://doi.org/10.1016/j.jclepro.2020.122011>

Choi, M. H., & Kim, G. H. (2002). Quality changes in *Pleurotus ostreatus* during modified atmosphere storage as affected by temperatures and packaging material. XXVI International Horticultural Congress: Issues and Advances in Postharvest Horticulture 628, 357–362.

Chung, N., Jenkins, G., Hannun, Y. A., Heitman, J., & Obeid, L. M. (2000). Sphingolipids signal heat stress-induced ubiquitin-dependent proteolysis. *Journal of Biological Chemistry*, 275(23), 17229–17232.

Cona, A., Tisi, A., Ghuge, S. A., Franchi, S., De Lorenzo, G., & Angelini, R. (2014). Wound healing response and xylem differentiation in tobacco plants over-expressing a fungal endopolygalacturonase is mediated by copper amine oxidase activity. *Plant Physiology and Biochemistry*, 82, 54–65.

Conesa, A., Götz, S., García-Gómez, J. M., Terol, J., Talón, M., & Robles, M. (2005). Blast2GO: a universal tool for annotation, visualization and analysis in functional genomics research. *Bioinformatics*, 21(18), 3674–3676.

Conesa, A., Madrigal, P., Tarazona, S., Gomez-Cabrero, D., Cervera, A., McPherson, A., Szczesniak, M. W., Gaffney, D. J., Elo, L. L., & Zhang, X. (2016). A survey of best practices for RNA-seq data analysis. *Genome Biology*, 17(1), 1–19.

Corrêa, R. C. G., Brugnari, T., Bracht, A., Peralta, R. M., & Ferreira, I. C. F. R. (2016). Biotechnological, nutritional and therapeutic uses of *Pleurotus* spp. (Oyster mushroom) related with its chemical composition: A review on the past decade findings. *Trends in Food Science & Technology*, 50, 103–117. <https://doi.org/10.1016/J.TIFS.2016.01.012>

Croan, S. C. (2004). Conversion of conifer wastes into edible and medicinal mushrooms. *Forest Products Journal*. Vol. 54, No. 2 (Feb. 2004). Pages 68-76. <https://www.fs.usda.gov/research/treesearch/6353>

Cui, L., Liu, Q. H., Wang, H. X., & Ng, T. B. (2007). An alkaline protease from fresh fruiting bodies of the edible mushroom *Pleurotus citrinopileatus*. *Applied Microbiology and Biotechnology*, 75, 81–85.

Dawidowicz, L. (2021). Cultivation of oyster mushrooms (*Pleurotus* spp.) using organic waste: an example with *Pleurotus pulmonarius* (Fr.) Quel. *Folia Biologica et Oecologica*, 17, 104–110. <https://doi.org/10.18778/1730-2366.16.21>

de Queiroz Cancian, M. A., de Almeida, F. G., Terhaag, M. M., de Oliveira, A. G., de Souza Rocha, T., & Spinosa, W. A. (2018). *Curcuma longa* L.-and *Piper nigrum*-based hydrolysate, with high dextrose content, shows antioxidant and antimicrobial properties. *LWT*, 96, 386–394.

Debivort. (2006). Basidium schematic.

[https://upload.wikimedia.org/wikipedia/commons/a/a6/Basidium\\_schematic.svg](https://upload.wikimedia.org/wikipedia/commons/a/a6/Basidium_schematic.svg)

Diaz, J. M., & Plummer, S. (2018). Production of extracellular reactive oxygen species by phytoplankton: past and future directions. *Journal of Plankton Research*, 40(6), 655–666.

Dickson, R. C., Nagiec, E. E., Skrzypek, M., Tillman, P., Wells, G. B., & Lester, R. L. (1997). Sphingolipids Are Potential Heat Stress Signals in *Saccharomyces*. *Journal of Biological Chemistry*, 272(48), 30196–30200.

Dupuis, J. R., Roe, A. D., & Sperling, F. A. H. (2012). Multi-locus species delimitation in closely related animals and fungi: one marker is not enough. *Molecular Ecology*, 21(18), 4422–4436.

Edgar, R. C. (2004). MUSCLE: multiple sequence alignment with high accuracy and high throughput. *Nucleic Acids Research*, 32(5), 1792. <https://doi.org/10.1093/NAR/GKH340>

Elisashvili, V., Kachlishvili, E., & Penninckx, M. (2008). Lignocellulolytic enzymes profile during growth and fruiting of *Pleurotus ostreatus* on wheat straw and tree leaves. *Acta Microbiologica et Immunologica Hungarica*, 55(2), 157–168.

Erjavec, J., Kos, J., Ravnikar, M., Dreo, T., & Sabotič, J. (2012). Proteins of higher fungi—from forest to application. *Trends in Biotechnology*, 30(5), 259–273.

Estrada, A. E. R., Jimenez-Gasco, M. del M., & Royse, D. J. (2010). *Pleurotus eryngii* species complex: sequence analysis and phylogeny based on partial EF1 $\alpha$  and RPB2 genes. *Fungal Biology*, 114(5–6), 421–428.

<https://doi.org/10.1016/J.FUNBIO.2010.03.003>

Estrada, A. E. R., & Royse, D. J. (2007). Yield, size, and bacterial blotch resistance of *Pleurotus eryngii* grown on cottonseed hulls/oak sawdust supplemented with manganese, copper and whole ground soybean. *Bioresource Technology*, 98(10), 1898–1906.

Festa, R. A., & Thiele, D. J. (2011). Copper: an essential metal in biology. *Current Biology*, 21(21), R877–R883.

Frøslev, T. G., Matheny, P. B., & Hibbett, D. S. (2005). Lower level relationships in the mushroom genus *Cortinarius* (Basidiomycota, Agaricales): a comparison of RPB1, RPB2, and ITS phylogenies. *Molecular Phylogenetics and Evolution*, 37(2), 602–618.

Ge, S. X., Jung, D., & Yao, R. (2020). ShinyGO: a graphical gene-set enrichment tool for animals and plants. *Bioinformatics*, 36(8), 2628–2629.

<https://doi.org/10.1093/bioinformatics/btz931>

Gil-Ramírez, A., Pavo-Caballero, C., Baeza, E., Baenas, N., Garcia-Viguera, C., Marín, F. R., & Soler-Rivas, C. (2016). Mushrooms do not contain flavonoids. *Journal of Functional Foods*, 25, 1–13. <https://doi.org/https://doi.org/10.1016/j.jff.2016.05.005>

Girmay, Z., Gorems, W., Birhanu, G., & Zewdie, S. (2016). Growth and yield performance of *Pleurotus ostreatus* (Jacq. Fr.) Kumm (oyster mushroom) on different substrates. *AMB Express*, 6(1), 1–7. <https://doi.org/10.1186/S13568-016-0265-1/TABLES/4>

- Golak-Siwulska, I., Kałużewicz, A., Spizewski, T., Siwulski, M., & Sobieralski, K. (2018). Bioactive compounds and medicinal properties of Oyster mushrooms (*Pleurotus* spp.). *Folia Horticulturae*, 30(2), 191–201. <https://doi.org/10.2478/FHORT-2018-0012>
- Goldschmidt, S., & Renn, K. (1922). Zweiwertiger Stickstoff: Über das  $\alpha$ ,  $\alpha$ -Diphenyl- $\beta$ -trinitrophenyl-hydrazyl.(IV. Mitteilung über Amin-Oxydation). *Berichte Der Deutschen Chemischen Gesellschaft (A and B Series)*, 55(3), 628–643.
- Gonzalez, P., & Labarère, J. (2000). Phylogenetic relationships of *Pleurotus* species according to the sequence and secondary structure of the mitochondrial small-subunit rRNA V4, V6 and V9 domains. *Microbiology*, 146(1), 209–221.
- Gume, B., Muleta, D., & Abate, D. (2013). Evaluation of locally available substrates for cultivation of oyster mushroom (*Pleurotus ostreatus*) in Jimma, Ethiopia. *African Journal of Microbiology Research*, 7(20), 2228–2237.
- Guimarães, L. L., Toledo, M. S., Ferreira, F. A. S., Straus, A. H., & Takahashi, H. K. (2014). Structural diversity and biological significance of glycosphingolipids in pathogenic and opportunistic fungi. *Frontiers in Cellular and Infection Microbiology*, 4, 138.
- Gupta, B., Niranjana Reddy, B. P., & Kotasthane, A. S. (2011). Molecular characterization and mating type analysis of oyster mushroom (*Pleurotus* spp.) using single basidiospores for strain improvement. *World Journal of Microbiology and Biotechnology*, 27(1), 1–9. <https://doi.org/10.1007/s11274-010-0419-2>
- Gupta, D. (2015). Methods for determination of antioxidant capacity: A review. *International Journal of Pharmaceutical Sciences and Research*, 6(2), 546.
- Hakomori, S. (2008). Structure and function of glycosphingolipids and sphingolipids: recollections and future trends. *Biochimica et Biophysica Acta (BBA)-General Subjects*, 1780(3), 325–346.
- Halliwell, B., & Gutteridge, J. M. C. (2007). *Free radicals in biology and medicine*. Oxford university press, USA.

He, X.-L., Li, Q., Peng, W.-H., Zhou, J., Cao, X.-L., Wang, D., Huang, Z.-Q., Tan, W., Li, Y., & Gan, B.-C. (2017). Intra- and inter-isolate variation of ribosomal and protein-coding genes in *Pleurotus*: implications for molecular identification and phylogeny on fungal groups. *BMC Microbiology*, 17(1), 139. <https://doi.org/10.1186/s12866-017-1046-y>

Hebert, P. D. N., Cywinska, A., Ball, S. L., & DeWaard, J. R. (2003). Biological identifications through DNA barcodes. *Proceedings of the Royal Society of London. Series B: Biological Sciences*, 270(1512), 313–321.

Hillis, D. M., & Bull, J. J. (1993). An empirical test of bootstrapping as a method for assessing confidence in phylogenetic analysis. *Systematic Biology*, 42(2), 182–192.

Hirano, Y., Chonan, K., Murayama, K., Sakasegawa, S., Matsumoto, H., & Sugimori, D. (2016). *Syncephalastrum racemosum* amine oxidase with high catalytic efficiency toward ethanolamine and its application in ethanolamine determination. *Applied Microbiology and Biotechnology*, 100(9), 3999–4013. <https://doi.org/10.1007/s00253-015-7198-5>

Ho, L.-H., Zulkifli, N. A., & Tan, T.-C. (2020). Edible mushroom: nutritional properties, potential nutraceutical values, and its utilisation in food product development. *An Introduction to Mushroom*, 10.

Horn, B. W., & Dorner, J. W. (2002). Effect of competition and adverse culture conditions on aflatoxin production by *Aspergillus flavus* through successive generations. *Mycologia*, 94(5), 741–751.

Hsu, C.-M., Hameed, K., Cotter, V. T., & Liao, H.-L. (2018). Isolation of Mother Cultures and Preparation of Spawn for Oyster Mushroom Cultivation: SL449/SS663, 1/2018. *EDIS*, 2018(1). <https://doi.org/10.32473/edis-ss663-2018>

Ijeh, I. I., Okwujiako, I. A., Nwosu, P. C., & Nnodim, H. I. (2009). Phytochemical composition of *Pleurotus tuber regium* and effect of its dietary incorporation on body/organ weights and serum triacylglycerols in albino mice. *Journal of Medicinal Plants Research*, 3(11), 939–943.

- Jang, K.-Y., Oh, Y.-L., Oh, M., Woo, S.-I., Shin, P.-G., Im, J., & Kong, W.-S. (2016). Introduction of the representative mushroom cultivars and groundbreaking cultivation techniques in Korea. *Journal of Mushroom*, 14(4), 136–141. <https://doi.org/10.14480/JM.2016.14.4.136>
- Jatwa, T. K., Apet, K. T., Wagh, S. S., Sayyed, K. S., Rudrappa, K. B., & Sornapriya, S. P. (2016). Evaluation of various agro-wastes for production of *Pleurotus* spp. (*P. Florida*, *P. Sajor-caju* and *P. Eous*). *Journal of Pure and Applied Microbiology*, 10(4), 2783–2792. <https://doi.org/10.22207/JPAM.10.4.37>
- Jegadeesh, R., Lakshmanan, H., Kab-Yeul, J., Sabaratnam, V., & Raaman, N. (2018). Cultivation of Pink Oyster mushroom *Pleurotus djamor* var. *roseus* on various agro-residues by low cost technique. *J Mycopathol Res*, 56(3), 213–220.
- Jeznabadi, E. K., Jafarpour, M., & Eghbalsaied, S. (2016). King oyster mushroom production using various sources of agricultural wastes in Iran. *International Journal of Recycling of Organic Waste in Agriculture*, 5(1), 17–24. <https://doi.org/10.1007/S40093-015-0113-3/FIGURES/4>
- Johnston, J. M., Ramos, E. R., Bilbrey, R. E., Gathman, A. C., & Lilly, W. W. (2000). Characterization of ScPrI, a small serine protease, from mycelia of *Schizophyllum commune*. *Mycological Research*, 104(6), 726–731.
- Jonathan, S., An, O., Garuba, E., & Babayemi, O. (2012). Bioconversion of sorghum stalk and rice straw into value added ruminant feed using *Pleurotus pulmonarius*.
- Kakon, A. J., Choudhury, M. B. K., & Saha, S. (2012). Mushroom is an ideal food supplement. *Journal of Dhaka National Medical College & Hospital*, 18(1), 58–62.
- Khan, M. A., & Tania, M. (2012). Nutritional and medicinal importance of *Pleurotus* mushrooms: an overview. *Food Reviews International*, 28(3), 313–329.



- Kibar, B., & Peksen, A. (2008). Modelling the effects of temperature and light intensity on the development and yield of different *Pleurotus* species. *Agric Trop Subtrop*, 41(2), 68–73.
- Kiss, L. (2012). Limits of nuclear ribosomal DNA internal transcribed spacer (ITS) sequences as species barcodes for Fungi. *Proceedings of the National Academy of Sciences*, 109(27), E1811–E1811.
- Knop, D., Yarden, O., & Hadar, Y. (2015). The ligninolytic peroxidases in the genus *Pleurotus*: divergence in activities, expression, and potential applications. *Applied Microbiology and Biotechnology*, 99, 1025–1038.
- Kudryavtseva, O. A., Dunaevsky, Y. E., Kamzolkina, O. V., & Belozersky, M. A. (2008). Fungal proteolytic enzymes: Features of the extracellular proteases of xylotrophic basidiomycetes. *Microbiology* (00262617), 77(6).
- Kukurba, K. R., & Montgomery, S. B. (2015). RNA sequencing and analysis. *Cold Spring Harbor Protocols*, 2015(11), pdb-top084970.
- Kumar, S., Stecher, G., & Tamura, K. (2016). MEGA7: Molecular Evolutionary Genetics Analysis Version 7.0 for Bigger Datasets. *Molecular Biology and Evolution*, 33(7), 1870–1874. <https://doi.org/10.1093/MOLBEV/MSW054>
- Kwok, L. Y., Schlüter, D., Clayton, C., & Soldati, D. (2004). The antioxidant systems in *Toxoplasma gondii* and the role of cytosolic catalase in defence against oxidative injury. *Molecular Microbiology*, 51(1), 47–61.
- Lahaye, R., Van der Bank, M., Bogarin, D., Warner, J., Pupulin, F., Gigot, G., Maurin, O., Duthoit, S., Barraclough, T. G., & Savolainen, V. (2008). DNA barcoding the floras of biodiversity hotspots. *Proceedings of the National Academy of Sciences*, 105(8), 2923–2928.

- Lederkremer, G. Z., Cheng, Y., Petre, B. M., Vogan, E., Springer, S., Schekman, R., Walz, T., & Kirchhausen, T. (2001). Structure of the Sec23p/24p and Sec13p/31p complexes of COPII. *Proceedings of the National Academy of Sciences*, 98(19), 10704–10709.
- Lee, H.-J., Kim, S.-W., Ryu, J.-S., Lee, C.-Y., & Ro, H.-S. (2014). Isolation of a variant strain of *Pleurotus eryngii* and the development of specific DNA markers to identify the variant strain. *Mycobiology*, 42(1), 46–51.
- Li, A., Begin, M., Kokurewicz, K., Bowden, C., & Horgen, P. A. (1994). Inheritance of strain instability (sectoring) in the commercial button mushroom, *Agaricus bisporus*. *Applied and Environmental Microbiology*, 60(7), 2384–2388.
- Li, J., He, X., Liu, X.-B., Yang, Z. L., & Zhao, Z.-W. (2017). Species clarification of oyster mushrooms in China and their DNA barcoding. *Mycological Progress*, 16, 191–203.
- Li, R., Zheng, Q., Lu, J., Zou, Y., Lin, J., Guo, L., Ye, S., & Xing, Z. (2021). Chemical composition and deterioration mechanism of *Pleurotus tuoliensis* during postharvest storage. *Food Chemistry*, 338, 127731.
- Li, Wang, Y., Pan, Y., Yu, H., Zhang, X., Shen, Y., Jiao, S., Wu, K., La, G., Yuan, Y., & Zhang, S. (2017). Mechanisms of Cd and Cr removal and tolerance by macrofungus *Pleurotus ostreatus* HAU-2. *Journal of Hazardous Materials*, 330, 1–8.  
<https://doi.org/https://doi.org/10.1016/j.jhazmat.2017.01.047>
- Li, & Yao. (2005). Revision of the taxonomic position of the Phoenix Mushroom. *Mycotaxon*, 91, 61–73. <https://eurekamag.com/research/004/305/004305106.php>
- Liew, S. S., Ho, W. Y., Yeap, S. K., & Sharifudin, S. A. bin. (2018). Phytochemical composition and in vitro antioxidant activities of *Citrus sinensis* peel extracts. In PeerJ.
- Liimatainen, K., Niskanen, T., Dima, B., Kytövuori, I., Ammirati, J. F., & Frøslev, T. G. (2014). The largest type study of Agaricales species to date: bringing identification and nomenclature of *Phlegmacium* (*Cortinarius*) into the DNA era. *Persoonia : Molecular Phylogeny and Evolution of Fungi*, 33, 98. <https://doi.org/10.3767/003158514X684681>

- Liu, Y. J., Whelen, S., & Hall, B. D. (1999). Phylogenetic relationships among ascomycetes: evidence from an RNA polymerase II subunit. *Molecular Biology and Evolution*, 16(12), 1799–1808.
- Livak, K. J., & Schmittgen, T. D. (2001). Analysis of relative gene expression data using real-time quantitative PCR and the  $2^{-\Delta\Delta CT}$  method. *Methods*, 25(4), 402–408.  
<https://doi.org/10.1006/meth.2001.1262>
- Loredana, L., Francesca, M., Florinda, F., Filomena, N., Paola, O., & Donatella, A. (2023). Effect of argon-enriched modified atmosphere on the over quality and bioactive compounds of ready-to-use broccoli rabe (*Brassica rapa sylvestris* L. var. *esculenta*) during the storage. *Food Science and Technology International*, 29(1), 84–94.
- MacPherson, I. S., & Murphy, M. E. P. (2007). Type-2 copper-containing enzymes. *Cellular and Molecular Life Sciences*, 64, 2887–2899.
- Maftoun, P., Johari, H., Soltani, M., Malik, R., Othman, N. Z., & El Enshasy, H. A. (2015). The edible mushroom *Pleurotus* spp.: I. Biodiversity and nutritional values. *International Journal of Biotechnology for Wellness Industries*, 4(2), 67.
- Manandhar, K. (2004). Oyster Mushroom Cultivation. *Cellulose*, 33(33.5), 22–28.
- Mandeel, Q. A., Al-Laith, A. A., & Mohamed, S. A. (2005). Cultivation of oyster mushrooms (*Pleurotus* spp.) on various lignocellulosic wastes. *World Journal of Microbiology and Biotechnology*, 21, 601–607.
- Mandon, E. C., Ehses, I., Rother, J., van Echten, G., & Sandhoff, K. (1992). Subcellular localization and membrane topology of serine palmitoyltransferase, 3-dehydrosphinganine reductase, and sphinganine N-acyltransferase in mouse liver. *Journal of Biological Chemistry*, 267(16), 11144–11148.
- Mapayi, T. T., Oluduro, A. O., Omoboye, O. O., & Taiwo, A. M. (2021). Medicinal plant assisted cultivation of *Pleurotus florida* using different lignocellulosic waste substrates. *Vegetos*, 34(3), 485–494.

- Mata, G., Cortes, E. G., & Salmones, D. (2007). Mycelial growth of three *Pleurotus* (Jacq.: Fr.) P. Kumm. species on sugarcane bagasse: Production of hydrolytic and oxidative enzymes. *International Journal of Medicinal Mushrooms*, 9(3 & 4).
- Matheny, P. B., Curtis, J. M., Hofstetter, V., Aime, M. C., Moncalvo, J.-M., Ge, Z.-W., Yang, Z.-L., Slot, J. C., Ammirati, J. F., & Baroni, T. J. (2006). Major clades of Agaricales: a multilocus phylogenetic overview. *Mycologia*, 98(6), 982–995.
- Moonmoon, M., Uddin, Md. N., Ahmed, S., Shelly, N. J., & Khan, Md. A. (2010). Cultivation of different strains of king oyster mushroom (*Pleurotus eryngii*) on saw dust and rice straw in Bangladesh. *Saudi Journal of Biological Sciences*, 17(4), 341–345.  
<https://doi.org/https://doi.org/10.1016/j.sjbs.2010.05.004>
- Morin, E., Kohler, A., Baker, A. R., Foulongne-Oriol, M., Lombard, V., Nagye, L. G., Ohm, R. A., Patyshakuliyeva, A., Brun, A., & Aerts, A. L. (2012). Genome sequence of the button mushroom *Agaricus bisporus* reveals mechanisms governing adaptation to a humic-rich ecological niche. *Proceedings of the National Academy of Sciences*, 109(43), 17501–17506.
- Moriya, Y., Itoh, M., Okuda, S., Yoshizawa, A. C., & Kanehisa, M. (2007). KAAS: an automatic genome annotation and pathway reconstruction server. *Nucleic Acids Research*, 35(suppl\_2), W182–W185.
- Mostak Ahmed, Noorlidah Abdullah, & Nuruddin, M. M. (2016). Yield and nutritional composition of oyster mushrooms: an alternative nutritional source for rural people. [http://www.ukm.my/jsm/malay\\_journals/jilid45bil11\\_2016/KandunganJilid45Bil11\\_2016.htm](http://www.ukm.my/jsm/malay_journals/jilid45bil11_2016/KandunganJilid45Bil11_2016.htm)
- Musieba, F., Okoth, S., Mibey, R. K., Wanjiku, S., & Moraa, K. (2013a). Proximate composition, amino acids and vitamins profile of *Pleurotus citrinopileatus singer*: An indigenous mushroom in Kenya. *American Journal of Food Technology*, 8(3), 200–206.  
<https://doi.org/10.3923/AJFT.2013.200.206>

- Myronycheva, O., Bandura, I., Bisko, N., Gryganskyi, A. P., & Karlsson, O. (2017). Assessment of the growth and fruiting of 19 oyster mushroom strains for indoor cultivation on lignocellulosic wastes. *BioResources*, 12(3), 4606–4626.
- Naraian, R., Sahu, R. K., Kumar, S., Garg, S. K., Singh, C. S., & Kanaujia, R. S. (2009). Influence of different nitrogen rich supplements during cultivation of *Pleurotus florida* on corn cob substrate. *The Environmentalist*, 29, 1–7.
- National Center for Biotechnology Information (US). (2008). BLAST® Command Line Applications User Manual. <https://www.ncbi.nlm.nih.gov/books/NBK279690/>
- Nielsen, S. S. (1998). *Food analysis*. Springer.
- Nielsen, S. S. (2017). *Food analysis laboratory manual*. Springer.
- Noguchi, R., Banno, S., Ichikawa, R., Fukumori, F., Ichiishi, A., Kimura, M., Yamaguchi, I., & Fujimura, M. (2007). Identification of OS-2 MAP kinase-dependent genes induced in response to osmotic stress, antifungal agent fludioxonil, and heat shock in *Neurospora crassa*. *Fungal Genetics and Biology*, 44(3), 208–218.
- Norat, T., Aune, D., Chan, D., & Romaguera, D. (2014). Fruits and Vegetables: Updating the Epidemiologic Evidence for the WCRF/AICR Lifestyle Recommendations for Cancer Prevention. In V. Zappia, S. Panico, G. L. Russo, A. Budillon, & F. Della Ragione (Eds.), *Advances in Nutrition and Cancer* (pp. 35–50). Springer Berlin Heidelberg.
- Nwoko, M. C., Onyeizu, U. R., Okwulehie, I. C., & Ukoima, H. N. (2017). Nutritional and Bioactive Compounds: Evaluation of *Pleurotus pulmonarius* (Fries) Quel. Fruit Bodies Grown on Different Wood Logs in Abia State, Nigeria. *J Bioremediat Biodegrad*, 8(393), 2.
- Obodai, M., Cleland-Okine, J., & Vowotor, K. A. (2003). Comparative study on the growth and yield of *Pleurotus ostreatus* mushroom on different lignocellulosic by-products. *Journal of Industrial Microbiology and Biotechnology*, 30(3), 146–149.

- Olveira-Bouzas, V., Pita-Calvo, C., Vázquez-Odériz, M. L., & Romero-Rodríguez, M. Á. (2021). Evaluation of a modified atmosphere packaging system in pallets to extend the shelf-life of the stored tomato at cooling temperature. *Food Chemistry*, 364, 130309.
- Owaid, M. N., Abed, A. M., & Nassar, B. M. (2015). Recycling cardboard wastes to produce blue oyster mushroom *Pleurotus ostreatus* in Iraq. *Emirates Journal of Food and Agriculture*, 537–541.
- Özünlü, O., & Ergezer, H. (2021). Possibilities of using dried oyster mushroom (*Pleurotus ostreatus*) in the production of beef salami. *Journal of Food Processing and Preservation*, 45(2), e15117.
- Palmieri, G., Giardina, P., Bianco, C., Fontanella, B., & Sannia, G. (2000). Copper induction of laccase isoenzymes in the ligninolytic fungus *Pleurotus ostreatus*. *Applied and Environmental Microbiology*, 66(3), 920–924.
- Papaspyridi, L.-M., Aligiannis, N., Christakopoulos, P., Skaltsounis, A.-L., & Fokialakis, N. (2011). Production of bioactive metabolites with pharmaceutical and nutraceutical interest by submerged fermentation of *Pleurotus ostreatus* in a batch stirred tank bioreactor. *Procedia Food Science*, 1, 1746–1752.
- Pereira, M., Malta, F., Freire, M., & Couto, P. (2017). Application of next-generation sequencing in the era of precision medicine. *Applications of RNA-Seq and Omics Strategies: From Microorganisms to Human Health*. London, England, UK: InTechOpen, 293–318.
- Persky, L.-L., Kerem, Z., Tel-Or, E., & Hadar, Y. (2002). Extracellular Catalase Activity in the Edible and Medicinal Mushroom *Pleurotus ostreatus* (Jacq.: Fr.) Kumm.(Basidiomycota). *International Journal of Medicinal Mushrooms*, 4(1).
- Peter, C., Laliberté, J., Beaudoin, J., & Labbé, S. (2008). Copper distributed by Atx1 is available to copper amine oxidase 1 in *Schizosaccharomyces pombe*. *Eukaryotic Cell*, 7(10), 1781–1794.

- Piska, K., Sułkowska-Ziaja, K., & Muszyńska, B. (2017). Edible mushroom *Pleurotus ostreatus* (oyster mushroom): its dietary significance and biological activity. *Acta Scientiarum Polonorum. Hortorum Cultus*, 16(1).
- Pomeranz, Y., Meloan, C. E., Pomeranz, Y., & Meloan, C. E. (1994). Determination of moisture. *Food Analysis: Theory and Practice*, 575–601.
- Puttaraju, N. G., Venkateshaiah, S. U., Dharmesh, S. M., Urs, S. M. N., & Somasundaram, R. (2006). Antioxidant activity of indigenous edible mushrooms. *Journal of Agricultural and Food Chemistry*, 54(26), 9764–9772.
- Raja, H. A., Baker, T. R., Little, J. G., & Oberlies, N. H. (2017). DNA barcoding for identification of consumer-relevant mushrooms: A partial solution for product certification? *Food Chemistry*, 214, 383–392.
- Raman, J., Jang, K. Y., Oh, Y. L., Oh, M., Im, J. H., Lakshmanan, H., & Sabaratnam, V. (2021). Cultivation and Nutritional Value of Prominent *Pleurotus* Spp.: An Overview. *Mycobiology*, 49(1), 1–14.  
<https://doi.org/10.1080/12298093.2020.1835142/FORMAT/EPUB>
- Raman, J., Lakshmanam, H., Sabaratnam, V., Kab-yeul, J., & Raaman, N. (2018). Cultivation of pink Oyster mushroom *Pleurotus djamor var. roseus* on various agro-residues by low-cost technique. In Article in *Journal of Mycopathological Research*.  
<https://www.researchgate.net/publication/328630516>
- Ravash, R., Shiran, B., Alavi, A.-A., Bayat, F., Rajaei, S., & Zervakis, G. I. (2010). Genetic variability and molecular phylogeny of *Pleurotus eryngii* species-complex isolates from Iran, and notes on the systematics of Asiatic populations. *Mycological Progress*, 9, 181–194.
- Reis, F. S., Barros, L., Martins, A., & Ferreira, I. C. F. R. (2012). Chemical composition and nutritional value of the most widely appreciated cultivated mushrooms: an inter-species comparative study. *Food and Chemical Toxicology*, 50(2), 191–197.

Ro, H.-S., Kim, S. S., San Ryu, J., Jeon, C.-O., Lee, T. S., & Lee, H.-S. (2007). Comparative studies on the diversity of the edible mushroom *Pleurotus eryngii*: ITS sequence analysis, RAPD fingerprinting, and physiological characteristics. *Mycological Research*, 111(6), 710–715.

Rosmiza, M. Z., Davies, W. P., Aznie CR, R., Jabil, M. J., & Mazdi, M. (2016). Prospects for Increasing Commercial Mushroom Production in Malaysia: Challenges and Opportunities. *Mediterranean Journal of Social Sciences*, 7(1 S1), 406.  
<https://www.richtmann.org/journal/index.php/mjss/article/view/8766>

Royse, D. J., Baars, J., & Tan, Q. (2017). Current Overview of Mushroom Production in the World. *Edible and Medicinal Mushrooms*, 5–13.  
<https://doi.org/10.1002/9781119149446.CH2>

Saito, T., Tanaka, N., & Shinozawa, T. (2002). Characterization of subrepeat regions within rDNA intergenic spacers of the edible basidiomycete *Lentinula edodes*. *Bioscience, Biotechnology, and Biochemistry*, 66(10), 2125–2133.

Sánchez-Rangel, J. C., Benavides, J., Heredia, J. B., Cisneros-Zevallos, L., & Jacobo-Velázquez, D. A. (2013). The Folin–Ciocalteu assay revisited: improvement of its specificity for total phenolic content determination. *Analytical Methods*, 5(21), 5990–5999.

Sardar, H., Ali, M. A., Anjum, M. A., Nawaz, F., Hussain, S., Naz, S., & Karimi, S. M. (2017). Agro-industrial residues influence mineral elements accumulation and nutritional composition of king oyster mushroom (*Pleurotus eryngii*). *Scientia Horticulturae*, 225, 327–334. <https://doi.org/10.1016/J.SCIENTA.2017.07.010>

Savoie, J., Salmones, D., & Mata, G. (2007). Hydrogen peroxide concentration measured in cultivation substrates during growth and fruiting of the mushrooms *Agaricus bisporus* and *Pleurotus* spp. *Journal of the Science of Food and Agriculture*, 87(7), 1337–1344.

Schlesier, K., Harwat, M., Böhm, V., & Bitsch, R. (2002). Assessment of antioxidant activity by using different in vitro methods. *Free Radical Research*, 36(2), 177–187.



Schoch, C. L., & Seifert, K. A. (2012). Reply to Kiss: Internal transcribed spacer (ITS) remains the best candidate as a universal DNA barcode marker for Fungi despite imperfections. *Proceedings of the National Academy of Sciences*, 109(27), E1812–E1812. <https://doi.org/10.1073/PNAS.1207508109>

Schoch, C. L., Seifert, K. A., Huhndorf, S., Robert, V., Spouge, J. L., Levesque, C. A., Chen, W., Bolchacova, E., Voigt, K., Crous, P. W., Miller, A. N., Wingfield, M. J., Aime, M. C., An, K. D., Bai, F. Y., Barreto, R. W., Begerow, D., Bergeron, M. J., Blackwell, M., ... Schindel, D. (2012). Nuclear ribosomal internal transcribed spacer (ITS) region as a universal DNA barcode marker for Fungi. *Proceedings of the National Academy of Sciences of the United States of America*, 109(16), 6241–6246. [https://doi.org/10.1073/PNAS.1117018109/SUPPL\\_FILE/SD01.XLS](https://doi.org/10.1073/PNAS.1117018109/SUPPL_FILE/SD01.XLS)

Shannon, E., Jaiswal, A. K., & Abu-Ghannam, N. (2017). Polyphenolic content and antioxidant capacity of white, green, black, and herbal teas: a kinetic study.

Shnyreva, A. A., & Shnyreva, A. V. (2015). Phylogenetic analysis of *Pleurotus* species. *Russian Journal of Genetics*, 51, 148–157.

Singh, M., & Kamal, S. (2017). Genetic Aspects and Strategies for Obtaining Hybrids. *Edible and Medicinal Mushrooms*, 35–87. <https://doi.org/10.1002/9781119149446.CH4>

Smiderle, F. R., Olsen, L. M., Ruthes, A. C., Czelusniak, P. A., Santana-Filho, A. P., Sasaki, G. L., Gorin, P. A. J., & Iacomini, M. (2012). Exopolysaccharides, proteins and lipids in *Pleurotus pulmonarius* submerged culture using different carbon sources. *Carbohydrate Polymers*, 87(1), 368–376.

Sousa, M. A. C., Zied, D. C., Marques, S. C., Rinker, D. L., Alm, G., & Dias, E. S. (2016). Yield and enzyme activity of different strains of almond mushroom in two cultivation systems. *Sydowia*, 68, 35–40.

Sousa-Santos, C., Robalo, J. I., Collares-Pereira, M. J., & Almada, V. C. (2005). Heterozygous indels as useful tools in the reconstruction of DNA sequences and in the assessment of ploidy level and genomic constitution of hybrid organisms. *DNA*

Sequence : The Journal of DNA Sequencing and Mapping, 16(6), 462–467.

<https://doi.org/10.1080/10425170500356065>

Soylu, M. K., & Kang, M. (2016). Mushroom Cultivation in South Korea. Turkish Journal of Agriculture - Food Science and Technology, 4(3), 225–229.

<https://doi.org/10.24925/TURJAF.V4I3.225-229.624>

Stajic, M., Sikorski, J., Wasser, S. P., & Nevo, E. (2005). Genetic similarity and taxonomic relationships within the genus *Pleurotus* (higher Basidiomycetes) determined by RAPD analysis. Mycotaxon, 93, 247–256.

Su, D., Lv, W., Wang, Y., Wang, L., & Li, D. (2020). Influence of microwave hot-air flow rolling dry-blanching on microstructure, water migration and quality of *Pleurotus eryngii* during hot-air drying. Food Control, 114, 107228.

Sugawara, A., Matsui, D., Yamada, M., Asano, Y., & Isobe, K. (2015). Characterization of two amine oxidases from *Aspergillus carbonarius* AIU 205. Journal of Bioscience and Bioengineering, 119(6), 629–635.

<https://doi.org/https://doi.org/10.1016/j.jbiosc.2014.10.023>

Sulistiany, H., Sudirman, L. I., & Dharmaputra, O. S. (2016). Production of fruiting body and antioxidant activity of wild *Pleurotus*. HAYATI Journal of Biosciences, 23(4), 191–195.

Tam, L. S., Li, E. K., Leung, V. Y. F., Griffith, J. F., Benzie, I. F. F., Lim, P. L., Whitney, B., Lee, V. W. Y., Lee, K. K. C., Thomas, G. N., & Tomlinson, B. (2005). Effects of vitamins C and E on oxidative stress markers and endothelial function in patients with systemic lupus erythematosus: A double blind, placebo controlled pilot study. Journal of Rheumatology, 32(2), 275–282.

Tan, Y.-S., Baskaran, A., Nallathamby, N., Chua, K.-H., Kuppusamy, U. R., & Sabaratnam, V. (2015). Influence of customized cooking methods on the phenolic contents and antioxidant activities of selected species of oyster mushrooms (*Pleurotus* spp.). Journal of Food Science and Technology, 52, 3058–3064.

Tang, Y.-J., Zhu, L.-W., Li, H.-M., & Li, D.-S. (2007). Submerged culture of mushrooms in bioreactors—challenges, current state-of-the-art, and future prospects. *Food Technology and Biotechnology*, 45(3), 221–229.

Tenney, A. E., Jia, Q. W., Langton, L., Klueh, P., Quatrano, R., & Brent, M. R. (2007). A tale of two templates: automatically resolving double traces has many applications, including efficient PCR-based elucidation of alternative splices. *Genome Research*, 17(2), 212–218. <https://doi.org/10.1101/GR.5661407>

The Business Research Company. (2023). Mushroom Global Market Report 2023. Research and Markets. <https://www.researchandmarkets.com/reports/5766651/mushroom-global-market-report#rvp-1>

Urbanelli, S., Della Rosa, V., Punelli, F., Porretta, D., Reverberi, M., Fabbri, A. A., & Fanelli, C. (2007). DNA-fingerprinting (AFLP and RFLP) for genotypic identification in species of the *Pleurotus eryngii* complex. *Applied Microbiology and Biotechnology*, 74(3), 592–600. <https://doi.org/10.1007/s00253-006-0684-z>

Vicente, M. F., Basilio, A., Cabello, A., & Peláez, F. (2003). Microbial natural products as a source of antifungals. *Clinical Microbiology and Infection*, 9(1), 15–32.

Vilgalys, R., & Sun, B. L. (1994). Ancient and recent patterns of geographic speciation in the oyster mushroom *Pleurotus* revealed by phylogenetic analysis of ribosomal DNA sequences. *Proceedings of the National Academy of Sciences of the United States of America*, 91(10), 4599. <https://doi.org/10.1073/PNAS.91.10.4599>

Wang, Guo, H., Li, J. J., Li, W., Wang, Q., & Yu, X. (2019). Evaluation of five regions as DNA barcodes for identification of *Lepista* species (Tricholomataceae, Basidiomycota) from China. *PeerJ*, 7(7). <https://doi.org/10.7717/PEERJ.7307>

Wang, Wu, X., Gao, W., Zhao, M., Zhang, J., & Huang, C. (2017). Differential expression patterns of *Pleurotus ostreatus* catalase genes during developmental stages and under heat stress. *Genes*, 8(11), 335.

- Wang, Z., Gerstein, M., & Snyder, M. (2009). RNA-Seq: a revolutionary tool for transcriptomics. *Nature Reviews Genetics*, 10(1), 57–63.
- Wang, Zhou, J., Cao, Z., Hu, B., Wang, J., Guo, J., & Zheng, S. (2022). De Novo Assembly Transcriptome Analysis Reveals the Preliminary Molecular Mechanism of Primordium Formation in *Pleurotus tuoliensis*. *Genes*, 13(10), 1747.
- Wani, B. A., Bodha, R. H., & Wani, A. H. (2010). Nutritional and medicinal importance of mushrooms. *Journal of Medicinal Plants Research*, 4(24), 2598–2604.
- Wan-Mohtar, W. A. A. Q. I., Klaus, A., Cheng, A., Salis, S. A., & Abdul Halim-Lim, S. (2019). Total quality index of commercial oyster mushroom *Pleurotus sapidus* in modified atmosphere packaging. *British Food Journal*, 121(8), 1871–1883.
- Watkinson, S. C., Burton, K. S., & Wood, D. A. (2001). Characteristics of intracellular peptidase and proteinase activities from the mycelium of a cord-forming wood decay fungus, *Serpula lacrymans*. *Mycological Research*, 105(6), 698–704.
- Wink, D. A., Hines, H. B., Cheng, R. Y. S., Switzer, C. H., Flores-Santana, W., Vitek, M. P., Ridnour, L. A., & Colton, C. A. (2011). Nitric oxide and redox mechanisms in the immune response. *Journal of Leukocyte Biology*, 89(6), 873–891.  
<https://doi.org/10.1189/jlb.1010550>
- Wojewoda, W. (2003). Checklist of Polish Larger Basidiomycetes. W. Szafer Institute of Botany, Polish Academy of Sciences.  
<https://books.google.com.my/books?id=UhmpAAAACAAJ>
- Wong, M. M. L., Cannon, C. H., & Wickneswari, R. (2011). Identification of lignin genes and regulatory sequences involved in secondary cell wall formation in *Acacia auriculiformis* and *Acacia mangium* via de novo transcriptome sequencing. *BMC Genomics*, 12, 1–13.
- Won-sik, K. (2004). Description of Commercially Important *Pleurotus* Species.

- Xia, F., Fan, J., Zhu, M., & Tong, H. (2011). Antioxidant effects of a water-soluble proteoglycan isolated from the fruiting bodies of *Pleurotus ostreatus*. *Journal of the Taiwan Institute of Chemical Engineers*, 42(3), 402–407.
- Xiao, G., Zhang, M., Shan, L., You, Y., & Salokhe, V. M. (2011). Extension of the shelf-life of fresh oyster mushrooms (*Pleurotus ostreatus*) by modified atmosphere packaging with chemical treatments. *African Journal of Biotechnology*, 10(46), 9509–9517.
- Xie, C., Gong, W., Zhu, Z., Yan, L., Hu, Z., & Peng, Y. (2018). Comparative transcriptomics of *Pleurotus eryngii* reveals blue-light regulation of carbohydrate-active enzymes (CAZymes) expression at primordium differentiated into fruiting body stage. *Genomics*, 110(3), 201–209.
- Xu, Chen, P., Li, H., Qiao, S., Wang, J., Wang, Y., Wang, X., Wu, B., Liu, H., Wang, C., & Xu, H. (2021). Comparative transcriptome analysis reveals the differential response to cadmium stress of two *Pleurotus fungi*: *Pleurotus cornucopiae* and *Pleurotus ostreatus*. *Journal of Hazardous Materials*, 416, 125814.
- Yamagishi, K., Kimura, T., Suzuki, M., Shinmoto, H., & Yamaki, K.-J. (2004). Elevation of intracellular cAMP levels by dominant active heterotrimeric G protein alpha subunits ScGP-A and ScGP-C in homobasidiomycete, *Schizophyllum commune*. *Bioscience, Biotechnology, and Biochemistry*, 68(5), 1017–1026.
- Yamanaka, K. (2011). Mushroom Cultivation in Japan. *World Society Mushroom Biology and Mushroom Products Bulletin*, 1–10.
- Yan, Z., Zhao, M., Wu, X., & Zhang, J. (2020). Metabolic response of *Pleurotus ostreatus* to continuous heat stress. *Frontiers in Microbiology*, 10, 3148.
- Yin, J., Xin, X., Weng, Y., & Gui, Z. (2017). Transcriptome-wide analysis reveals the progress of *Cordyceps militaris* subculture degeneration. *PLOS ONE*, 12(10), e0186279. <https://doi.org/10.1371/JOURNAL.PONE.0186279>

Yin, Zheng, L., Chen, L., Tan, Q., Shang, X., & Ma, A. (2014). Cloning, expression, and characterization of a milk-clotting aspartic protease gene (Po-Asp) from *Pleurotus ostreatus*. *Applied Biochemistry and Biotechnology*, 172, 2119–2131.

Yu, G. J., Wang, M., Huang, J., Yin, Y. L., Chen, Y. J., Jiang, S., Jin, Y. X., Lan, X. Q., Wong, B. H. C., Liang, Y., & Sun, H. (2012). Deep Insight into the *Ganoderma lucidum* by Comprehensive Analysis of Its Transcriptome. *PLOS ONE*, 7(8), e44031.  
<https://doi.org/10.1371/JOURNAL.PONE.0044031>

Zámocký, M., Gasselhuber, B., Furtmüller, P. G., & Obinger, C. (2012). Molecular evolution of hydrogen peroxide degrading enzymes. *Archives of Biochemistry and Biophysics*, 525(2), 131–144.

Zengin, G., Sarikurkcu, C., Uyar, P., Aktumsek, A., Uysal, S., Kocak, M. S., & Ceylan, R. (2015). *Crepis foetida* L. subsp. *rhoadifolia* (Bieb.) Celak. as a source of multifunctional agents: Cytotoxic and phytochemical evaluation. *Journal of Functional Foods*, 17, 698–708.

Zervakis, G., Sourdis, J., & Balis, C. (1994). Genetic variability and systematics of eleven *Pleurotus* species based on isozyme analysis. *Mycological Research*, 98(3), 329–341.

Zervakis, Ntougias, S., Gargano, M. L., Besi, M. I., Polemis, E., Typas, M. A., & Venturella, G. (2014). A reappraisal of the *Pleurotus eryngii* complex—New species and taxonomic combinations based on the application of a polyphasic approach, and an identification key to *Pleurotus* taxa associated with *Apiaceae* plants. *Fungal Biology*, 118(9–10), 814–834.

Zervakis, Venturella, G., & Papadopoulou, K. (2001). Genetic polymorphism and taxonomic infrastructure of the *Pleurotus eryngii* species-complex as determined by RAPD analysis, isozyme profiles and ecomorphological characters. *Microbiology* (Reading, England), 147(Pt 11), 3183–3194. <https://doi.org/10.1099/00221287-147-11-3183>

- Zhang, W.-R., Liu, S.-R., Kuang, Y.-B., & Zheng, S.-Z. (2019). Development of a Novel Spawn (Block Spawn) of an Edible Mushroom, *Pleurotus ostreatus*, in Liquid Culture and its Cultivation Evaluation. *Mycobiology*, 47(1), 97–104.  
<https://doi.org/10.1080/12298093.2018.1552648>
- Zhao, M., Zhang, J., Chen, Q., Wu, X., Gao, W., Deng, W., & Huang, C. (2016). The famous cultivated mushroom Bailinggu is a separate species of the *Pleurotus eryngii* species complex. *Scientific Reports*, 6(1), 33066.
- Zheng, Q., Yu, Z., Yuan, Y., Sun, D., Abubakar, Y. S., Zhou, J., Wang, Z., & Zheng, H. (2021). The GTPase-Activating Protein FgGyp1 Is Important for Vegetative Growth, Conidiation, and Virulence and Negatively Regulates DON Biosynthesis in *Fusarium graminearum*. *Frontiers in Microbiology*, 12, 621519.
- Zhong, Y., & Shahidi, F. (2015). 12 - Methods for the assessment of antioxidant activity in foods. *Journal of Functional Foods*. In F. Shahidi (Ed.), *Handbook of Antioxidants for Food Preservation* (pp. 287–333). Woodhead Publishing.  
<https://doi.org/https://doi.org/10.1016/B978-1-78242-089-7.00012-9>
- Zmitrovich, I. V., & Wasser, S. P. (2016). Is Widely Cultivated “*Pleurotus sajor-caju*”, Especially in Asia, Indeed an Independent Species? *International Journal of Medicinal Mushrooms*, 18(7), 583–588. <https://doi.org/10.1615/INTJMEDMUSHROOMS.V18.I7.30>
- Zygler, A., Słomińska, M., & Namieśnik, J. (2012). 2.04 - Soxhlet Extraction and New Developments Such as Soxtec. In J. Pawliszyn (Ed.), *Comprehensive Sampling and Sample Preparation* (pp. 65–82). Academic Press.  
<https://doi.org/https://doi.org/10.1016/B978-0-12-381373-2.00037-5>

## Appendix

### Appendix 1

Table 1 Detailed identification BLAST results of *Pleurotus* sample based on ITS marker gene from the aligned sequence of each marker gene.

Number	Sample ID	Species	% Identity	Accession length	Accession number
1	MP5	<i>P. eryngii</i>	99.00%	1777	OL687127.1
2	MP11	<i>P. eryngii</i>	99.88%	1777	OL687127.1
3	MP14	<i>P. eryngii</i>	99.63%	1777	OL687127.1
4	MP16	<i>P. eryngii</i>	99.88%	1777	OL687127.1
5	MP22	<i>P. eryngii</i>	99.88%	1777	OL687127.1
6	MP27	<i>P. eryngii</i>	99.88%	1777	OL687127.1
7	MP30	<i>P. eryngii</i>	99.88%	1777	OL687127.1
8	MP50	<i>P. eryngii</i>	99.63%	1777	OL687127.1
9	MP2	<i>P. pulmonarius</i>	100.00%	1542	AY450349.1
10	MP9	<i>P. pulmonarius</i>	100.00%	1542	AY450349.1
11	MP12	<i>P. pulmonarius</i>	100.00%	1542	AY450349.1
12	MP24	<i>P. pulmonarius</i>	99.88%	1542	AY450349.1
13	MP25	<i>P. pulmonarius</i>	100.00%	1542	AY450349.1
14	MP28	<i>P. pulmonarius</i>	100.00%	1542	AY450349.1
15	MP31	<i>P. pulmonarius</i>	100.00%	1542	AY450349.1
16	MP34	<i>P. pulmonarius</i>	100.00%	1542	AY450349.1
17	MP35	<i>P. pulmonarius</i>	100.00%	1542	AY450349.1
18	MP36	<i>P. pulmonarius</i>	100.00%	1542	AY450349.1
19	MP41	<i>P. pulmonarius</i>	100.00%	1542	AY450349.1
20	MP42	<i>P. pulmonarius</i>	100.00%	1542	AY450349.1
21	MP43	<i>P. pulmonarius</i>	99.89%	1542	AY450349.1
22	MP51	<i>P. pulmonarius</i>	100.00%	1542	AY450349.1
23	MP52	<i>P. pulmonarius</i>	100.00%	1542	AY450349.1
24	MP53	<i>P. pulmonarius</i>	100.00%	1542	AY450349.1



Table 2 Detailed identification BLAST results of *Pleurotus* sample based on IGS1 marker gene from the aligned sequence of each marker gene.

Number	Sample ID	Species	% Identity	Accession length	Accession number
1	MP5	<i>P. eryngii</i>	99.72%	922	KF743840.1
2	MP11	<i>P. eryngii</i>	100.00%	922	HM998804.1
3	MP14	<i>P. eryngii</i>	100.00%	922	HM998804.1
4	MP16	<i>P. eryngii</i>	100.00%	921	HM998784.1
5	MP22	<i>P. eryngii</i>	100.00%	922	HM998804.1
6	MP27	<i>P. eryngii</i>	100.00%	921	HM998784.1
7	MP30	<i>P. eryngii</i>	100.00%	921	HM998784.1
8	MP50	<i>P. eryngii</i>	100.00%	922	HM998804.1
9	MP2	<i>P. pulmonarius</i>	98.75%	791	AB234031.1
10	MP9	<i>P. pulmonarius</i>	98.00%	791	AB234031.1
11	MP12	<i>P. pulmonarius</i>	99.09%	791	AB234031.1
12	MP24	<i>P. pulmonarius</i>	99.71%	791	AB234031.1
13	MP25	<i>P. pulmonarius</i>	99.44%	541	JX271868.1
14	MP28	<i>P. pulmonarius</i>	98.91%	791	AB234031.1
15	MP31	<i>P. pulmonarius</i>	98.71%	791	AB234031.1
16	MP34	<i>P. pulmonarius</i>	99.43%	791	AB234031.1
17	MP35	<i>P. pulmonarius</i>	99.57%	791	AB234031.1
18	MP36	<i>P. pulmonarius</i>	99.72%	791	AB234031.1
19	MP41	<i>P. pulmonarius</i>	99.42%	791	AB234031.1
20	MP42	<i>P. pulmonarius</i>	99.72%	791	AB234031.1
21	MP43	<i>P. pulmonarius</i>	99.71%	791	AB234031.1
22	MP51	<i>P. pulmonarius</i>	99.08%	791	AB234031.1
23	MP52	<i>P. pulmonarius</i>	99.07%	791	AB234031.1
24	MP53	<i>P. pulmonarius</i>	98.91%	791	AB234031.1

Table 3 Detailed identification BLAST results of *Pleurotus* sample based on rpb2 marker gene from the aligned sequence of each marker gene.

Number	Sample ID	Species	% Identity	Accession length	Accession number
1	MP5	<i>P. eryngii</i>	100.00%	1965	KU727131.1
2	MP11	<i>P. eryngii</i>	100.00%	1965	KU727131.1
3	MP14	<i>P. eryngii</i>	100.00%	1118	HG964261.1
4	MP16	<i>P. eryngii</i>	99.88%	1965	KU727131.1
5	MP22	<i>P. eryngii</i>	100.00%	1965	KU727131.1
6	MP27	<i>P. eryngii</i>	100.00%	1965	KU727131.1
7	MP30	<i>P. eryngii</i>	99.88%	1965	KU727131.1
8	MP50	<i>P. eryngii</i>	100.00%	1118	HG964261.1
9	MP2	<i>P. pulmonarius</i>	99.12%	2164	JQ513872.1
10	MP9	<i>P. pulmonarius</i>	99.24%	2164	JQ513872.1
11	MP12	<i>P. pulmonarius</i>	99.27%	2164	JQ513872.1
12	MP24	<i>P. pulmonarius</i>	99.13%	2164	JQ513872.1
13	MP25	<i>P. pulmonarius</i>	99.06%	2164	JQ513872.1
14	MP28	<i>P. pulmonarius</i>	99.12%	2164	JQ513872.1
15	MP31	<i>P. pulmonarius</i>	99.06%	2164	JQ513872.1
16	MP34	<i>P. pulmonarius</i>	98.98%	2164	JQ513872.1
17	MP35	<i>P. pulmonarius</i>	98.89%	2164	JQ513872.1
18	MP36	<i>P. pulmonarius</i>	98.94%	2164	JQ513872.1
19	MP41	<i>P. pulmonarius</i>	98.93%	2164	JQ513872.1
20	MP42	<i>P. pulmonarius</i>	99.13%	2164	JQ513872.1
21	MP43	<i>P. pulmonarius</i>	99.13%	2164	JQ513872.1
22	MP51	<i>P. pulmonarius</i>	99.05%	2164	JQ513872.1
23	MP52	<i>P. pulmonarius</i>	99.02%	2164	JQ513872.1
24	MP53	<i>P. pulmonarius</i>	99.06%	2164	JQ513872.1

## Appendix 2

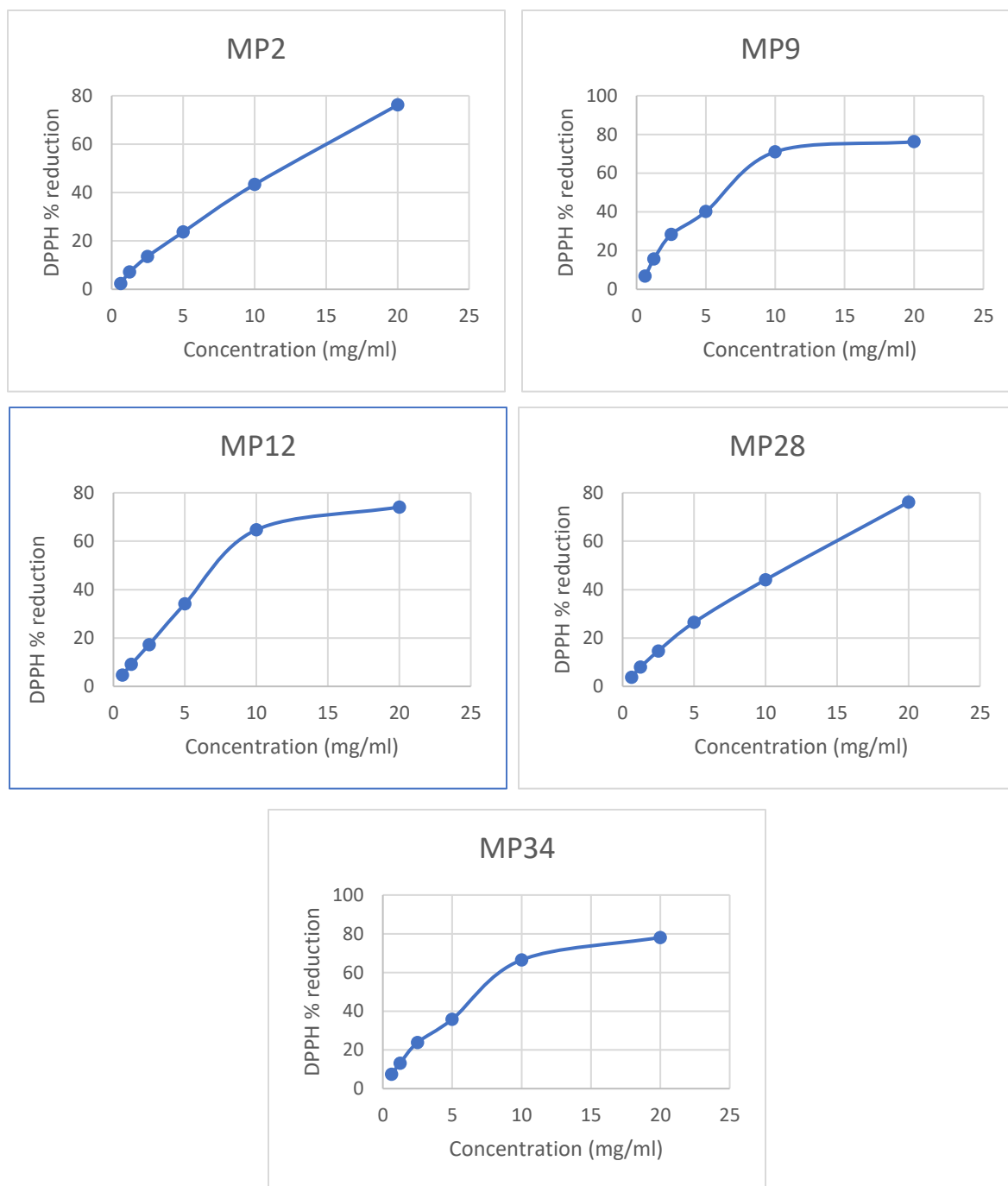


Figure 1 Scatter plot of DPPH % reduction againsts various concentrations of MP2, MP9 , MP12, MP28 and MP34 fruiting bodies aqueous extracts.

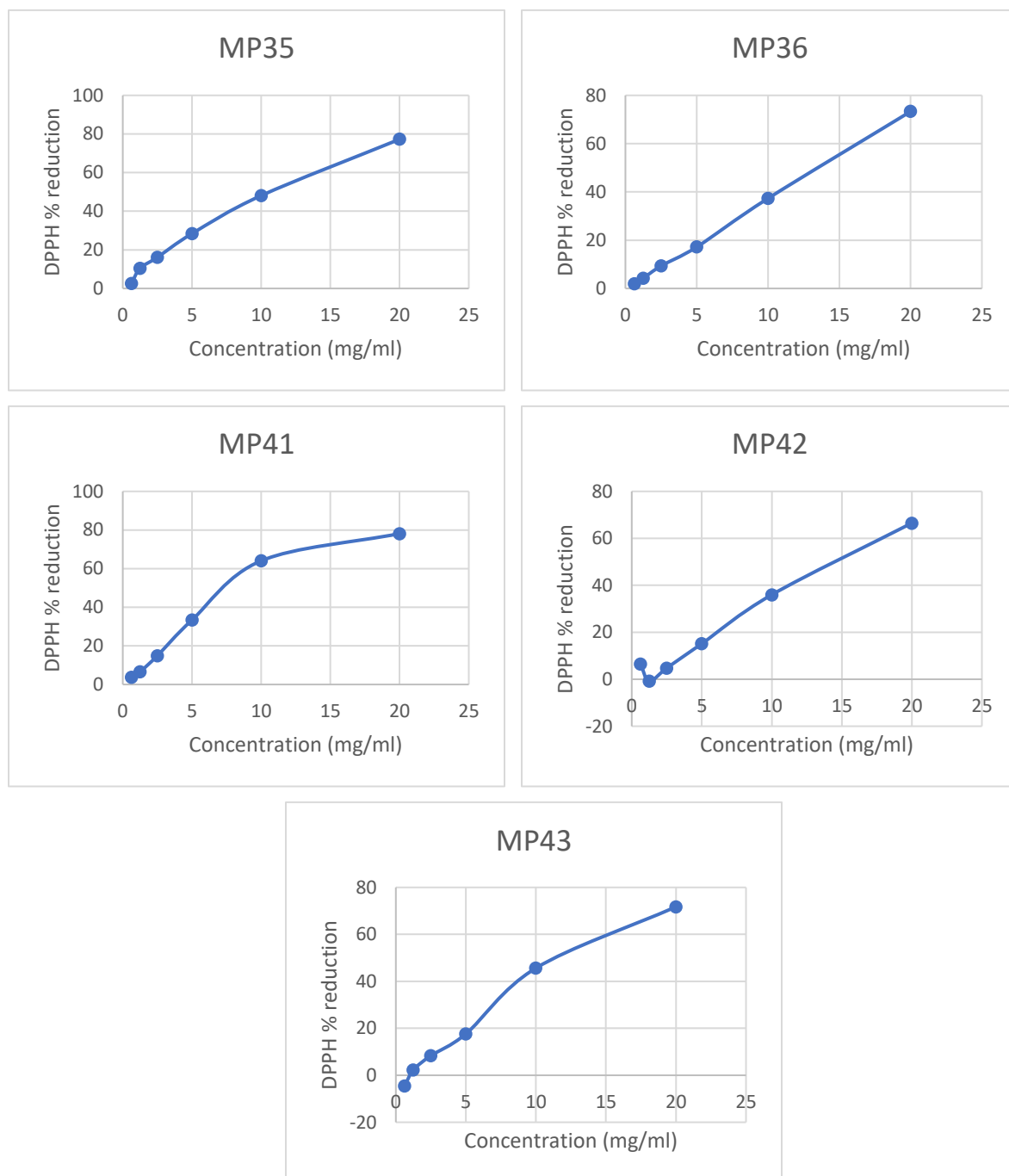


Figure 2 Scatter plot of DPPH % reduction againsts various concentrations of MP35, MP36 , MP41, MP42 and MP43 fruiting bodies aqueous extracts.

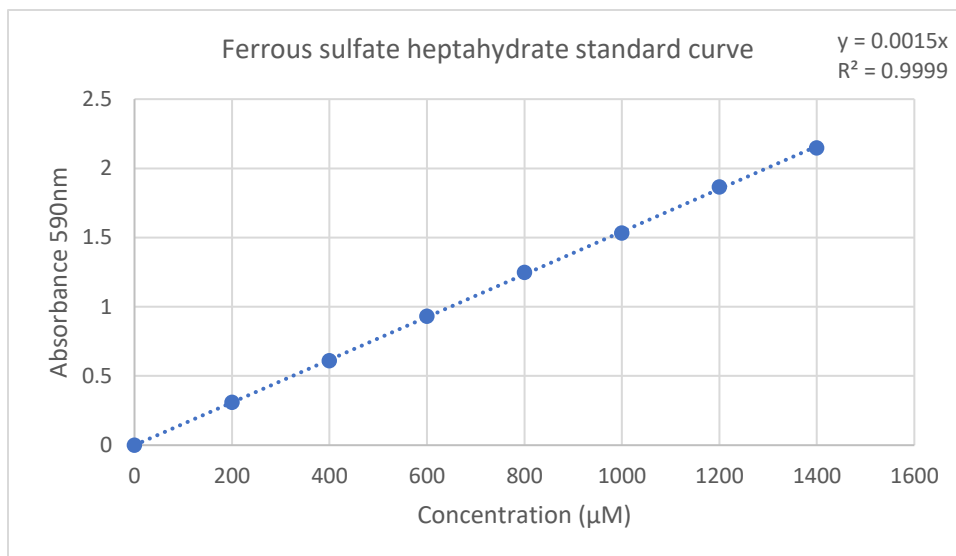


Figure 3 Standard calibration curve of Absorbance 590nm against increasing concentrations of ferrous sulfate heptahydrate used for FRAP analysis.

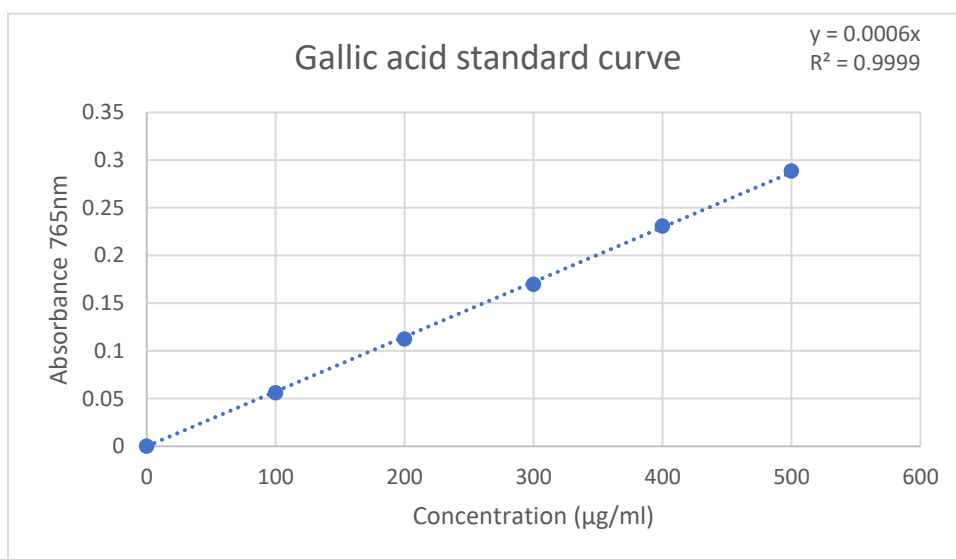


Figure 4 Standard calibration curve of Absorbance 765nm against increasing concentrations of gallic acid used for total phenolic content evaluation.

## Appendix 3

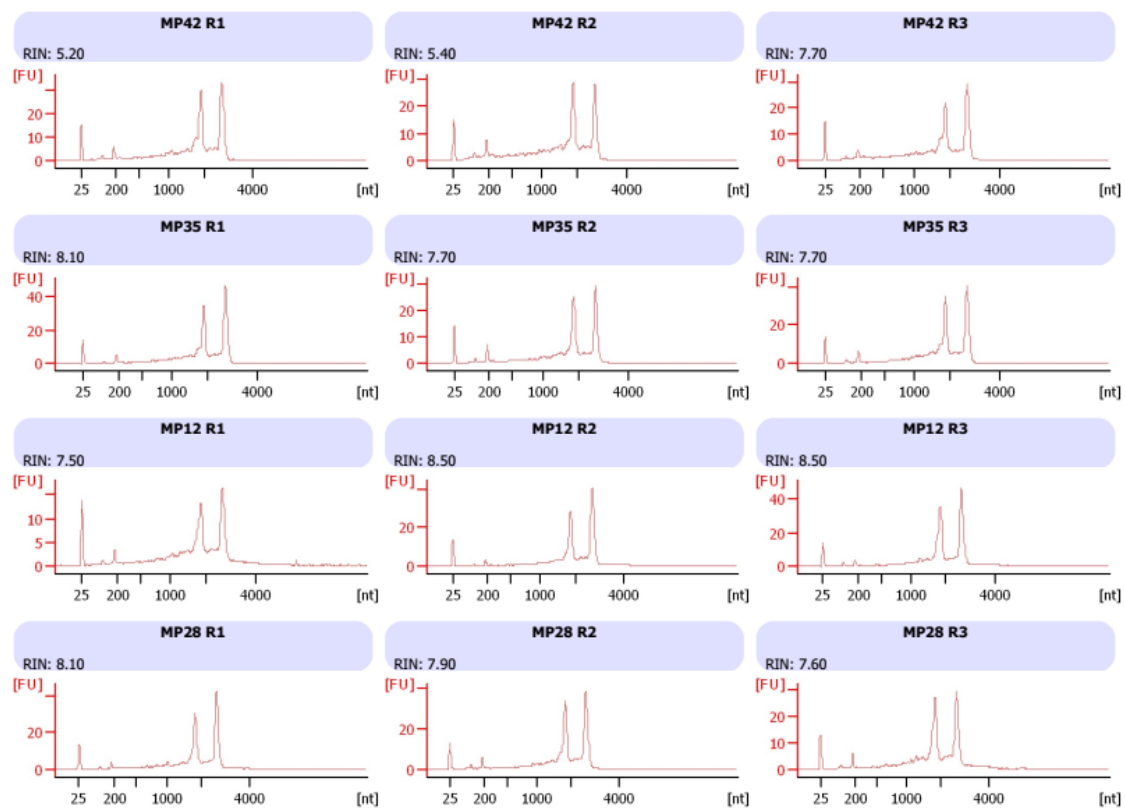


Figure 1 Electropherograms of RNA samples of high and low yield *P. pulmonarius*

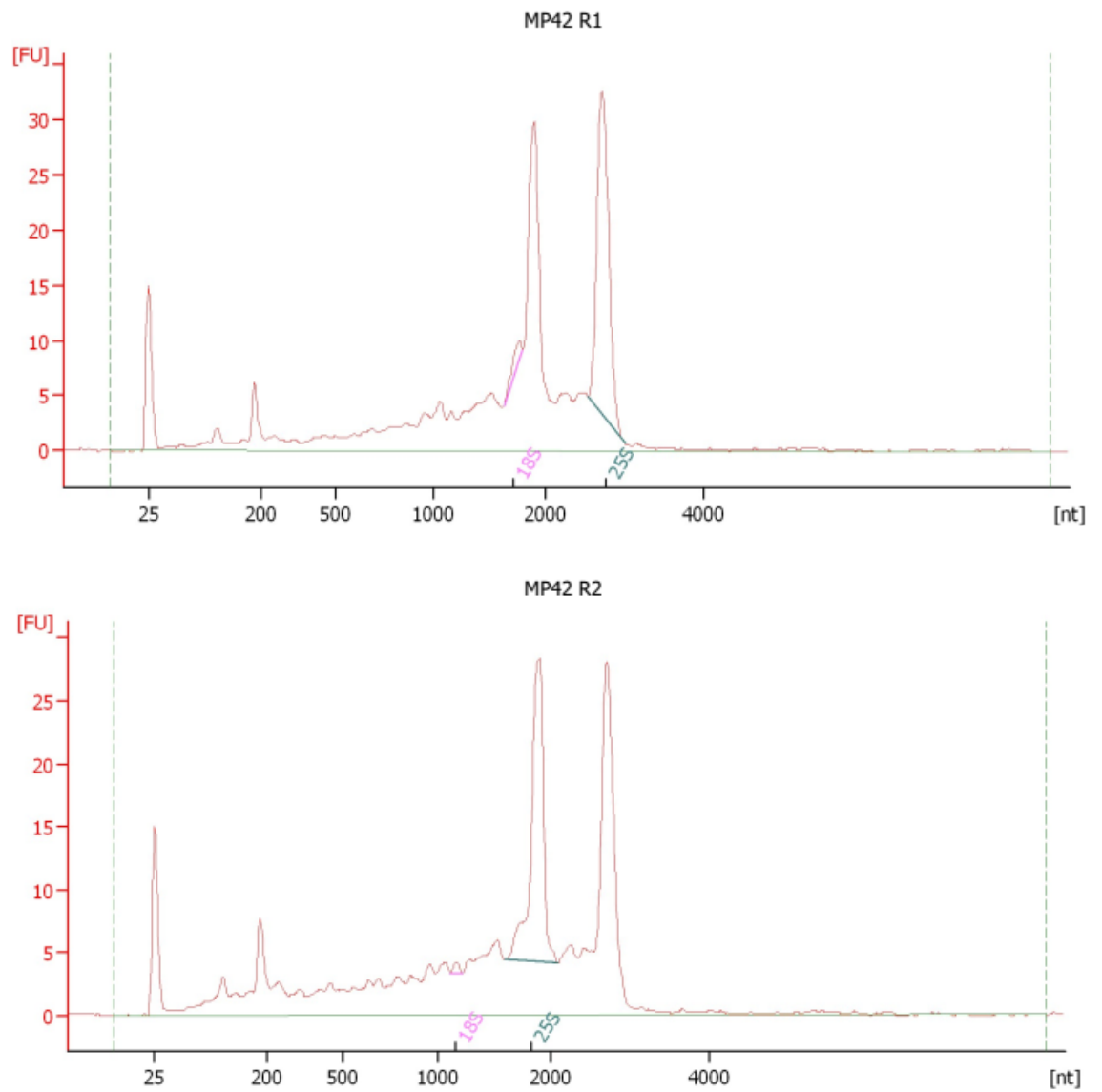


Figure 2 MP42 Replicate 1 and Replicate 2 Electropherograms with inaccurate pink and green line position.

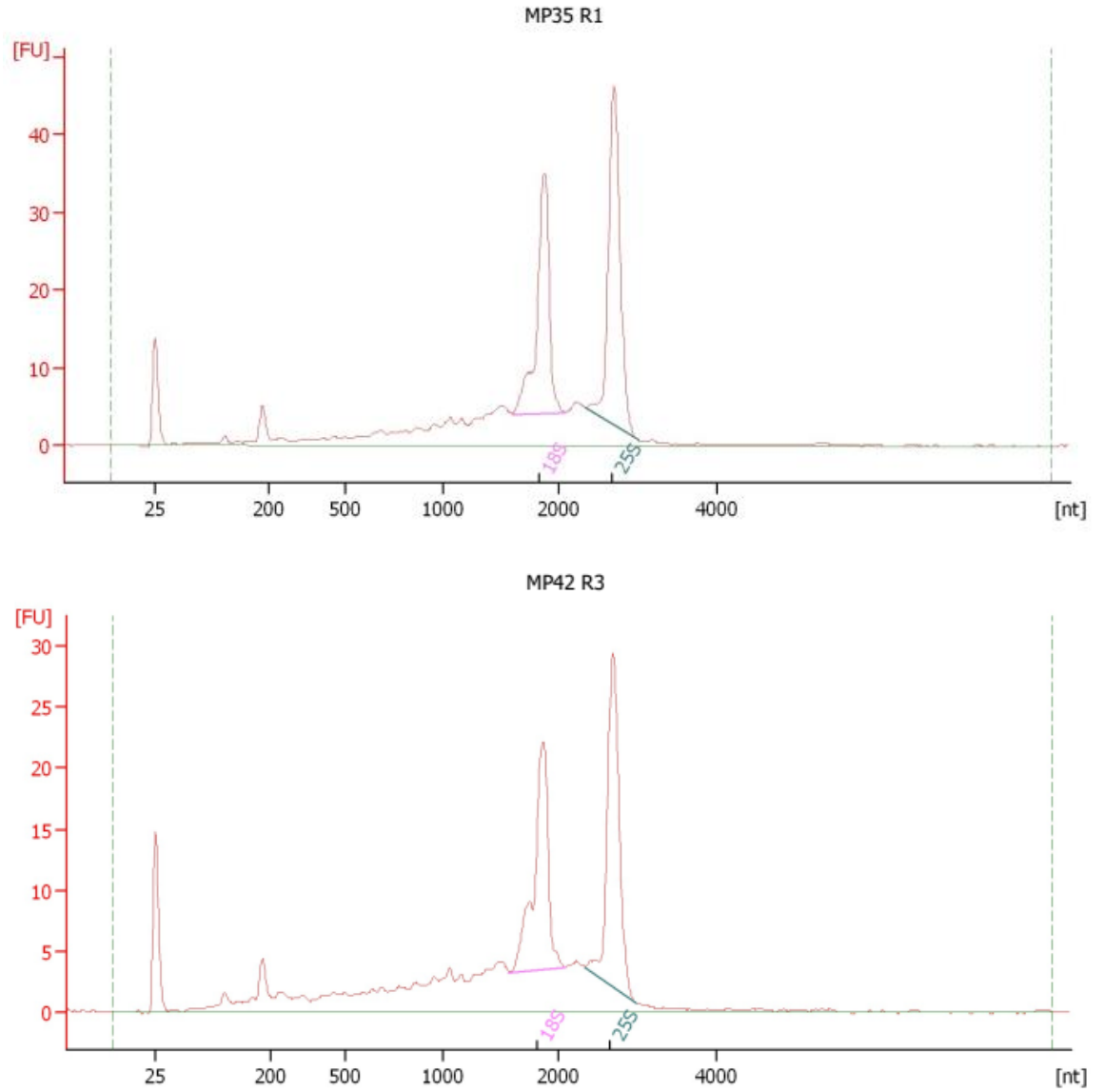


Figure 3 MP42 Replicate 3 and MP35 Replicate 2 Electropherograms with pink and green line position at the base of 18S and 26S peaks respectively.



## Appendix 4

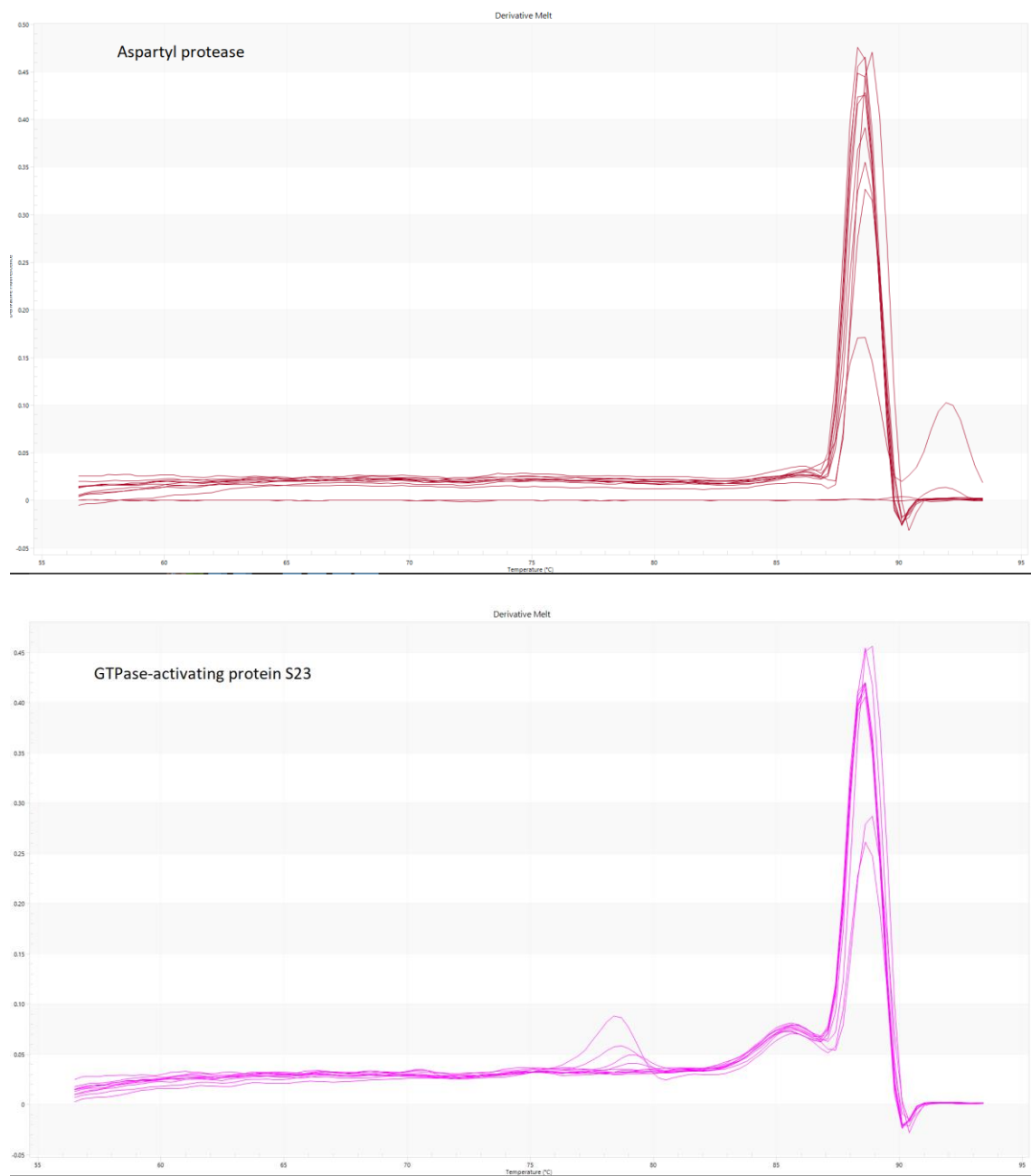


Figure 1 Melt curve of profile of Aspartyl protease and GTPase-activating protein S23.

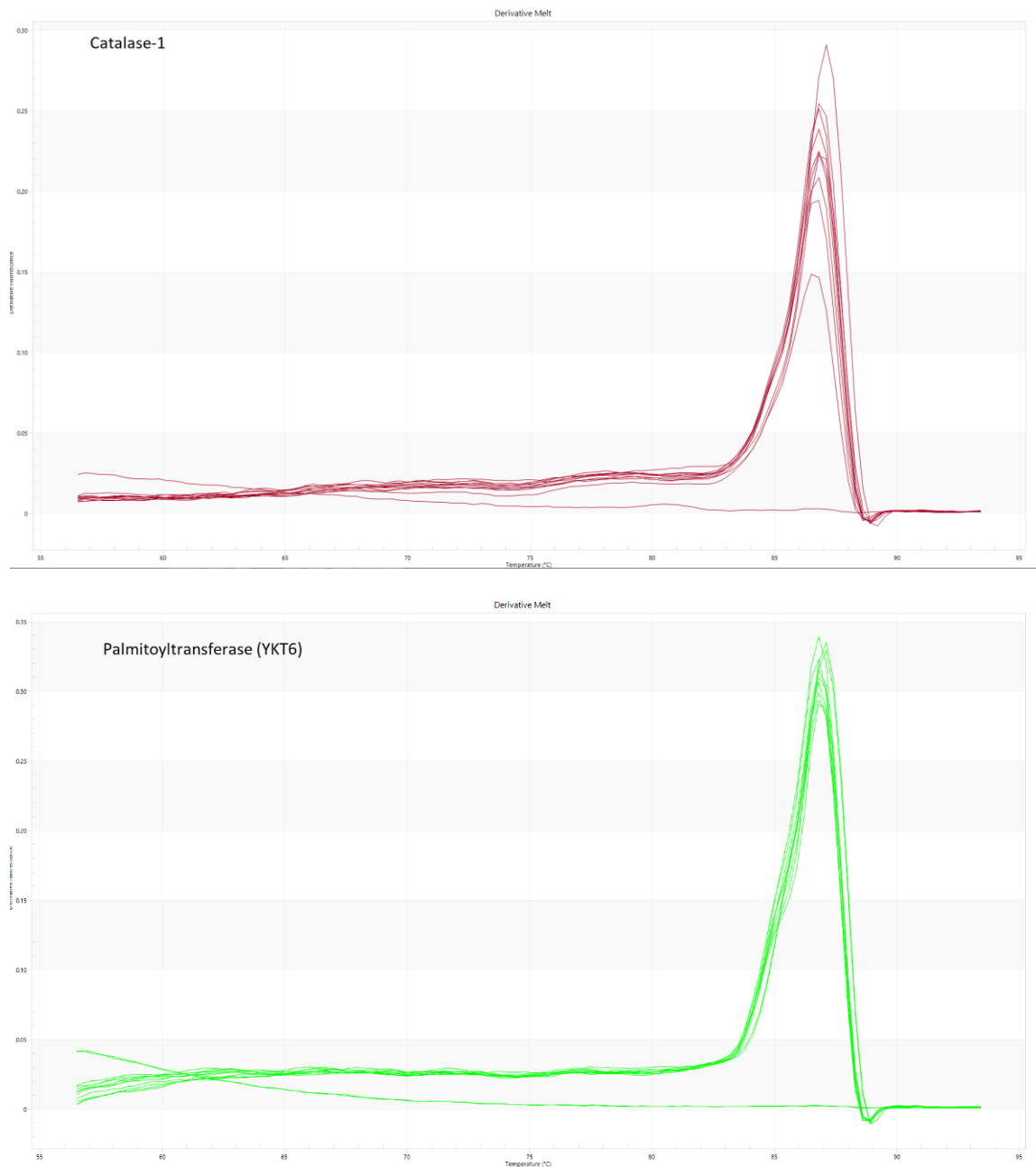


Figure 2 Melt curve of profile of *CATALASE1* and Palmitoyltransferase.

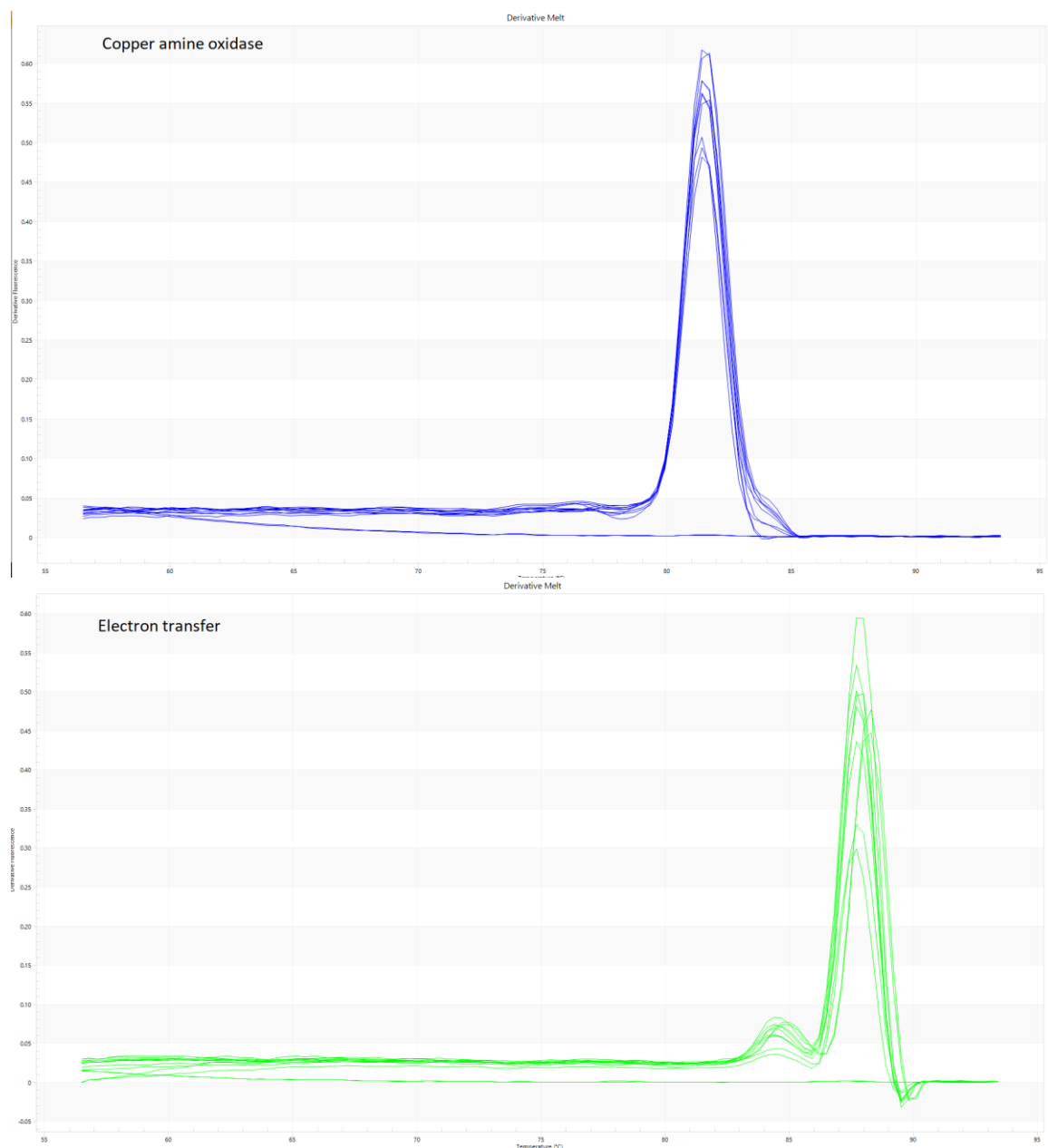


Figure 3 Melt curve of profile of Copper amine oxidase and Electron transfer.

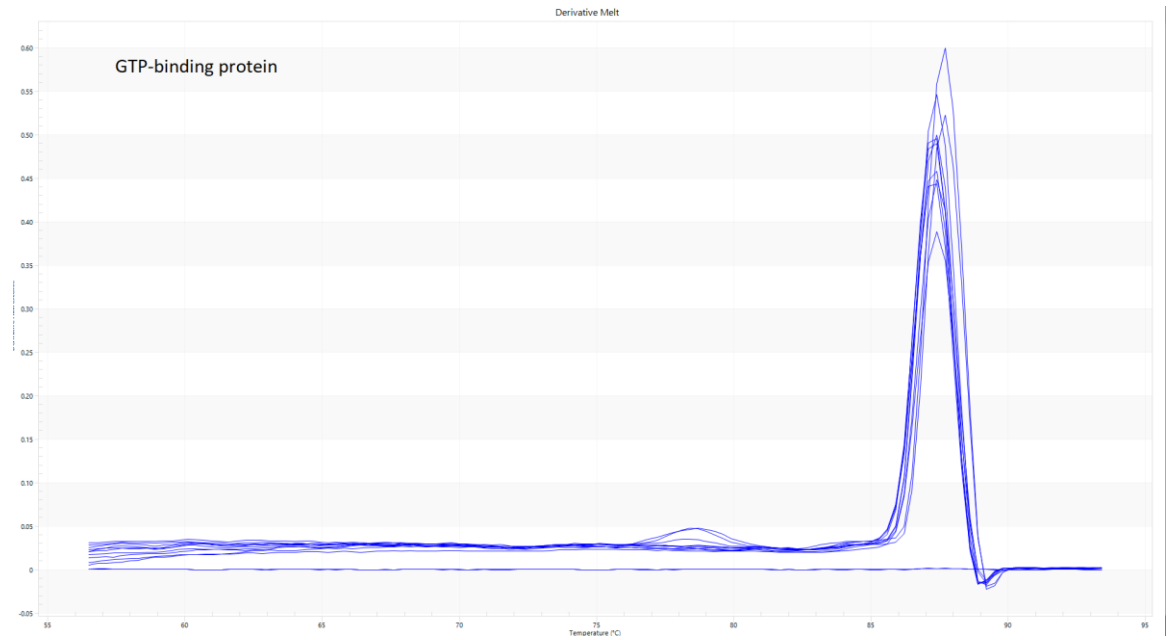


Figure 4 Melt curve of profile of GTP-binding protein.

## Appendix 5

Table 1 Detailed NGS results of the selected five DEG with its appropriate annotation NT: NCBI blast, PFAM (The prediction of protein structure domain).

Gene name	Study ID	Log <sub>2</sub> fold change	Fold change	P-value	FDR p-value	Bonferroni	NT	Pfam
Copper Amine Oxidase	640	-15.9219	-62081.1	0	0	0	<i>Pleurotus ostreatus</i> uncharacterized protein (PC9H_003002)	Copper amine oxidase, enzyme domain
Palmitoyltransferase	10258	-13.7924	-14188.3	2.22E-16	2.54E-15	1.84E-11	<i>Pleurotus ostreatus</i> palmitoyltransferase (YKT6)	Regulated-SNARE-like domain
GTPase-activating protein S23	10629	11.94306	3937.477	9.19E-13	8.26E-12	7.6E-08	<i>Pleurotus ostreatus</i> GTPase-activating protein S23 (SEC23)	Sec23/Sec24 helical domain
<i>CATALASE1</i>	3921	-10.9168	-1933.25	0	0	0	<i>Pleurotus ostreatus</i> catalase 1 mRNA	C-terminal domain found in long catalases
Aspartyl protease	885	14.14762	18149.26	0	0	0	<i>Pleurotus ostreatus</i> uncharacterized protein (PC9H_009941)	Eukaryotic aspartyl protease

Table 2 Detailed BLAST results of the selected genes.

Gene name	ID	Description	Score	Query Cover	E-value	% Identity	Accession Length	Accession Number
Copper Amine Oxidase	640	Pleurotus ostreatus uncharacterized protein (PC9H_003002)	1519	99%	0	88.03%	2208	XM_036772602.1
Palmitoyltransferase	10258	Pleurotus ostreatus palmitoyltransferase (YKT6)	652	64%	0	93.37%	603	XM_036771556.1
GTPase-activating protein S23	10629	Pleurotus ostreatus GTPase-activating protein S23 (SEC23)	536	99%	2.00E-147	90.77%	2295	XM_036777882.1
<i>CATALASE1</i>	3921	Pleurotus ostreatus catalase 1 mRNA	588	83%	7.00E-163	86.86%	2238	MH645357.1
Aspartyl protease	885	Pleurotus ostreatus uncharacterized protein (PC9H_009941)	1760	44%	0	88.60%	1455	XM_036779438.1

Table 3 Sequence data of the five differentially expressed gene.

Gene name	Sequence
Aspartyl protease	<p> CTTTAAAGTCGACACTCGTTTCTCGCCACTGCCTATGCCGCAACCTGCAAAATAATCCGA  AACTCAAACACCATGTTGCCCCAGGCGTTGTTTCTTCTGCTAGCGGCTTTCCTGGCGCCC  CCCCTGCAAGTTTATGGCACAGTATCGACACGGCATGCAGTCCCCTTCGCGCAGCACATC  TCGCTGCCTGCTCTCCAGGGTCATCTCCTCGAATACGGAAGCGAGCTATGAACGAACT  AATATCGGAATAGCGTCTGCTACTCTGGCGAGCGATGGACAATCGTATTATTCGATTATC  GAGGTCGGCGGGATGAATTTAGGGTGGCTTTGGACACCGCATCGTCAGATCTATGGCTT  GCATCTTCTGCGTGACCACGGAGACTTGCAATGCCATCCCGAGGTACCCTCTCTCGTAC  GAGAGCCCCTCGTTCGCAGCCGTCATGGGAACCAAACTGCCTTCAATGCTAGCTACGCA  GACGGGACATCTTCCAACGGCTTCGTCGCTCGCGAAAGGGTGACTTTGGCGAATTTAACC  ATCCCGGATCAGGCGCTGGGAGTCATCACGGATTGCAATGTCACTCTTACGGACAGAACG  ACTGGGTACTTGGGCTGGGCTTCCCGCTCTATCTGGCGTGAATCAAACGGTTACAAAT  TCTACGCCATTCTAGTCAACCTGGCGCAACGAGGCCTCTTGAATACCCCTTGTTGCGC  CTTCATCTAACTAGAAACACCTCCGGCACGATTTGATTGGTGCTATCGATGCGTCCGTT  GTAATGCAACCAGCCAATATCTCATGGAACCCAGTTGTCCAATTTGCCCCCTTTGCATCT  GAAAGTAATGTATCTTCGTATCTCCAATGGGCCATCCCCTTAGGCGGATTCTCTGTAAAC  CATACTCAGTTGGCACCAATGCCAACATATACCAATGTCACACACAATATGTCTATTGCC  TTGATCGACATAGGAACACCTGGTTTATACGGCCCTTTCCAAGATGTCTCCCGCCTTTTC  TCATTGATTGATGGAGCCCGGCTTGTTGACAGCTCTGGACAATGGGCTATCCCATGTGAC  ACTTCTGTACCGATATCGTTCACCTTCGGCGGGCGTGAGTTATGATCTACAAGCATATGAA  TATATCGTCGGCCCCGCCGCTGGTAACCCGAATCTTGCCTGAGCTGGCCCATGGCTGCG  CCGCTCAGCTCAGACGGAATTGACTGGCAAATCGGTGCCAATTTCTGCGCAGAGTATAC  TCGATCTTCAGCTATGGTATCAACCGCAAGGAACCCCGATGATCGGCTTCTATTCCCTC  CGCAACCAACAGCTGCGTCGTCGCCCCGTAGACGCAGTGTCTCCATATTGAGATCATC  TCCGGTATATCCACGGTCGCCACCACCCTCCCCAACTTCCCGCTCCCCACGCCGACCTTC  ACCACTCCCCCTACGCATTTAACACCTCAGTCCCCACCTCGAACGGCGGCATCGTATCC  TCCGGATTAGCGACAAGCACGTATAGGCCGGTTTTGGGCGGCCCCAATGGCGTCAATGCG  TCCGCTATACCGACGATTTCTCCGAAACCGGCGCTGCAGACGTTGATTATGACGGATGCG  CAGGGCTTGCTGACGACTTCCACTAAAACACTGGAGGAGCCGACGGTGACTTTGGCCCTG  CCGCCGGGATGGAATGCGGCGCCTTGACATACGTGTTAATTCGTTTGCCGTGTTGTTAATG </p>

	<p> TTTATGCTGTCGTGCACTTGGTTGGTTCTGTAGATGGACTTCGTTCTAGTAGTACATAGT  AAATATTGATGTATATCTTCTCAGCATTCGTACATAAGGACTTTCGTAGATATATACGA  GTAATCATCATTTGGTTCAGGCAGGAACTAGAAGACTAAAGTGCGAGTAAGTATCCATCG  TTGGAACATTTTGCGCCATACGGTGTCCCATTACTAAGTATCTGAATATTGAACGTGGA  ACATTGGTCAGTAGTTAGTATCCCAAACTCAAGCAGACACAACATTCATAAGAACTAC  AAAGATACAGCAATAATGATATTTACTATTCCGGTCTCCAGCATATGTTGTTTCGTACGCA  ATATATAAATCATCTACATATCCCATTTCATCCCACATCCCGGGTTGGCTAGATGCAGATG  CGGGAGTGGCGGCAGTGCTTTGAATCTCCACCGTCGGCTCCAGCGCAACGACTTTCTCCC  TTGAGTTTGTATCATCCTTGCTGTTCTTCATAGCTATCAACGTGACATCTTGAATTTCGC  CCTGCAAGGGACCGCTATAGAGCAAGCGGATATCATTTGCTTCGATGACTTGTACAAGAC  GCGCCGACTCGATTTTCGCGGACTTCGATGAACGACGCTGAGAAGAGGAGGATGTGGGGTC  CGCGGTGAGCGTACGAAGTTGCTTTTGTCTCCCATTTGATGTACCCAGATTTCCGTCGAG  GGACTCCGTGTTTCGAGATGTAGCAACCAAGGTATCATATATGACCAGCAATTCCTCAT  CATTACTACGCACCAGGCCAGCGGCCTCGCATCCGAAGTGTGTTCTTTGAGATCAGCCA  TGGGCGGATCCTTTATTGCATCAGAGAAATCAGGAACAAGTCTGATCTGCGATTTGGCGA  CGTTTGTAGGATCCGCAATTACTATGGCCTCGGCAGTGCAAACGCCAATTGTCTTGACGA  GGACCGTCACATCATGTGCGTCTTTAGGTATATAGCCGGGCTCGCCCAACGGTCGAAATG  ACATGGTGGGGCCACTACGCCTGGGCACCGTGGCAGTCGCGCCAACGTCAACTGCTTCAA  GTACATTGAGGCTGAGGGAAAGGCTCAATGTCTTTCTGGAGGCGTATATCACTAGCATCC  GTTGGCCAACCTTCGCATGTTTAAAGAACAACACATTCCTCCGTGCCGGCACTAGAATCAC  TGCCGGCGATATGCTCCAATGAAGCATCCAACGCCGTTTTGGTGCATCCCCCAGAGCGA  CGCGAGCGAGTATGTCCAGCGAATAAGACACTAAGGATGTGTCATAATGAACGAGGAACT  TATTGAAGTTCTTTTCGCCTAGGGACTGAATTGCCGCCATGGAAATCGGGTTGTTGTAGC  CGAGTACTCTGCGGAACGCTTCATATTGTGCTCCGTCAACCTTCGGAGCCACAAATATCC  CAGTAGTGCAGCCACGGCGATGAATTTTTGCCGCTGCTGACGAATGGTACCGCACACA  CTATCCTT </p>
<i>CATALASE1</i>	<p> CAGGCGCACCTGCAGAGCGCGCTCGCCTTCGAGCTCAGCCACTGCGAGGACCCGATTGTA  TACCGCAACTACATCAACGTTCTCAACAATATTGACTATGAACTCGCCAAATACGTCGCA  GTCGCCGTGGGTGGCGACGTCCCCGATGCTCCAGGGAAGCAGAACGAGGGGCACAAAAGC  GCGAAACTAAGCCAAGTGTACTACGCACCGAAGGAACCGACCATCAAAGGCCGGCGCGTT  GCCATACTGCTGGCGGACGGCTTTGATAAGGCGGAGGTTGTGGGTATCAAAGCGCTCATT  GCATCTGCGTCGGCGAATGCGTTCGTTATTGGGCCGAGGAGGGGGAAGGTCTTTGCGGCC </p>



	GGCGAGAAAATTGGTGTCGAGGGAGGTGGGATCGATGCAGATCATCACTTCGAAGGTCAG CGCAGTACGATGTTTGATGCGCTCGTTATCCAGTGGGGAGCATGCCGCTCTGTTGATG AAGAGTGGGCGCGCTGTTCAATTGGCTGAGGGAGGCATTGCGGCATTGCAAGCCAATAGGC TTTGAAGATGACGCTGAATATTGGGGAGAAAGGATTCATGGAAAGGTTGCGCTTCGAGCT TAGCAAGCATAGGTGCTTCAAGAGGGAGG
GTPase-activating protein S23	CGTGGGCTCATCCAATTCGTCACGCATTACCAACATTTCGTCTGGTCAACAACGTCTTCGT GTTACGACTATTGCTCGCAACTTCGCTGAAGCAAACGCGCCAAGTATCGCGGCCTCATT GACCAAGAAGCTGCCGCCGTTCTCATGGCTAGGATCGCGGTCTTCAAGGCCGAGATTGAC GACTCTCCGATGTCTTGAGGTGGCTGGATCGTATGCTTATCCGGCTGTGCCAGAAATTC GCCGACTACAGGAAAGAAGACCCAACGTCGTTTCAGGCTGACGGACAATTTAGTATTTAT CCTCAGTTCATGTTCCATCTCCGCAGAAGTCAGTTCCTACAGGTGTTCAACAACAGTCCG GACGAAACAGCGTTCTATAGACGCGTACTTAACGAAGAGGATGT
Palmitoyltransferase	ATGAAACACCGCTCCATCGAGGACTGCTTCTTGAATATTTCACTACTCATTGTAAGTGTC AATTGTCCTCCCGTTAGAATTGCCTCGCAAATCTACGGCCAGAAAGCTATAATTGTATC CTCATAGGGGCAGCATAGGAGCGGTCTAATATGGCAACGGATAAGCGCCTTGGCTGCGCC TCATTGCCAGGCAGCAAGACGGTAAGTGGGAGCAACCTCTCAAGACATCCACCATGGTC AAGATCTTCTCTCTCTCCGTCGTTCTTGCGCCTCCGTCGGGTTCTTGCACTGTTCTCAGC AATGCCACCGATCTTCTTCATTTCTTTCTACCAGAGAGGCTCCGTTGGAGAGTTCATG ACCTTCTCTCCCGAACGGTCGCAGAACGGACCCCTCAAGGTCAGCGCCAGAGCGTCCAG GAGAACAAATTACGTTGCTCACGTCTACAACCGTGGCGGAGCCGAGCAACTTGCGGCTGTG ATCATCACCGACCAAGAGTACCCTGTTGCGCCTGCCTTCTCCCTGCTCACCAAGATTCTG GACGACTTCACTGCCAAAGTCCCGCAGTCTTCTTCTCCAATCCATCGGCCATCAGCTTC TCTGAAATCAATGGTTACATCAAAGATATCAGGACCCTCGTCAGGCTGATACGATCATG AAAGT
Copper Amine Oxidase	TATTGTGATGGTTGGTCCATTGGCTACGACGAACGGTTCCTCAGAGCAGGCGGGTGCAA CAGGCGCTAGTGTTGCTCGGTATGGTCAGCACGAGAACCTGTACGCCCCACCCCTTAGAC TTTGTGCCCGTCATTGACGCCAATACAGAAGAGGTACTGCATGTGACTTTCCACCAGTG TGGAACCTTCGCCCAATGGGCCCGTATTATCCGTGAAATCCACTGCGCCCCAACGCCG

	<p> TTGCCAACCCACAGGATGCCTTCGCCTTCGCGAACAGGGACCGAATCCCTCCCCGGTC  AAGAAATTCGACTTCTTACCGGACTTGATGAAAGAGAATGACCCAGAGTTTAAACCGCGC  GACGATATCAAGCCGCTGCACGTCGTACAGCCCGAAGGCGTGAGCTTCAAGATGAATGGG  CATGAGCTCGAGTGGCAGAATTGGAAGATGCACATCGCTTTCAGCCACAGGGAAGGTTTG  GTCCTTTCGACTATCACCTATAACGATCATGGTGAAGTGCGGCCGATTTTCTACCGCCTG  TCCCTCGCGGAGATGGTTGTACCGTACGGGGCGCCGGAATATCCTCATCCAAGGAAGTTT  GCGTTTGATTCTGGCGAATACGGAATGGGAACGATGGCAAATGAATTGTCCCTAGGATGT  GATTGTCTGGGACAAATCCATTATTTACCCGGAGCATTCTGTGTCGCATGCCGGAACCGCC  ATCGTTATTAAGAATGTCATCTGCATCCACGAGGAGGATGCTGGTGTCTTTGGAAGCAT  ACGGACTACCGGCCTGACGGTCGCTCACAACCGTTTCGGAGGCGAAGGCTCGTCGTCAGC  ATGGTCTGCACCCTTGCAAATTACGAGTACATCTGGAATTACCACTTCTATCAGGACGGC  ACCATCGAGTTCGAGATCAGACTGTCTGGCATCCTCCAGGTCTACGTTTCAGCTGACGGC  GAACCCAATCCCCATGGTACGACTGTGGCGCCGAATGTCAACGCGCATTATCACCAACAT  TTATTCTGTGTCCGCGTTGACCCCATGGTGGACGGGCTGAATAATTCAGTCATCGAATCT  GACATCATTCCATTACCAGAGCCGAAGGGATCCGCGACGAATTATGGCGGTAACGGATT  ATCTCAATAGATACTCCTCTCAAGACCGAGGCGGGCCGTCCATATGACTTTGCGAAGGAG  CGCCGATGGAGGATTGTCAATCCATCGAGGAAGCACTACGCTTCAGGAAAGGACGTGGGG  TATCCCTTGGTGTGAAGGGCGGCGT </p>
--	---